annual report 1987

nuclear physics laboratory
university of washington

ANNUAL REPORT

Nuclear Physics Laboratory
University of Washington
May, 1987

Supported in part by the United States Department of Energy
under contract DE-AC06-81ER40048

INTRODUCTION

This has been a watershed year for the Nuclear Physics Laboratory here at the University of Washington. After 35 years, the Laboratory's original accelerator, a classical 60-inch cyclotron, was finally shut down. (A commemoration by Fred Schmidt of the early days at the cyclotron follows this introduction.) This past year has also seen the completion of the installation of the new linac-booster. We enthusiastically look ahead to the next 35 years for our Laboratory, as we plan the exciting physics program made possible by the new facility.

There have been an unusual number of personnel changes during this transition year and we were sorry to see a number of long-time co-workers retiring or otherwise leaving the Laboratory. Among those who officially retired are two of the Lab's founding fathers, Professors George Farwell and Fred Schmidt. As one might have predicted, they continue to pursue their research here with unabated intensity.

We were very pleased this year to welcome to the Laboratory, Dr. Charles Hyde-Wright, a new faculty member in the Physics Department. Charles is already reporting on his recent work and plans in the medium energy section of this Annual Report.

At this time a year ago about one-third of the linac-booster had been installed. So had the beam transport from the tandem to the booster. During the past year we have completed the installation of all of the remaining cryostats, resonators, bending magnets, diagnostics and beam lines. The individual systems have been debugged and are operating satisfactorily. The automatic control for these systems has been completed and is in use. We are now beginning to study the performance of the accelerator as an accelerator rather than as a collection of subsystems. To date, we have accelerated a beam of ^{16}O through the entire linac to an energy of 170 MeV. We look forward to the delivery of beams to the experimental areas by late summer.

The new polarized ion source is expected to be an important component of the new facility. In tests it has produced a 1 μa beam of H^- at 40 keV polarized to 86%.

As in other recent years, the experiments conducted by the members of the Laboratory have been carried out using accelerators at other laboratories as well as with our local Van de Graaff. Among the experiments which have attracted more than average interest is one that used no accelerator at all. The original "Fifth Force" hypothesis of Ephraim Fishbach was designed to explain gravitational anomalies that had been observed by Eötvös et al. and Stacey et al. This hypothesis has been ruled out by a local experiment employing a sensitive highly symmetric torsion pendulum containing beryllium and copper test bodies. The apparatus used is now being improved to test generalizations of the theory that can accommodate very small effects in our Be-Cu comparison.

In the field of Nuclear Astrophysics, preliminary results indicate the feasibility of determining the γ-branch of the unbound 5.17 MeV level in ^{14}O via the $^{12}C(^3He,n\gamma)$ reaction. We are now in the process of understanding and eliminating the sources of background, which is our limiting factor at the moment. In the area of symmetry studies, results have been obtained from the Washington-Wisconsin experiment measuring parity mixing in ^{14}N. The parity violating asymmetry measurement is smaller than the best theoretical estimates. An extensive effort is underway to solidify our description of the

^{14}N wave functions so that the experimental results can be used to deduce a parity violating nucleon–nucleon interaction.

Using a 21 MeV beam of antiprotons from the LEAR facility at CERN we have succeeded in trapping hundreds of antiprotons of keV energies in a Penning trap for the first time. With this capability demonstrated, we look forward to the development of precision systems to measure the antiproton inertial mass, to improve tests of CPT invariance for hadrons and to other experiments with protonium and antihydrogen.

As in other years, there have been a fair number of investigations involving the emission or absorption of photons by nuclei. In the continuing studies of the giant resonances built upon excited states, we have completed a detailed analysis of the proton capture systematics for the A=28–52 mass region. A study in ^{90}Zr of the statistical emission of photons with giant-dipole resonance energies suggests a possible change of mean nuclear shape from spherical to deformed as temperature and spin increase. A comparison of the decays of ^{92}Mo and ^{100}Mo (respectively, spherical and vibrational near the ground state) shows that the large width difference observed for the GDR's built on the ground states persists to higher spins and temperatures.

We have been trying to interpret our results on the energy dependence of the fore–aft asymmetries observed in the (γ,n) reaction on calcium. Our goal is to see in a consistent way how the properties of the E2 isovector resonance depend on the type and size of target nucleus. To complete our rough survey of this resonance, we have still to study a carbon target. Here the use of an active scintillator target will make it possible to study neutron emissions to much higher residual excitations than we have been able to do for heavier targets.

We have studied the emission of high energy γ-rays in bombardments of several targets with 19 MeV/nucleon ^{19}F ions. Our measured cross-sections are in reasonable agreement with calculations of bremsstrahlung from individual n–p collisions occurring at an early stage of the nucleus–nucleus collision. The forward peaked distribution of the observed radiation is roughly consistent with isotropic emission from a radiating source which is moving at half the beam velocity, i.e., at the speed of the nucleon–nucleon c.m.–system, supporting the view that the photons are products of n–p bremsstrahlung.

The main effort in our pion–reaction program has been the analysis of our comparative inclusive scattering cross-sections for ^{2}H, ^{3}He, and ^{4}He at 100 MeV with both + and – pions. The goal here has been to see how the quasi-elastic scattering from the individual nucleons is affected by the increasing probability for pion absorption as the target mass in this set of nuclei is increased.

A new medium energy activity involves the study of the $^{3}He(e,e'pp)n$ reaction at Saclay. In this reaction, the absorption takes place on a correlated pair of protons and there is strong suppression of transverse photons: the proton pair has no dipole moment and pion exchange currents are suppressed. The main features of the reaction should therefore be understandable in terms of the wave functions of the nucleons. The study of ^{3}He with the (e,e'pp) reaction may be a useful first step for the study of nucleon correlations in larger nuclei.

One of the ongoing studies in our heavy ion program is that of projectile breakup (e.g., in the bombardment of ^{181}Ta with 20 MeV/nucleon). Earlier investigation

demonstrated that the breakup of the projectile into two fragments of comparable charge was primarily sequential rather than instantaneous. In the most recent experiment we have addressed the question of charge balance in the projectile breakup. We determined in a coincidence experiment that most of the difference between the projectile's charge and the sum of the fragment charges goes into the emission of light charged particles (e.g., α and p) rather than into particle transfer to the target.

In a very different type of heavy ion study, we have used 35 and 50 MeV per nucleon carbon beams from the MSU/NSCL facility to bombard targets of ^{12}C, ^{40}Ca, ^{90}Zr, and ^{208}Pb. The data, extending up to angles at which the cross-section has dropped to less than 10^{-3} of the Rutherford cross-section, is now being analyzed. It is expected to provide new information on optical potentials, on the previously observed breakdown of the M3Y folding model and on total reaction cross-sections in this relatively unexplored energy region.

For the accelerator mass spectrometry (AMS) program, measurements of organic ^{14}C concentrations in deep-sea surface sediments from several locations were completed. Modeling studies of the data suggest that much of the organic carbon in the sedimentary mixed layer (the top few cm) is degradable on a time scale of a thousand years or less. Work continues on the NASA-supported collaborative study of methane cycling in high-northern-latitude wetland environments, and on further analysis and reduction of our already very low ^{14}C background for AMS measurements.

We close this introduction with a reminder that the articles in this report describe work in progress and are not be regarded as publications or quoted without permission of the investigators. In each article the names of the investigators have been listed alphabetically, but where appropriate the names of those primarily responsible for the report have been underlined.

As always, we welcome applications from outsiders for the use of our facilities. As a convenient reference for potential users, the table on the following page lists the vital statistics of our accelerator. For further information please write or telephone Dr. W.G. Weitkamp, Technical Director, Nuclear Physics Laboratory, University of Washington, Seattle, WA 98195; (206) 543-4080.

We are grateful to Barbara Fulton for her contributions to the design and production of this report.

Isaac Halpern
Editor

TANDEM VAN DE GRAAFF ACCELERATOR

A High Voltage Engineering Corp. Model FN purchased in 1966 with NSF funds; operation funded primarily by the U.S. Department of Energy. See W.G. Weitkamp and F.H. Schmidt, "The University of Washington Three Stage Van de Graaff Accelerator," Nucl. Instrum. Meth. 122, 65 (1974).

Available Energy Analyzed Beams:

Ion	Max. Current (pμA)	Max. Practical Energy (MeV)
p,d	20	18
He	1.5	27
Li	0.2	36
C	1.8	63
N	0.2	62
O	1	72
Si	0.1	90
Cl	0.2	90
Ni	0.005	99
Br	0.05	108
Ag	0.001	108

60-INCH CYCLOTRON

A fixed energy cyclotron constructed in 1950-52 with State of Washington funds; operated with income from outside users. See F.H. Schmidt, G.W. Farwell, J.E. Henderson, T.J. Morgan, and J.F. Streib, "The University of Washington Sixty-Inch Cyclotron," Rev. Sci. Instrum. 25, 499 (1954).

Available Target Box Beams:

Ion	Maximum Current (μA)	Energy (MeV)
p	100	11
d	150	22
^{4}He	30	42

The University of Washington Sixty-Inch Cyclotron

F.H. Schmidt

The Nuclear Physics Laboratory's cyclotron was shut down in late 1986. It had served us well for 35 years. This short history is to commemorate this productive machine, as one does an old friend.

The cyclotron became a gleam in the eye of the Physics Department in the Spring of 1947, and was conceived during three marathon staff meetings between September 10th and 15th of that year; its pulse was detected with an internal beam on July 27, 1951, and it reached childhood with a large and robust external beam in November 1952. From early 1953 through 1970 it matured, and enjoyed a full and fruitful physics research life. By 1972, the greater fraction of cyclotron operating time was devoted to diverse out-side user activities. From then on, total cyclotron use slowly declined, but various medical and other non-physics uses continued Until October 9, 1986 when the last run was made and the cyclotron was shut down permanently after 35 years of faithful operation. So far as we know, no other cyclotron of its type can lay claim to a similar record of longevity.

The birth-pains of the cyclotron were severe: An 18-month period from summer 1951 to late fall 1952 was devoted almost completely to a veritable struggle with the high-powered oscillator, and the critically shaped magnetic field. When it was over, the cyclotron produced very large beams to a target chamber: $>$ 100 μA of 22 MeV deuterons; $>$ 100 μA of 11 MeV protons; and $>$ 30 μA of 44 MeV α-particles. This success warranted construction of an external system to focus and analyze the beam to a large scattering chamber, all of which was fully operational by 1958.

A vigorous research program was initiated as soon as beam became available in the target chamber in 1952. This program included some of the first precise determinations of nuclear sizes (from measurements of the elastic scattering of alpha particles); early studies of the effects of angular momentum on angular distributions of nuclear reactions (including fission and particle evaporation); a study of the time reversal invariance of nuclear forces (through a comparison of a nuclear reaction and its inverse); explorations of the effects of parity non-conservation in short lived β decays, and a number of other seminal studies.

The physics research done with the cyclotron served to give the University of Washington Nuclear Physics Laboratory a substantial reputation world-wide; a reputation which helped to spawn the 3-stage Tandem Van de Graaff Program.

The medical uses of the cylcotron included an extensive neutron cancer therapy program, and in vivo whole body calcium activation studies. With considerable help from the NPL to keep it alive, the cancer work done with the 60-inch cyclotron assisted the University to obtain its own clinical cyclotron at the University Hospital.

Obviously, these programs all rested on good cyclotron operation. So, why were we successful? Was it luck? What did we do that was different?

Our initial intention was to carbon-copy the 60-inch "Rad-Lab" Berkeley machine. We were provided all available designs by Professor Ernest Lawrence, and so the project appeared simple - even to a small department which had never before contemplated such a

major undertaking. However, it soon became apparent that considerable improvements could be made in the Berkeley designs;

These included:[1]

1. A shielded vault (or building) to house the cyclotron instead of concrete blocks for shielding, thus facilitating access and servicing.
2. Provision in the original design of the building for an external beam system for scattering experiments, even though it was not clear that a cyclotron could be so employed.
3. A much improved and faster vacuum pumping system, achieved in part by relocation of a large pump from the position in the Berkeley machine.
4. An innovative welded aluminum vacuum chamber housing the dees, (indeed, we were pioneers in the use of welded aluminum for vacuum systems), which cut down radioactive activation.
5. An improved dee–stem shorting system (the so called spiders) which could be shifted in position for tuning purposes.
6. A thin graphite septum, or beam splitter, at the exit of the dee in the deflector channel. The graphite was bent to conform to the ion trajectories. It did not become severely radioactive (as would tungsten). It withstood the severe heating from 5 K.W. of beam power, and it had a long life due to the minimal sputtering of graphite.
7. Graphite barriers inside the dees to protect the vital parts such as water pipes.
8. Graphite source and central region parts instead of the customary tungsten.

So far as we know, other cyclotrons of that era lacked many of these features.

Other technical innovations installed after the initial construction also contributed to the success of the cyclotron as a research tool. We took a big step by construction of a double magnet external system – one magnet to direct and focus the beam to a distant, well–shielded experimental "cave," and a second to focus and energy–analyze the beam into a large and versatile scattering chamber. A magnetic spectrometer, in turn, was used to analyze reaction products.

When we first attempted particle–gamma coincidence studies, the accidental coincidence rates exceeded calculations. This led us to examine the time–structure of the beam and resulted in our discovery of separated ion orbit spirals in the cyclotron. At a meeting in Berkeley in the summer of 1946, a group of cyclotron experts had concluded that residual gas scattering caused complete amalgamation of the ion orbits, so that no vestige of the spirals would survive to the exit radius. Our observation of separated orbits therefore came as a surprise.

Once we understood the origin of the deleterious time–structure of the beam, we were led to construct a regulated power system, "the dee voltage regulator" to drive the dee potentials. Concurrently, we installed an automatic frequency control system. These improvements produced controlled ion orbits and converted the cyclotron into a precision tool for reaction and scattering experiments. Our success in these areas set the stage for

sophisticated experiments with the Three-Stage Tandem Van de Graaff accelerator.

The success of the cyclotron rested heavily on devoted graduate students, staff, and faculty. The energy, spirit, and drive of many individuals was, we believe, exceptional. Of course, we also needed money.[2]

Professor Ernest Lawrence died prematurely in 1958. As one of his former students, the author of this short history of our cyclotron deeply regrets that "E.O.L." never knew how greatly his influence contributed to our success.

References:

1. F.H. Schmidt, G.W. Farwell, J.E. Henderson, T.J. Morgan, and J.F. Streib, The Rev. of Sci. Instr. 25, 449 (1954).
2. The total cost, up to successful operation, was about $7 M (1987 dollars), and was shared about equally by the State of Washington and the Office of Naval Research.

TABLE OF CONTENTS

1. ASTROPHYSICS AND COSMOLOGY

1.1 Search for a γ-Branch of the Unbound 5.17 MeV level of ^{14}O

E.G. Adelberger, P.B. Fernandez, A. Garcia, M. Khandaker, and M. Hindi

As described in last year's Annual Report, we are attempting to measure the γ branching ratio of the unbound first excited state in ^{14}O, via the $^{12}C(^3He,n\gamma)$ reaction. Knowledge of Γ_γ/Γ will allow us to determine the rate for $^{13}N(p,\gamma)$ at astrophysical energies, and to predict stellar environments where the so-called "hot" CNO cycle can occur.[1] The predicted[2] value of Γ_γ/Γ is $\approx 5\times10^{-5}$.

We obtained a carefully prepared ^{12}C target: approximately 240 $\mu g/cm^2$ of isotopically enriched ^{12}C evaporated onto a 20 mil 99.9985% ^{197}Au backing. The $(n\gamma)$ coincidence spectra measured when it was bombarded with a ^3He beam showed two salient features: an exponential γ-ray background extending up to ≈ 7 MeV, and a 5.2 MeV peak.

We examined $(n\gamma)$ coincidence spectra from several possible contaminants (silicon, iron, nickel, sodium chloride), but they all failed to account for the observed continuum background in the $^{12}C(^3He,n\gamma)$ data. We identified the $^{14}N(^3He,np)^{15}O$ reaction as the source of the 5.2 MeV γ-ray yield. We measured the amount of ^{14}N in the target using the $(p,p'\gamma)$ reaction, and subtracted its contribution to the $(n\gamma)$ coincidence yield. After subtracting the contributions from the peak and exponential backgrounds, we obtained a limit for the γ branching ratio Γ_γ/Γ of $(1.4\pm0.5)\times10^{-4}$. This indicated that the experiment could reach the required sensitivity.

In an effort to reduce our background, we made a ^{12}C target by ion implantation. We used the NPL sputter ion source to implant ^{12}C ions into a 20 mil thick ^{197}Au substrate that had been cleaned by glow discharge. This target showed (4.2 ± 1.1) times less ^{14}N and (8.1 ± 5.8) times less ^{13}C than our previous best evaporated ^{12}C target. But when bombarded with 9.4 MeV ^3He, the γ-ray exponential background in coincidence with 2 MeV neutrons persisted. We are now investigating whether this background is due to secondary reactions taking place in the Au backing, i. e. $^{197}Au(p,n\gamma)$, where the energetic protons come from the $^{12}C(^3He,p)$ reaction. To test this hypothesis we are going to make a second target by implanting ^{12}C ions into a 1 mil thick Au substrate; this should reduce the $(n\gamma)$ coincidence background by a factor of 2.

References:

1. Nuclear Physics Laboratory Annual Report, University of Washington (1986) p. 1.
2. K. Langanke, O.S. van Roosmalen and W.A. Fowler, Nucl. Phys. A 435, 657 (1985).

******

1.2 Study of the Delayed Proton Decay Scheme of ^{37}Ca

E.G. Adelberger, P.B. Fernandez, S. Gil, A. Garcia, W.F. Rogers, D. Mikolas,* and T. Murakami*

We plan to determine the B(GT) distribution for the ^{37}Ca β^+ decay by an improved measurement of the ^{37}K delayed proton spectrum. This information helps in determining the solar neutrino capture cross section of ^{37}Ca, which is important in light of the current solar neutrino problem.[1,2] The currently accepted cross section value is partially based on ^{37}Ca delayed proton spectrum measurements by Sextro et al.[3] which were analyzed assuming that all ^{37}K decays proceed to the ^{36}Ar ground state. Adelberger and Haxton[4] have pointed out that neglecting decays to the first excited state of ^{36}Ar at 1.97 MeV yields a B(GT) distribution that is too weak and shifted to lower excitation energies. This effect produces a ^{37}Cl neutrino capture cross section that is too low by roughly 4%. We plan to measure the B(GT) spectrum more accurately by taking account of proton decays to the ^{36}Ar first excited state. Our measurements would also provide a useful benchmark for studies of quenching of spin observables, and yield a calibration of (p,n) B(GT) determinations over an unusually broad range of excitation energies,[5] since the ^{37}Ca beta decay is the most energetic in the sd-shell.

We will produce ^{37}Ca via ^{3}He(^{36}Ar,^{37}Ca)2n at $E_{lab} \simeq 12$ MeV/A (the kinematically reversed reaction used by Sextro et al.) using the Recoil Product Mass Separator (RPMS) facility at MSU.[6] Our first run (for which our proposal has already been accepted) will probe ^{37}Ca production yield to ascertain the feasibility of performing proton-gamma coincidences to measure the ^{37}Ca beta-decay ft spectrum.

The experimental set-up will consist of two separate detector arrangements and a rotating catcher wheel. The first detector arrangement located at the focal plane of the RPMS, will identify the ^{37}Ca reaction products. The catcher wheel will be rotated every 0.25 seconds ($T_{1/2}$(^{37}Ca)=0.173 sec) to the position of the second detector arrangement which will measure inclusive proton spectra, proton-gamma coincidences and proton-positron coincidences. This setup will employ two identical 500 μm Si E detectors located on each side of the catcher wheel, each of which is backed by a 5" by 6" NaI gamma detector. Current efforts are devoted to design and construction of the detector arrangements and the target gas cell.

References:

* National Superconductor Cyclotron Lab, Michigan State University, East Lansing, MI 48824.

1. J.N. Bahcall, W.F. Huebner, S.H. Lubow, P.D. Parker, and R.K. Ulrich, Rev. Mod. Phys. 54, 767 (1982).
2. J.N. Bahcall, Rev. Mod. Phys. 50, 881 (1978).
3. R.G. Sextro, R.A. Gough, and J. Cerny, Nucl. Phys. A 234, 130 (1974).
4. E.G. Adelberger and W. Haxton, Phys. Rev. C (1987), in press.
5. J. Rapaport et al., Phys. Rev. Lett. 47, 1518 (1981).
6. J.A. Nolen, Jr., L.H. Harwood, M.S. Curtin, E. Ormand, and S. Briker, "Instrumentation for Heavy Ion Nuclear Research," Proc. of the Int. Conf. on Inst. for Heavy Ion Nuclear Research, ORNL, Tennessee, October 22-25, Harwood Academic Publishers (1984).

******

1.3 Nucleosynthesis of ^{180}Ta

S.E. Kellogg and E.B. Norman*

It has been proposed by Beer and Ward that the abundance of nature's rarest isotope, ^{180}Ta, could be quantitatively accounted for in the standard stellar slow (s) and/or rapid (r) neutron-capture processes through the existence of small, previously unmeasured β-branches which drain and feed the population of the $t_{1/2}$ = 5.5 hour isomer of ^{180}Hf.[1] As described in previous laboratory reports,[2] we have conducted a series of experiments designed to measure these small β-branches. This work has now been completed and can be summarized as follows. We have:

(1) Measured the direct (isomer-to-isomer) 214-keV-endpoint β branch from ^{180}Hf^{m} to ^{180}Ta^{m} to be f_{β} = 0.30±0.07±0.07% (Ref. 3).

(2) Observed a new γ ray in the decay of ^{180}Hf^{m} which indicated a small β-branch of 0.023% to an excited state in ^{180}Ta (Ref. 4).

(3) Established a stringent limit of 0.023% on the fraction f_{m} of ^{180}Lu decays which populate ^{180}Hf^{m} (Ref. 5).

(4) Sought to identify a possible high-spin, short-lived isomer of ^{180}Lu, and established upper limits on its possible half-life (Ref. 6).

(5) Established limits on the ^{180}Ta^{m} photodeexcitation cross-section via resonant and nonresonant processes (Ref. 7), and

(6) Calculated upper-limits on the life-time of ^{180}Ta^{m} in a stellar environment (Ref. 3).

Taken together, this body of work rules out an exclusive s- or r-process production mechanism for ^{180}Ta^{m} via the Beer and Ward theory.

References:

* Lawrence Berkeley Laboratory, University of California, Berkeley, CA 94720.

1. H. Beer and R. Ward, Nature 291, 308 (1981).
2. Nuclear Physics Laboratory Annual Report, University of Washington (1983) p. 1; ibid (1985) p. 1; ibid. (1986) p. 3.
3. S.E. Kellogg, "The Nucleosynthesis of ^{180}Ta^{m}," Ph.D. Thesis, University of Washington (1987).
4. S.E. Kellogg and E.B. Norman, Phys. Rev. C 31, 1505 (1985).
5. S.E. Kellogg and E.B. Norman, Phys. Rev. C 34, 2248 (1986).
6. K.T. Lesko et al., Phys. Rev. C 34, 2256 (1986).
7. E.B. Norman et al., Astrophys. J. 281, 360 (1984).

******

2. GIANT RESONANCES IN EXCITED NUCLEI

2.1 Excited-State Giant Dipole Resonances in Proton Capture

J.A. Behr, D.H. Dowell,* G. Feldman, C.A. Gossett, J.H. Gundlach, M. Kicinska-Habior, and K.A. Snover

We have studied, via (p,γ) reactions, the GDR built on excited final states up to $E_f \sim 10$–15 MeV in ^{28}Si, ^{40}Ca, ^{46}Ti and ^{52}Cr, and up to $E_f \sim 3$–6 MeV in ^{29}P and ^{41}Sc. All cases show clear evidence of a resonance structure for capture to discrete final states. Measured excitation functions were analyzed by three separate methods. First, to extract GDR parameters in a model-independent manner, a Lorentzian function was fitted to the inverse (γ,p_0) excitation curves, after accounting for the statistical decay component of the cross section. Gamma-ray resonance energies so obtained are roughly constant as a function of E_f for ^{29}P, ^{41}Sc, ^{46}Ti and ^{52}Cr, while ^{28}Si and ^{40}Ca show a pronounced decrease ($\sim$3 MeV) for the higher energy final states. The GDR widths increase from 4 to 10 MeV in ^{28}Si and ^{40}Ca and from 6 to 11 MeV in ^{46}Ti with increasing final state energy, but they remain relatively constant at an intermediate value of 6–8 MeV in ^{29}P, ^{41}Sc and ^{52}Cr. Remarkable similarities in energy and width trends are apparent for ^{28}Si compared to ^{40}Ca and for ^{29}P compared to ^{41}Sc.

Next, an analysis was performed with the direct-semidirect (DSD) model.[1] A fixed complex GDR coupling strength was used for all states in the model calculations for $A \leq 41$; for states in the A=46 and 52 nuclei, a 20% larger strength was necessary. Calculations were fitted to the data by varying the GDR energy, width and spectroscopic factor for each final state. The DSD calculations reproduce the (p,γ) excitation functions quite well; the resultant energies and widths are similar to the Lorentzian results described above (except DSD widths were typically lower by $\sim$1 MeV), and the fitted C^2S values are in reasonable agreement with the literature values.

Finally, we investigated the applicability of a simple schematic model, using harmonic oscillator wave functions, for computing integrated (γ,p_0) strengths.[2] In the extreme limit of neglecting penetrability differences for different nucleon decay channels, the model results agree with the A=28–41 data[3-4] but overpredict the measured strengths in the $1f_{7/2}$ nuclei ^{46}Ti and ^{52}Cr. Attempts to improve the calculations using Coulomb penetrabilities together with a weak-coupling approximation for the nucleon decay energies reduced the discrepancies between calculation and experiment in ^{46}Ti and ^{52}Cr but worsened the agreement in the other cases.

In conclusion, we have established the systematics of the energy, width and strength of the GDR built on a wide range of excited states in the A=28–52 mass region. The validity of the DSD model in predicting the energy dependence and magnitude of the cross section for capture to states at moderate excitation has also been demonstrated.

References:

* Present address: Boeing Aerospace Co., Seattle, WA 98124

1. M. Potokar et al., Nucl. Phys. A 277, 29 (1977).
2. K.A. Snover, J. de Phys. 45, C4-337 (1984).
3. D.H. Dowell et al., Phys. Rev. Lett. 50, 1191 (1983).
4. D.H. Dowell, 5th Capture γ-Ray Spec. Symp. (Knoxville, 1984), 597.

2.2 Spin Dependence of the Giant Dipole Resonance Strength Function in Highly Excited Nuclei in the Mass Region A=39–45

J.A. Behr, C.A. Gossett, J.H. Gundlach, G. Feldman, M. Kicinska-Habior, and K.A. Snover

In our previous study[1] of the strength function of the giant dipole resonance (GDR) built on highly excited states of ^{63}Cu, the energy E_D and strength S of the GDR were found to be independent of spin and temperature. The width Γ of the GDR was found to increase as a function of both temperature and spin, and their relative importance was difficult to resolve. In order to study the pure spin dependence of the GDR strength function we have measured continuum γ-ray spectra from decays of ^{39}K*, ^{40}K*, ^{42}Ca* and ^{45}Sc* compound nuclei produced by heavy-ion-fusion reactions. For such light compound nuclei, the effective temperature associated with the states upon which the GDR is built is nearly constant or even decreases with increasing projectile energy in the entrance channel for projectiles of mass A $\sim$ 12–18.

Nuclei of interest were produced by bombarding self-supporting aluminum targets of 1.0 and 1.5 mg/cm^2 thickness with 33.8, 48.2 and 62.7 MeV ^{12}C, 39.7 MeV ^{13}C, 29.2 and 44.7 MeV ^{15}N and 31.5, 44.9, 61.5 and 72.5 MeV ^{18}O ions from the University of Washington FN tandem accelerator. Our experimental technique has been described previously.[1,2]

The parameters of the GDR strength function have been extracted using the modified isospin-dependent version of the computer code CASCADE in a nonlinear least-squares fitting routine. Different level density formulations were tested as described in our previous work.[1] All measured spectra were well-reproduced by statistical calculations with a one-component GDR using a level density calculated in the Reisdorf approach[1,3] (see Fig. 2.2-1). The effective temperature of states upon which the GDR is built was estimated to be in the range of 1.6–1.7 MeV for all cases except ^{12}C + ^{27}Al at E=62.7 MeV which corresponded to T=1.45 MeV, and ^{13}C + ^{27}Al at E=29.2 MeV which corresponded to T=1.8 MeV. The mean spin range studied here was 7.7–18.7 $\hbar$, corresponding to a range of grazing angular momentum ℓ_0 of 11.5–28.0 $\hbar$.

GDR parameters extracted from the best fits to the data are presented in Fig. 2.2-2. In all compound nuclei studied here a strong spin dependence of the GDR width is found. For example, in the case of ^{45}Sc, Γ increases from 12.1±0.3 to 16.2±0.6 MeV in the mean spin range 7.7–18.7 $\hbar$ and constant temperature 1.6 MeV. Our results show that the GDR in highly excited nuclei in the mass range A=39–45 is 2–5 MeV broader than the GDR in A$\approx$63 nuclei at similar temperatures.[1]

Within a given reaction channel, GDR energies extracted from CASCADE fits using the most reliable level density show some spin dependence. The average value of E_D for decays of ^{45}Sc* appears somewhat lower than for the other nuclei, although isospin splitting differences (the difference between the mean GDR energy and the expected $T_<$ energy) are expected to be similar for all cases. Also, the GDR strength appears significantly larger than 1.0 for the T_z=1 ^{40}K and ^{42}Ca cases. Further study of the level density is required before definite conclusions concerning differences in E_D and S in the nuclei studied can be made. Recently we have measured the angular distribution of high energy γ rays from the decay of ^{45}Sc at 50 and 66.6 MeV excitation energy and ^{39}K at 60 MeV. Once these data are analyzed we will be able to determine possible nonstatistical enhancement of the high-energy γ-ray spectra at the highest projectile energies. We are also hoping to extract some information about deformation from the angular distributions.

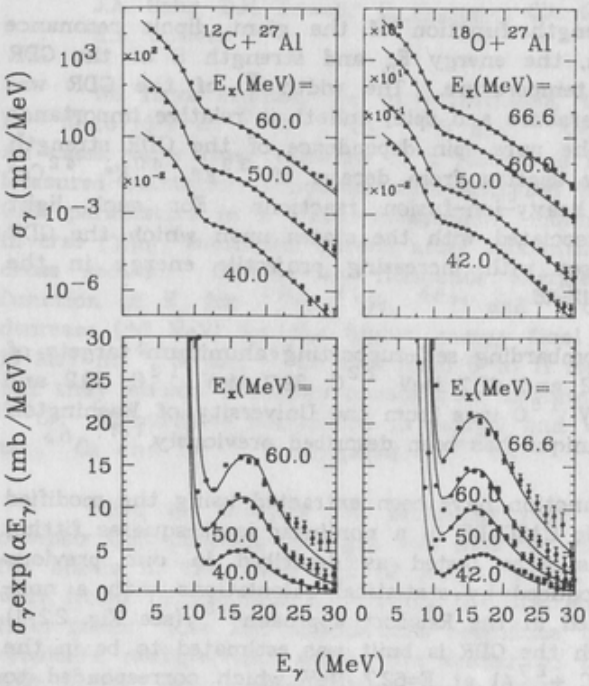

Fig. 2.2-1 Measured γ-ray spectra from the decay of $^{39}K^*$ and $^{45}Sc^*$ together with least-squares-fitted statistical model calculations. Bottom part shows the same spectra multiplied by an energy-dependent factor $\exp(\alpha E_\gamma)$ to permit convenient comparision of the fit quality on a linear scale.

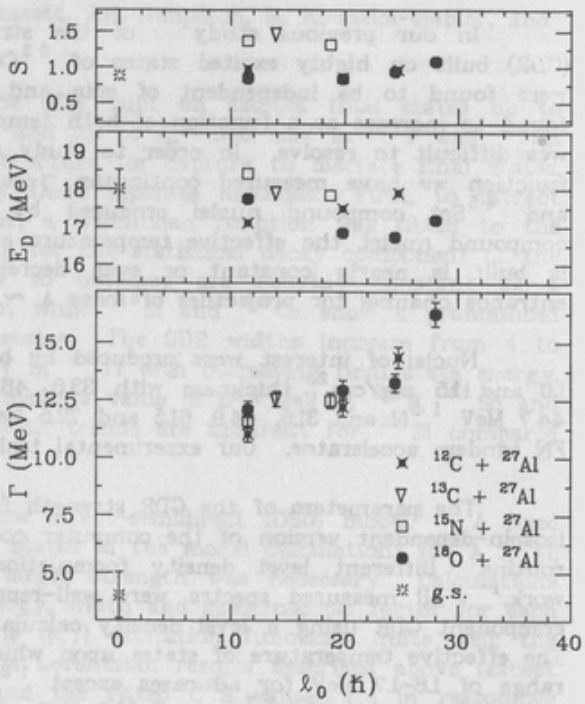

Fig. 2.2-2 The extracted GDR parameters from decays of $^{39}K^*$, $^{40}K^*$, $^{42}Ca^*$ and $^{45}Sc^*$ as a function of the grazing angular momentum ℓ_0.

References:

1. M. Kicinska-Habior, K.A. Snover, C.A. Gossett, J.A. Behr, G. Feldman, H.K. Glatzel, J.H. Gundlach, and E.F. Garman, Phys. Rev. C 36, #2 (August, 1987), in press.
2. C.A. Gossett, K.A. Snover, J.A. Behr, G. Feldman, and J.L. Osborne, Phys. Rev. Lett. 54, 1486 (1985).
3. W. Reisdorf, Z. Phys. A 300, 227 (1981).

******

2.3 Nuclear Level Density for $23 \leq A \leq 63$ – Comparison of Experimental Data and Theoretical Expectations

M. Kicinska-Habior and K.A. Snover

The level density of atomic nuclei is a quantity of primary importance in statistical models of nuclear reactions, and has a strong impact on the quantitative results of calculations. For statistical decay of the Giant Dipole Resonance (GDR) built on highly excited states, where the γ-decay width is proportional only to the ratio of level densities of final and initial states, parameters of the GDR strength function extracted from fits of statistical model calculations to the measured γ-ray spectra as well as the quality of the fits are sensitive to the level density parameters.[1] To satisfactorily reproduce γ-decay spectra measured in heavy-ion induced reactions we should then know the level density of the initial compound nucleus and its daughters in the range from low ($\leq$ 5MeV) up to high ($\geq$50 MeV) excitation energies. Available experimental data consist of level density values determined from direct level counting, high resolution s- and p-wave neutron resonance and charged particle resonance measurements, one nucleon transfer reaction experiments and Ericson fluctuation measurements.[2-4] These data cover the range mainly up to ~10 MeV. Only for some nuclei level densities up to ~25 MeV are known, above which no information exists. We have considered the sensitivity of the statistical model calculations to the level density parameters as an opportunity for testing different level density formulations.

In our studies we have concentrated on nuclei with A=23-63. The range of masses chosen is connected with recently analyzed data from statistical decay of ^{39}K, ^{40}K, ^{42}Ca, ^{45}Sc and ^{63}Cu nuclei (see Secs. 2.4 and 2.2). We have investigated three different level density formulations: 1) the original CASCADE approach proposed by Pühlhofer[5] in which the level density is defined separately in different regions of excitation energy, and at energies above 20 MeV parameters $a_{LDM}=A/8$ MeV^{-1} and Δ_{LDM} calculated from the Myers droplet model mass formula without the Wigner term are used; 2) a variation of the Pühlhofer approach in which a_{LDM}, Δ_{LDM} and the location and size of the transition region in which the level density is interpolated from the low energy values obtained with empirical parameters to the high energy, liquid drop values, were varied; 3) the approach suggested by Reisdorf[6] in which the level density at all excitation energies is given by one smoothly varying formula treating the level density parameter a as dependent on the ground-state shell correction energy and the excitation energy of the nucleus. Our criteria in determining the acceptability of the level density description were that it should result in good fits of the statistical calculations to the measured γ-decay spectra of nuclei studied over a wide range of excitation energies, that the extracted GDR parameters should vary smoothly with excitation energy and spin, and that the calculated level density should agree with values determined experimentally.

In the case of the Pühlhofer approach and its variations the calculated level densities for most of the nuclei agree apriori with experimental values up to 8-10 MeV, because the level density parameters used in the calculation have been extracted from fits to those data. At higher energies, however, the magnitude of the level density calculated with $a_{LDM}=A/8$ MeV^{-1} and Δ_{LDM} calculated without the Wigner term is for most of the nuclei too large, resulting in an incorrect slope of the level density in the transition region. In such a case, if high-energy γ decay populates states in the transition region, then the high-energy γ-ray spectrum is given incorrectly and fits give often unreasonable GDR parameters. Our analysis shows that for nuclei with mass around A=60 the best CASCADE fits to the measured γ-ray spectra are obtained with level density parameters

a_{LM}=A/9 MeV^{-1} and Δ_{LDM} calculated with the Wigner term included or a_{LDM}=A/9.5 MeV^{-1} and Δ_{LDM} calculated without the Wigner term. These parameterizations also reproduce well the experimental values of the level density for all of the studied nuclei for which such data above 10 MeV have been measured. However, in the mass range A=35–45 the level density above 10 MeV was determined experimentally only for a few nuclei. We have found also that to reproduce γ-ray spectra from decay of ^{39}K and ^{45}Sc at the lowest measured excitation energies parameters $a_{LDM} \cong A/10$ MeV^{-1} and Δ_{LDM} calculated with the Wigner term would be required in the Pühlhofer approach.

Equally well fitted as in the Pühlhofer approach with the best level density parameters are γ-ray spectra from the decay of ^{63}Cu, ^{45}Sc, ^{42}Ca, ^{40}K and ^{39}K nuclei analyzed with the Reisdorf approach together with individual levels at very low excitation energy. The Reisdorf approach has been originally proposed and used for heavy nuclei. Characteristic parameters in this approach, the scaling parameter r_o=1.153 fm defining the smooth liquid drop part of the level density parameter a, as well as the damping factor for shell effects γ^{-1}=18.5 MeV, have been determined for masses A=100–253. Those parameters still reproduce well the level density data for masses around A=60. For nuclei with A=30–50 level spacings calculated with those parameters are 2–5 times smaller than level spacings observed experimentally. We have tested the sensitivity of the Reisdorf approach to both parameters r_o and γ^{-1} and we have found that the experimental level spacings in the range of masses A=23–63 are reproduced reasonably well in the Reisdorf approach when $r_o \cong$1.10 fm and γ^{-1}=18.5 MeV. The parameter r_o which compares usually with the radial constant in the droplet model r_{oDM}=1.16 fm has to be treated here as a free parameter, perhaps because light nuclei do not fulfill the assumption of being leptodermous.

References:

1. M. Kicinska-Habior, K.A. Snover, C.A. Gossett, J.A. Behr, G. Feldman, H.K. Glatzel, J.H. Gundlach, and E.F. Garman, Phys. Rev. C 36, #2 (August, 1987), in press.
2. W. Dilg et al., Nucl. Phys. A 217, 269 (1973).
3. C.C. Lu et al., Nucl. Phys. A 190, 229 (197.
4. M. Beckerman, Nucl. Phys. A 278, 333 (1977).
5. F. Pühlhofer, Nucl. Phys. A 280, 267 (1977).
6. W. Reisdorf, Z. Phys. A 300, 227 (1981).

******

2.4 Statistical GDR Decay of Highly Excited States of ^{63}Cu

J.A. Behr, C.A. Gossett, J.H. Gundlach, G. Feldman, M. Kicinska-Habior, and K.A. Snover

We have continued our studies of temperature and spin dependence of the GDR strength function in the ^{63}Cu nucleus. Our continuum γ-ray spectra from decays of $^{63}Cu^*$ formed at initial excitation energies of 22.5 to 77.4 MeV and mean spin up to 22 $\hbar$, measured in ^{18}O, ^{12}C, ^{6}Li and ^{4}He induced reactions on ^{45}Sc, ^{51}V, ^{57}Fe and ^{59}Co targets, have been analyzed using the statistical code CASCADE with the standard level density formulation proposed by Pühlhofer.[1] Because the fit quality as well as the extracted parameters of the GDR strength function (energy, width and strength) depend on level density, we performed detailed analysis of the level densities for the initial compound nucleus ^{63}Cu and its daughters. The large range of energies studied in this work permitted different level density formulations to be tested.[2] Final values of the GDR energy, width and strength at given temperatures and spins have been obtained by averaging over the different level density descriptions which resulted in good quality fits and which reproduced experimental values of level densities determined from direct level counting, high resolution (p,p) resonance measurements and Ericson fluctuation measurements.

The GDR energy and strength were shown not to depend on nuclear temperature in the studied range 0.7-1.9 MeV and final spin in the range 3-22 $\hbar$, which is consistent with theoretical expectations. The mean GDR energy of 16.8±0.4 MeV at finite temperature observed in the present work is in agreement with the average ground-state $T_<$ value of 16.7 MeV. The average strength of 0.99±0.10 (in units of the classical dipole sum rule) is in agreement with the ground-state value of 0.97. The GDR width increases smoothly from 7.5±0.4 MeV to 10.6±0.6 MeV with both increasing temperature and increasing spin in the studied range. These widths may be compared with 5±1 MeV for the $T_<$ component of the ground-state GDR estimated from neighbouring nuclei. The basic character of the width dependence on temperature and spin is not affected by changes in the level density parameters. Observed broadening of the GDR at higher temperature is presumably due to thermal averaging over a distribution of deformations. A similar effect was observed for GDR built on highly excited states in $^{108}Sn^*$ and $^{111}Sn^*$ nuclei.[3]

References:

1. F. Pühlhofer, Nucl. Phys. A 280, 267 (1977).
2. M. Kicinska-Habior, K.A. Snover, C.A. Gossett, J.A. Behr, G. Feldman, H.K. Glatzel, J.H. Gundlach, and E.F. Garman, Phys. Rev. C 36, #2 (August, 1987), in press.
3. J.J. Gaardhøje, C. Ellegaard, B. Herskind, R.M. Diamond, M.A. Deleplanque, G. Dines, A.O. Macchiavelli, and F.S. Stephens, Phys. Rev. Lett. 56, 1783 (1986).

******

2.5 The Giant Dipole Resonance in Highly Excited ^{92}Mo and ^{100}Mo

J.A. Behr, C.A. Gossett, J.H. Gundlach, G. Feldman, M. Kicinska-Habior, and K.A. Snover

Recently it has been shown[1-3] that in analogy with the well-known splitting of the giant dipole resonance (GDR) built on the ground state of statically deformed nuclei, the GDR strength function for compound nuclear γ decay provides information on the deformation of the ensemble of excited nuclear states populated by the γ decay. This result motivated our interest in studying the GDR strength function for spherical vibrational nuclei, the surface of which is dynamically deformed, which results in a modulation of the giant dipole vibration by the lower-frequency quadrupole surface vibration. The effect of the dipole-vibrational quadrupole coupling has been described in the framework of the Dynamic Collective Model (DCM)[4] which reproduces well the (γ,γ') data for ^{92}Mo and ^{96}Mo.[5] The GDR built on the ground states of even molybdenum isotopes (A=92-100) has been also observed in the (γ,n) reaction.[6] It was found experimentally[6] that the width of the GDR in these nuclei is strongly dependent on the "softness" of the nucleus, and increases from 5.4±0.2 MeV for ^{92}Mo up to 7.9±0.2 MeV for ^{100}Mo. These results are in good agreement with theoretical evaluations of the spreading width of the GDR in molybdenum isotopes in the framework of the DCM.[4,6]

In order to study the temperature and spin dependence of the dipole-quadrupole coupling we have measured continuum γ-ray spectra from decays of ^{92}Mo* and ^{100}Mo* compound nuclei formed at the same nuclear temperatures and spins. To produce the ^{92}Mo and ^{100}Mo compound nuclei we used the ^{16}O + ^{76}Se reaction at projectile energies E=50.0 and 72.2 MeV, and the ^{18}O + ^{82}Se reaction at E=49.1, 63.4 and 72.8 MeV. We have used water-cooled targets of ^{76}Se (1.7 mg/cm^2) and ^{82}Se (1.0 mg/cm^2), enriched to 96.5% and 96.7%, respectively, evaporated on platinum backings. We have used the same experimental technique as described previously.[2,7]

The parameters of the GDR strength function have been extracted using the statistical code CASCADE in a nonlinear least-squares fitting routine. All spectra are well-reproduced by statistical calculations with a one-component GDR (see Fig. 2.5-1). GDR parameters extracted from the best fits to the data are presented in Fig. 2.5-2. We have found that the mean energy E_D and strength S of the GDR from decays of ^{92}Mo* and ^{100}Mo* are close to the ground-state values, but the width Γ is broader and increases by ~1 MeV in the mean spin range 9-20 $\hbar$ and temperature range 1.35-1.55 MeV. The g.s. GDR in ^{100}Mo is broader than the g.s. GDR in ^{92}Mo by 2-2.5 MeV, and this width difference persists for the GDR built on excited states in the spin and temperature range studied here. It would be interesting to see if theoretical calculations could reproduce both the substantial broadening due to thermal fluctuations and the persistent width difference of the GDR in these two nuclei.

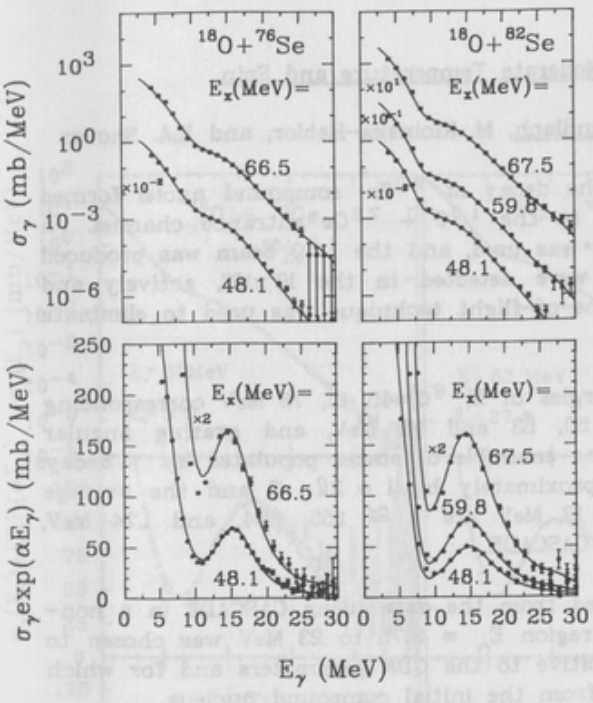

Fig. 2.5–1 Measured γ–ray spectra from the decays of ^{92}Mo* and ^{100}Mo* together with least–squares–fitted statistical model calculations. Bottom part shows the same spectra multiplied by an energy–dependent factor $\exp(\alpha E_\gamma)$ to permit convenient comparison of the fit quality on a linear scale.

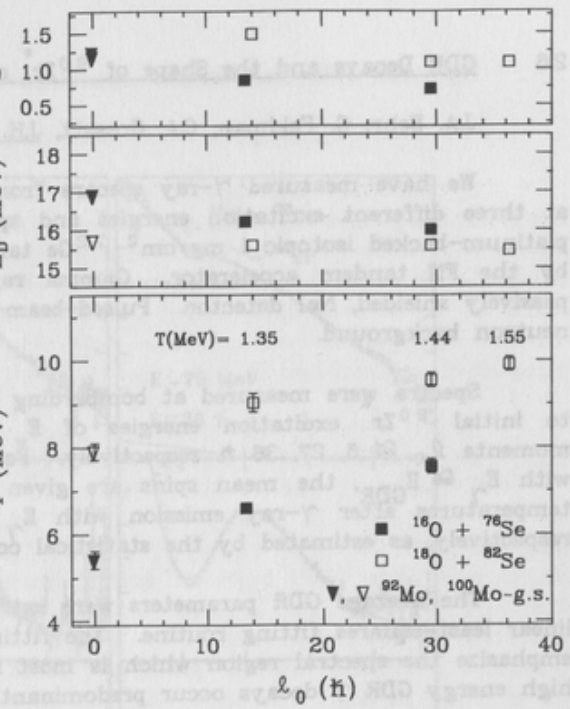

Fig. 2.5–2 The extracted GDR parameters from decays of ^{92}Mo* and ^{100}Mo* as a function of the grazing angular momentum ℓ_0.

References:

1. J.J. Gaardhøje, C. Ellegaard, B. Herskind, and S.G. Steadman, Phys. Rev. Lett. 53, 148 (1984).
2. C.A. Gossett, K.A. Snover, J.A. Behr, G. Feldman, and J.L. Osborne, Phys. Rev. Lett. 54, 1486 (1985).
3. D.R. Chakrabarty, M. Thoennessen, N. Alamanos, P. Paul, and S. Sen, Phys. Rev. Lett. 58, 1092 (1987).
4. M.G. Huber, M. Danos, H.J. Weber and W. Greiner, Phys. Rev. 155, 1073 (1967).
5. T.J. Bowles, R.J. Holt, H.E. Jackson, R.M. Laszewski, R.D. Mc Keown, A.M. Nathan, and J.R. Specht, Phys. Rev. C 24, 1940 (1981).
6. H. Beil, R. Bergere, P. Carlos, A. Lepretre, A. de Miniac, and A. Veyssiere, Nucl. Phys. A 227, 427 (1974).
7. M. Kicinska–Habior, K.A. Snover, C.A. Gossett, J.A. Behr, G. Feldman, H.K. Glatzel, J.H. Gundlach, and E.F. Garman, Phys. Rev. C 36, #2 (August, 1987), in press.

2.6 GDR Decays and the Shape of $^{90}Zr^*$ at Moderate Temperature and Spin

J.A. Behr, G. Feldman, C.A. Gossett, J.H. Gundlach, M. Kicinska-Habior, and K.A. Snover

We have measured γ-ray spectra from the decay of $^{90}Zr^*$ compound nuclei formed at three different excitation energies and spins in the $^{18}O + ^{72}Ge$ entrance channel. A platinum-backed isotopic 1 mg/cm^2 ^{72}Ge target was used, and the ^{18}O beam was produced by the FN tandem accelerator. Gamma rays were detected in the 10"x10", actively and passively shielded, NaI detector. Pulsed-beam-time-of-flight technique was used to eliminate neutron background.

Spectra were measured at bombarding energies of $E(^{18}O)$=45, 61, 76 MeV corresponding to initial $^{90}Zr^*$ excitation energies of E_x = 50, 63 and 75 MeV, and grazing angular momenta $\ell_0 \cong$ 5, 27, 36 $\hbar$ respectively. For the ensemble of states populated by γ decays with $E_\gamma \cong E_{GDR}$, the mean spins are given approximately by $I = 2\ell_0/3$ and the average temperatures after γ-ray emission with E_γ = 17 MeV are T $\cong$ 1.55, 1.64, and 1.74 MeV, respectively, as estimated by the statistical code CASCADE.

The average GDR parameters were extracted from the data using CASCADE in a non-linear least-squares fitting routine. The fitting region E_γ = 11.75 to 23 MeV was chosen to emphasize the spectral region which is most sensitive to the GDR parameters and for which high energy GDR γ decays occur predominantly from the initial compound nucleus.

The results are shown in Fig. 2.6-1. The lowest spin case, shown in the left hand column, has been discussed earlier.[1] For this case the excited state GDR strength function is well described by a single Lorentzian, as is characteristic of a spherical nucleus, with resonance energy and strength similar to the ground state GDR, but with a strongly broadened width, Γ = 8.8 MeV, compared to a width of 4 MeV for the g.s. GDR.[2] For the cases at higher energies and spins shown in the second and third columns, a 2-component GDR shape is required to obtain a good fit to the data, suggesting a spin and temperature-induced change to a preferred deformed shape. For all three cases, well determined, similar results are obtained for the total GDR strength of $\cong$ 1 classical sum rule, mean resonance energy of 16.8$\pm$0.1 MeV, and full width at half maximum of 8.6 to 9.5 MeV.

For the two higher energies and spins, the apparent splitting deduced from the 2-Lorentzian fits corresponds to $\delta \cong (E_2/E_1)-1 \cong$ 0.22 and 0.24 for the ℓ_0 = 27 and 36 $\hbar$ cases, respectively. The sense of the apparent deformations, prolate vs. oblate, is given by the strength ratio S_2/S_1 of the two components; however this quantity is in general difficult to determine since the two components are not resolved. The present fit results, based on 6 independently varied parameters, do not allow a clear determination of the sense of the deformation. In the near future, a reaction leading to a similar compound system at significantly higher spin is planned.

References:

1. Nuclear Physics Laboratory Annual Report, University of Washington (1986), p. 12.
2. B.L. Berman, S.C. Fultz, Rev. Mod. Phys. 47, 713, (1975).

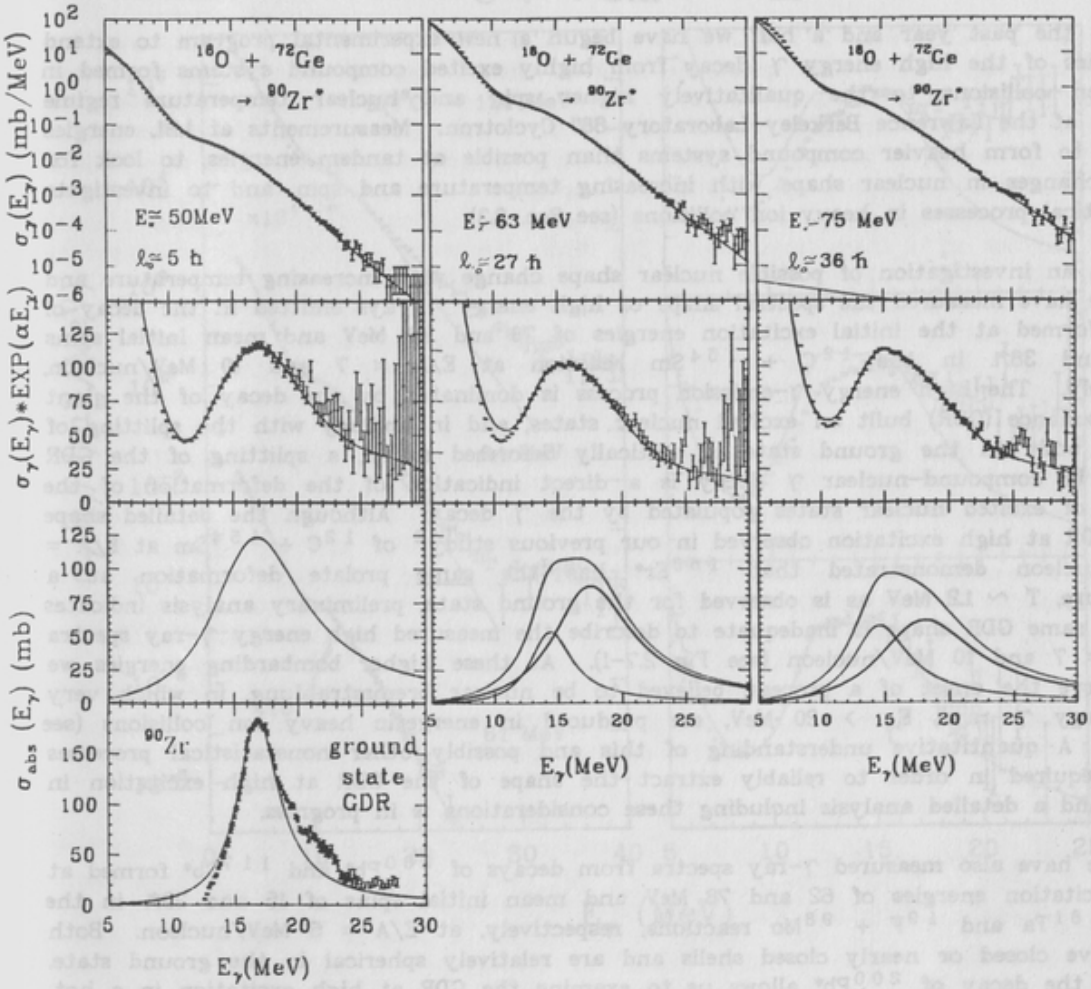

Fig. 2.6-1 Spectra from decays of $^{90}Zr^*$ formed at E_x = 50, 63, and 75 MeV, and ℓ_0 = 5, 27, 36 ħ, respectively. Top panel: the measured spectrum and the best-fit CASCADE calculations. Second panel: measured and calculated spectra multiplied by $\exp(\alpha E_\gamma)$ with α^{-1}=1.7, 2.0, and 2.2 MeV respectively. Third panel: fit GDR shape. Bottom left panel: ^{90}Zr g.s.-GDR.

******

2.7 Search for Nuclear Shape Changes at Elevated Temperature

J.A. Behr, C.A. Gossett, J.H. Gundlach, K.T. Lesko,* E.B. Norman,* and K.A. Snover

In the past year and a half we have begun a new experimental program to extend our studies of the high energy γ decay from highly excited compound systems formed in heavy ion collisions to the qualitatively higher spin and nuclear temperature regime accessible at the Lawrence Berkeley Laboratory 88" Cyclotron. Measurements at LBL energies allow us to form heavier compound systems than possible at tandem energies, to look for possible changes in nuclear shape with increasing temperature and spin, and to investigate nonstatistical processes in heavy ion collisions (see Sec. 3.3).

In an investigation of possible nuclear shape change with increasing temperature and spin,[1] we have measured the spectral shape of high energy γ rays emitted in the decay of $^{166}Er^*$ formed at the initial excitation energies of 70 and 105 MeV and mean initial spins of 26 and 38$\hbar$ in the $^{12}C + ^{154}Sm$ reaction at E/A = 7 and 10 MeV/nucleon, respectively. The high energy γ-emission process is dominated by the decay of the giant dipole resonance (GDR) built on excited nuclear states, and in analogy with the splitting of the GDR built on the ground state in statically deformed nuclei, a splitting of the GDR observed in compound-nuclear γ decay is a direct indication of the deformation of the ensemble of excited nuclear states populated by the γ decay. Although the detailed shape of the GDR at high excitation observed in our previous study[2] of $^{12}C + ^{154}Sm$ at E/A = 5 MeV/nucleon demonstrated that $^{166}Er^*$ has the same prolate deformation at a temperature, T $\sim$ 1.2 MeV as is observed for the ground state, preliminary analysis indicates that the same GDR shape is inadequate to describe the measured high energy γ-ray spectra at E/A = 7 and 10 MeV/nucleon (see Fig. 2.7-1). At these higher bombarding energies we also observe the onset of a process, believed to be nuclear bremsstrahlung, in which very high energy γ rays, E_γ > 20 MeV, are produced in energetic heavy ion collisions (see Sec. 3.3). A quantitative understanding of this and possibly other nonstatistical processes will be required in order to reliably extract the shape of the GDR at high excitation in $^{166}Er^*$ and a detailed analysis including these considerations is in progress.

We have also measured γ-ray spectra from decays of $^{200}Pb^*$ and $^{117}Sb^*$ formed at initial excitation energies of 62 and 78 MeV and mean initial spins of 15 and 29$\hbar$ in the $^{19}F + ^{181}Ta$ and $^{19}F + ^{98}Mo$ reactions, respectively, at E/A = 5 MeV/nucleon. Both nuclei have closed or nearly closed shells and are relatively spherical in the ground state. Study of the decay of $^{200}Pb^*$ allows us to examine the GDR at high excitation in a hot, spherical nucleus much heavier than previously studied, while the study of the decay of $^{117}Sb^*$ provides information on the properties of the GDR at high spin in a moderate mass nucleus. Preliminary analysis indicates that the measured γ-decay spectral shapes are reasonably well reproduced by a single-component Lorentzian shape for the GDR at high excitation, suggesting that the average shapes of $^{200}Pb^*$ and $^{117}Sb^*$ are not strongly deformed at the finite temperatures and spins studied in this work.

References:

* Lawrence Berkeley Laboratory, Berkeley, CA 94720.

1. J.J. Gaardhoje, et. al., Phys. Rev. Lett. 53, 148 (1984).
2. C.A. Gossett, et. al., Phys. Rev. Lett. 54, 1486 (1985).

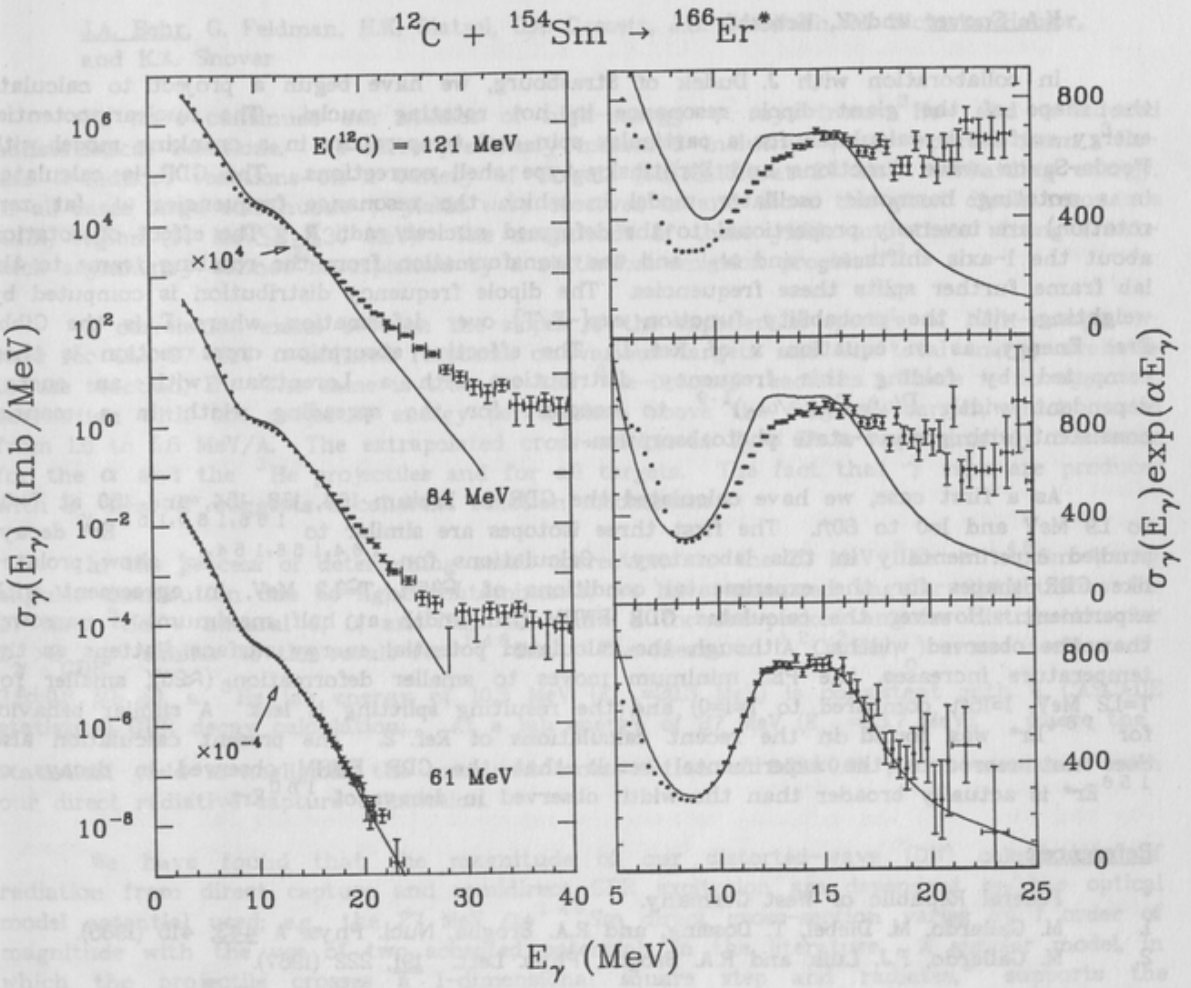

Fig. 2.7–1 Left: Measured continuum γ–ray spectra from decays of $^{166}Er^*$ formed in the $^{12}C + {}^{154}Sm$ reaction at E(^{12}C) = 84 and 121 MeV at the LBL 88″ Cyclotron along with previous measurements at 61 MeV (Ref. 2). Solid curves are calculations using fixed GDR parameters from the best fit to the high energy spectrum shape at 61 MeV in which the GDR shape at T $\sim$ 1.2 MeV indicates the same prolate deformation as in the ground state. Above $E_\gamma \approx 20$ MeV the spectra at 84 and 121 MeV exhibit the onset of nuclear bremsstrahlung. Detailed analysis of the spectra at 84 and 121 MeV including contributions from statistical and nonstatistical processes is in progress. Right: Data and calculations from the left rescaled by $\exp(\alpha E_\gamma)$ for better visual comparision. Values of α^{-1} = 2.05, 1.75 and 1.45 MeV were chosen in order that the resulting shapes for the rescaled spectra at 121, 84 and 61 MeV, respectively, roughly reproduce the shape of the GDR input into the calculation.

******

2.8 GDR Shape Calculations in Hot Nuclei

K.A. Snover and K. Weber*

In collaboration with J. Dudek of Strasbourg, we have begun a project to calculate the shape of the giant dipole resonance in hot rotating nuclei. The nuclear potential energy surface is calculated for a particular spin and temperature in a cranking model with Woods-Saxon wave functions and Strutinsky-type shell corrections. The GDR is calculated in a rotating harmonic oscillator model in which the resonance frequencies ω_i (at zero rotation) are inversely proportional to the deformed nuclear radii R_i. The effect of rotation about the 1-axis shifts ω_2 and ω_3, and the transformation from the rotating frame to the lab frame further splits these frequencies. The dipole frequency distribution is computed by weighting with the probability function exp[-F/T] over deformation, where F is the Gibbs Free Energy, as in equation x of Ref. 1. The effective absorption cross section is then computed by folding this frequency distribution with a Lorentzian with an energy dependent width $\Gamma(\omega)=\Gamma_0(\omega/\omega_0)^{1.9}$ to account for the spreading width in a manner consistent with ground-state photoabsorption.

As a first case, we have calculated the GDR in Erbium 164, 158, 154, and 150 at T=0.1 to 1.9 MeV and I=0 to 60$\hbar$. The first three isotopes are similar to ^{166,160,156}Er* decays studied experimentally in this laboratory. Calculations for ^{164,158,154}Er* show prolate-like GDR shapes for the experimental conditions of I$\cong$15$\hbar$, T$\cong$1.2 MeV, in agreement with experiment. However the calculated GDR FWHM (full width at half maximum) is narrower than the observed widths. Although the calculated potential energy surface flattens as the temperature increases, the PES minimum moves to smaller deformation ($\approx$20% smaller for T=1.2 MeV, I=15$\hbar$ compared to T=I=0) and the resulting splitting is less. A similar behavior for ^{164}Er* was found in the recent calculations of Ref. 2. The present calculation also does not reproduce the experimental result that the GDR FWHM observed in decays of ^{156}Er* is actually broader than the width observed in decays of ^{160}Er*.

References:

* Federal Republic of West Germany.

1. M. Gallardo, M. Diebel, T. Dossing, and R.A. Broglia, Nucl. Phys. A 443, 415 (1985).
2. M. Gallardo, F.J. Luis, and R.A. Broglia, Phys. Lett. 191, 222 (1987).

******

2.9 High-Energy γ Rays from ^{3}He- and α-Induced Nonstatistical Reactions

J.A. Behr, G. Feldman, H.K. Glatzel, C.A. Gossett, J.H. Gundlach, M. Kicinska-Habior, and K.A. Snover

We have continued our studies of high-energy γ rays from ^{3}He- and α-induced nonstatistical reactions. We have previously measured inclusive γ-ray spectra from ^{3}He- and α-induced reactions on a variety of targets ($61 \leq A \leq 181$) at 27 MeV bombarding energy. In all cases large continuous γ yields were observed in and above the giant dipole resonance (GDR) region (14 MeV$\leq E_\gamma \leq$30 MeV). The magnitude of these yields and their strong front-back asymmetry cannot be explained by a statistical emission process.[1,2]

A correlation exists between the slopes of the exponential spectra of high-energy γ-rays for the 27 MeV α-induced reactions on various targets and the total energy available in the reaction, E*. The same is true for the ^{3}He-induced reactions. There is no apparent correlation with the projectile energy per nucleon above the Coulomb barrier, which varies from 1.6 to 5.6 MeV/A. The extrapolated cross-section at $E_\gamma \approx E^*$ is approximately the same for the α and the ^{3}He projectiles and for all targets. The fact that γ rays are produced with E_γ near E* suggests a coherent reaction mechanism.

In the process of determining small corrections to the 27 MeV ^{3}He + ^{148}Sm γ-ray angular distribution due to light contaminants, we have measured angular distributions for 27 MeV ^{3}He + natural C, O, and Ta. All show a forward-peaked angular distribution for $E_\gamma > E_{GDR}$, similar to the result for ^{148}Sm. The measured ^{12}C(^{3}He,γ_o) cross section of 3.5±0.8 μb at a ^{3}He lab energy of 10.3 MeV ($E_{\gamma o}$=20.3 MeV) is consistent with a CASCADE statistical GDR decay calculation: At a lab energy of 27 MeV ($E_{\gamma o}$=33.7 MeV), where the statistical yield is negligible, the measured cross section of 0.20±0.07 μb is consistent with our direct radiative capture calculation.

We have found that the magnitude of our distorted-wave (DW) calculations of radiation from direct capture and semidirect GDR excitation are dependent on the optical model potential used; e.g., the 27 MeV α+^{148}Sm direct cross-section varies by 1 order of magnitude with the use of two accepted potentials in the literature. A simpler model, in which the projectile crosses a 1-dimensional square step and radiates,[3] supports the observation that while the magnitude of direct radiative capture can account for the experimental cross-sections at E_γ near E*, some other process is needed to account for the larger experimental yield at lower E_γ and for the exponential spectrum shape. Our DW direct calculations show that E2 radiation as well as E1 is important; this is consistent with an apparent lack of correlation of $\sigma(E_\gamma \approx E^*)$ with the E1 effective charge, which for ^{4}He depends more strongly on the target Z and A than for ^{3}He.

References:

1. K.A. Snover, Ann. Rev. Nucl. Part. Sci., 36, 597 (1986).
2. Nuclear Physics Laboratory Annual Report, University of Washington (1986) p. 17.
3. K. Nakayama and G.F. Bertsch, Phys. Rev. C 34, 2190 (1986).

3. HEAVY IONS

3.1 Light-particle Multiplicity Accompanying Projectile Breakup at 20 MeV/A

T.C. Awes,* R.C. Connolly, S. Gil, D.D. Leach, S. Sorensen,† R. Vandenbosch, and C.L. Wu†

We have continued our study of projectile breakup reactions at 20 MeV/A. In previous experiments[1,2] we have demonstrated that projectile breakup into fragments of approximately 1/2 the projectile charge is due to a sequential decay rather than to prompt fragmentation as assumed by previous workers. The first study of coincident fragments with Z between 3 and 8 revealed energy-energy correlations which could only be understood if the projectile breakup occurred outside the range of the Coulomb field of the target-like reaction partner. A second more detailed study showed that the relative energy spectra of these breakup events were consistent with statistical model expectations for decay of excited nuclei. One puzzle that remained after these studies was the fact that the most probable sum of the nuclear charges of the observed coincident events was appreciably less than that of the projectile ^{35}Cl. This could arise from transfer of protons from the projectile to the target at an early stage of the collision, or it could result from either (or both) pre-equilibrium emission of protons and alphas or to additional proton or alpha evaporation from the projectile-like or final fragments.

The most recent experiment was designed to distinguish between these possibilities by determining the number of protons and alpha particles accompanying events in which two heavier coincident fragments were emitted. We constructed an array of plastic phoswich detectors to detect protons and alphas. By moving these detectors to suitable places we were able in four configurations to cover the full solid angle between ±45 degrees in the reaction plane and ±20 degrees out of the reaction plane. The reaction plane was defined by the beam and the midpoint between the semiconductor telescopes for detection of the projectile breakup fragments. The telescopes were centered at ±7.5 degrees with respect to this plane with the midpoint at 11 degrees with respect to the beam. We analyzed coincident events in which both fragments fell in the Z range between 4 and 8.

The angular distributions of coincident protons and alpha particles are shown Fig. 3.1-1. They exhibit Gaussian distributions which are centered approximately on the beam direction on the opposite side of the beam from the telescopes. These observations are consistent with the majority of the protons and alpha particles being emitted at an early stage of the reaction, rather than by sequential decay of projectile-like fragments or their breakup products. The energy spectra exhibited a lot of high energy particles, with the proton spectra in particular having a considerable number of particles with velocities greater than the beam velocity.

A lower limit to the nuclear charge carried off by the light charged particles accompanying projectile breakup can be obtained by integrating the yields of particles with $Z \geq 1$ and $Z \geq 2$ observed in the phoswich detectors and integrating over all angles, using the Gaussian fits shown in the figure to extrapolate to larger angles. This yields an average charge carried away by the accompanying light particles of Z=3.4. When this is added to the average total charge of the triggering coincident breakup fragments of Z=12.5, one obtains a total charge of Z=15.9, which is rather close to the projectile charge (Z=17). Thus we conclude that most of the charge not appearing in the breakup fragments is lost to accompanying light charged particles rather than transferred to the target nucleus.

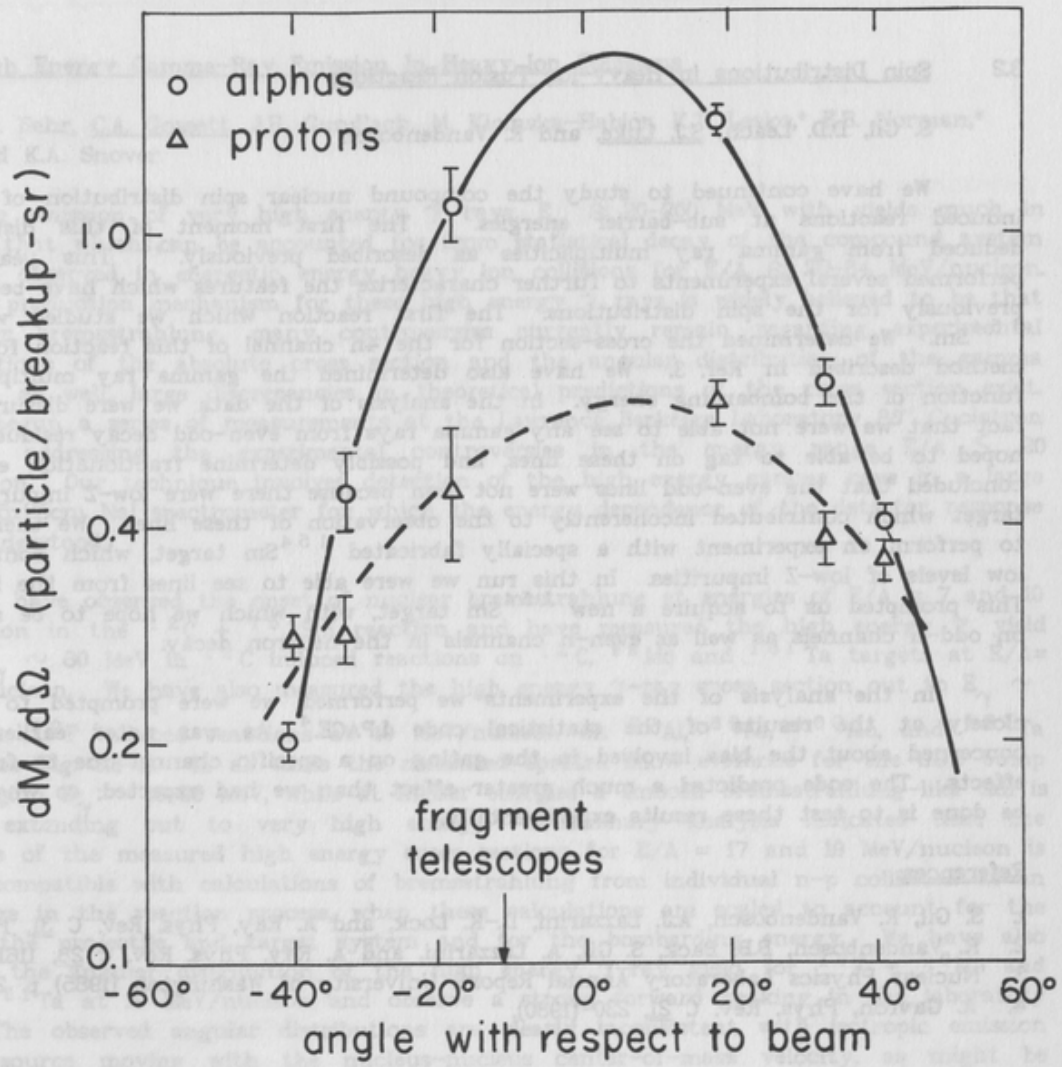

Fig. 3.1–1. Angular distributions of alpha particles and protons (with respect to the beam direction) for 20 MeV/A ^{35}Cl on ^{181}Ta. Only statistical contributions to the errors are shown. The full curves are Gaussian fits to the data.

References:

* Oak Ridge National Laboratory, Oak Ridge, TN 37831.

† University of Tennessee, Knoxville, TN 37996.

1. M.J. Murphy, S. Gil, M.N. Harakeh, A. Ray, A.G. Seamster, R. Vandenbosch, and T.C. Awes, Phys. Rev. Lett. 53, 1543 (1984).
2. M.J. Murphy, D.D. Leach, A. Ray, A.G. Seamster, and R. Vandenbosch, Phys. Rev. C 33, 165 (1986).

******

3.2 Spin Distributions in Heavy-Ion Fusion Reactions

S. Gil, D.D. Leach, S.J. Luke, and R. Vandenbosch

We have continued to study the compound nuclear spin distribution of heavy ion induced reactions at sub-barrier energies.[1] The first moment of this distribution is deduced from gamma ray multiplicities as described previously.[1,2] This year we have performed several experiments to further characterize the features which have been observed previously for the spin distributions. The first reaction which we studied was ^{18}O + ^{154}Sm. We determined the cross-section for the 4n channel of this reaction following the method described in Ref. 3. We have also determined the gamma ray multiplicity as a function of the bombarding energy. In the analysis of the data we were disturbed by the fact that we were not able to see any gamma rays from even-odd decay residues. We had hoped to be able to tag on these lines, and possibly determine fractionation effects.[3] We concluded that the even-odd lines were not seen because there were low-Z impurities in the target which contributed incoherently to the observation of these lines. We then proceeded to perform an experiment with a specially fabricated ^{154}Sm target, which contained very low levels of low-Z impurities. In this run we were able to see lines from the 5n channel. This prompted us to acquire a new ^{154}Sm target, with which we hope to be able to tag on odd-n channels as well as even-n channels in the neutron decay.

In the analysis of the experiments we performed, we were prompted to look more closely at the results of the statistical code LPACE.[4] As was noted earlier, we were concerned about the bias involved in the gating on a specific channel due to fractionation effects. The code predicted a much greater effect than we had expected; so what needs to be done is to test these results experimentally.

References:

1. S. Gil, R. Vandenbosch, A.J. Lazzarini, D.-K. Lock, and A. Ray, Phys. Rev. C 31, 1752 (1985).
2. R. Vandenbosch, B.B. Back, S. Gil, A. Lazzarini, and A. Ray, Phys. Rev. C 28, 1161 (1983).
3. Nuclear Physics Laboratory Annual Report, University of Washington (1985) p. 24.
4. A. Gavron, Phys. Rev. C 21, 230 (1980).

******

3.3 High Energy Gamma-Ray Emission In Heavy Ion Collisions

J.A. Behr, C.A. Gossett, J.H. Gundlach, M. Kicinska-Habior, K.T. Lesko,* E.B. Norman,* and K.A. Snover

The emission of very high energy γ rays, $E_\gamma \approx 20$–200 MeV with yields much in excess of that which can be accounted for from statistical decay of the compound system have been observed in energetic energy heavy ion collisions for E/A $\approx$ 20–84 MeV/nucleon. While the production mechanism for these high energy γ rays is widely believed to be that of nuclear bremsstrahlung, many controversies currently remain regarding experimental determinations of the absolute cross section and the angular distribution of the gamma yield, and as well, large discrepancies in theoretical predictions of the cross section exist. We have begun a series of measurements at the Lawrence Berkeley Laboratory 88" Cyclotron aimed at addressing the experimental controversies in the energy range E/A $\leq$ 20 MeV/nucleon. Our technique involves detection of the high energy gamma rays in a large shielded 25x25cm NaI spectrometer for which the energy dependence of the detector response is well understood.

We have observed the onset of nuclear bremsstrahlung at energies of E/A = 7 and 10 MeV/nucleon in the $^{12}C + {}^{154}Sm$ reaction and have measured the high energy γ yield out to $E_\gamma \sim 60$ MeV in ^{12}C induced reactions on ^{12}C, ^{98}Mo and ^{181}Ta targets at E/A= 17 MeV/nucleon. We have also measured the high energy γ-ray cross section out to $E_\gamma \sim$ 80 MeV in ^{19}F induced reactions at 19 MeV/nucleon on ^{27}Al, ^{60}Ni, ^{100}Mo, and ^{181}Ta targets (see Fig. 3.3-1). In all cases the measured spectra show evidence for the GDR bump in the region $E_\gamma \sim 10$–20 MeV, while at higher energies a smooth bremsstrahlung-like tail is observed extending out to very high energy. Preliminary analysis indicates that the magnitude of the measured high energy cross sections for E/A = 17 and 19 MeV/nucleon is roughly compatible with calculations of bremsstrahlung from individual n-p collisions at an early stage in the reaction process, when these calculations are scaled to account for the mass of the projectile and target system and for the bombarding energy. We have also measured the angular distribution of the high energy γ-ray yield for $^{19}F + {}^{98}Mo$ and $^{19}F + {}^{181}Ta$ at 19 MeV/nucleon and observe a strong forward peaking in the laboratory frame. The observed angular distributions are clearly inconsistent with isotropic emission from a source moving with the nucleus-nucleus center-of-mass velocity, as might be expected for emission from a fused compound system. The data are roughly consistent with isotropic emission from a source moving with the much larger velocity of the nucleon-nucleon center-of-mass system, supporting the suggestion that the high energy γ-production mechanism is that of bremsstrahlung from energetic n-p collisions.

Reference:

* Lawrence Berkeley Laboratory, Berkeley, CA 94720.

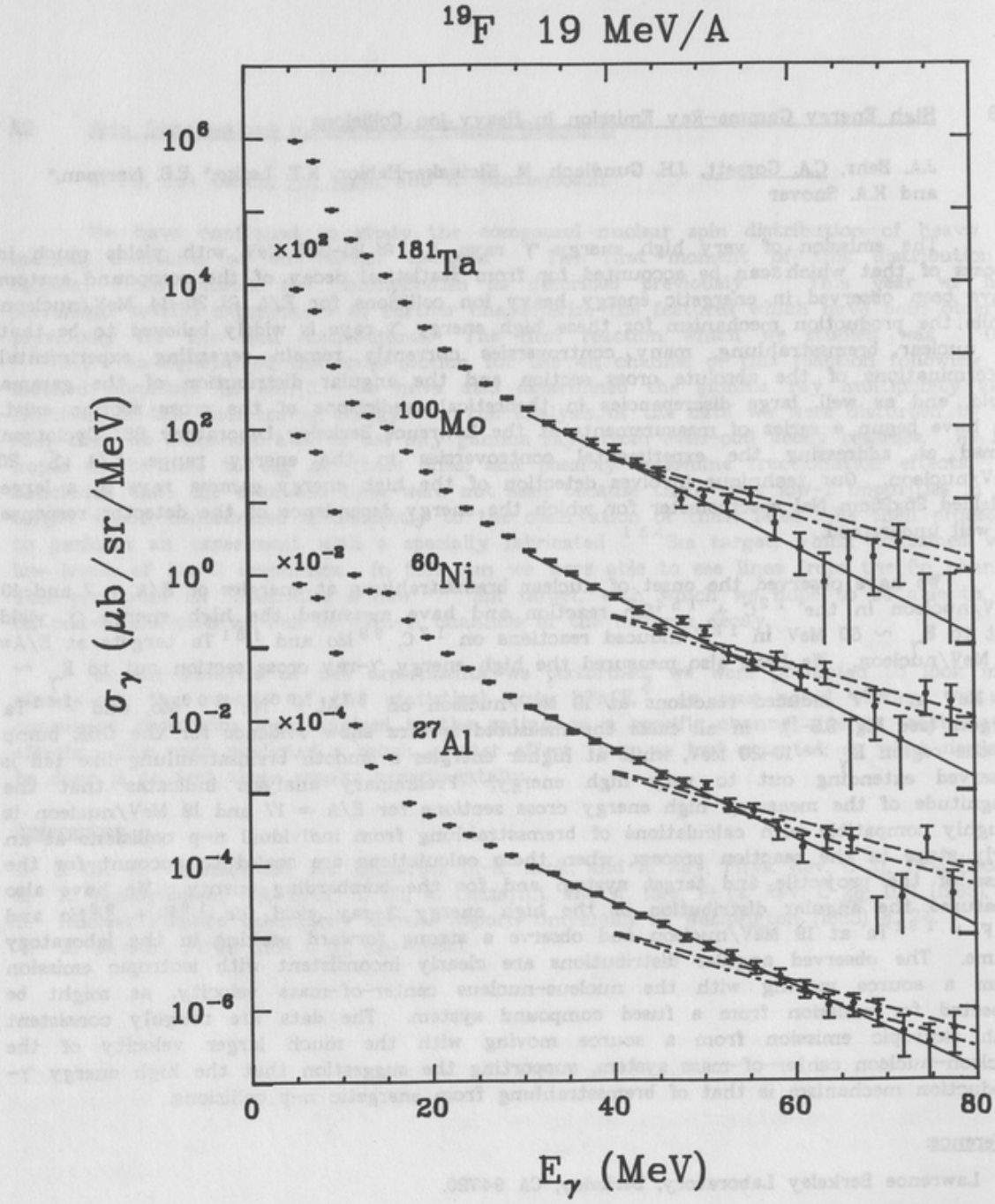

Fig. 3.3–1 High energy gamma ray spectra from 19 MeV/nucleon ^{19}F induced reactions on ^{27}Al, ^{60}Ni, ^{100}Mo, and ^{181}Ta targets at Θ(lab) = 90°. Dashed and dash–dotted curves are nuclear bremsstrahlung calculations (W. Cassing, private communication) using quantal phase space model and Boltzmann–Uehling–Uhlenbeck approaches respectively, for gamma–ray emission in ^{40}Ar + ^{40}Ca collisions at 20 MeV/nucleon and have been scaled approximately for the mass of the target and projectile systems in the present work. The solid curves are fits to the measured spectra assuming an exponential form for the energy dependence of the high energy gamma–ray cross section.

3.4 Heavy Ion Elastic Scattering at 25–50 MeV/Nucleon

J.G. Cramer, S. Gil, D.D. Leach, B. McLain, and L.T. Nirider

This work was done using the K–500 Cyclotron of the National Superconducting Cyclotron Laboratory of Michigan State University. In January of this year we used beams of ^{12}C ions at energies of 25, 35, and 50 Mev/nucleon to bombard targets of ^{12}C, ^{40}Ca, ^{90}Zr, and ^{208}Pb. The elastic scattering differential cross sections were measured using the S–320 magnetic spectrometer out to angles corresponding to about 10^{-3} of the Rutherford cross section. This provided new information on elastic scattering in this energy region. Optical model fits to these data (now being analysed) will provide optical potentials of interest for reaction studies and investigations of nuclear dynamics. Such fits will also determine the scattering S–matrix well enough to provide determination of the total reaction cross sections to about 5%.

Total reaction cross sections are of interest because a very simple and naive model, the optical limit of Glauber theory (usually referred to as "the Glauber model") has up to now shown remarkable and unexpected predictivity for such cross sections. The model, with no free parameters and using only electron scattering charge distributions, Hartree–Fock matter distributions, and measured nucleon–nucleon total cross sections (all from the literature), has been shown to reproduce with remarkable accuracy all measured nucleus–nucleus total reaction cross sections for both light and heavy ion systems on a variety of targets at all energies from 5 to 200 MeV/nucleon. The agreement between the experimental data and these naive Glauber model calculations is quite remarkable, particularly considering the large target mass range spanned and the parameter–free character of the calculations.

The success of this naive model over such a broad range of systems and energies is quite remarkable, since the model's simplicity is achieved by neglecting a number of physical effects that are expected to be important in nuclear reactions (for example, the nuclear strong–interaction potential). It is therefore of considerable interest to test stringently the limits of this broad predictivity to gain clues to the origins of the model's unexpected success. We plan to do this when the booster is operational with more fragile projectiles (e.g., ^{7}Li) and with more deformed nuclei than have previously been studied.

It is also worth noting in the present context that more sophisticated models of nuclear dynamics, for example intranuclear cascade models, have thus far done rather poorly in reproducing these same measured total reaction cross sections. This is surprising because such models contain far more "understanding" of nuclear dynamics, and they have done rather well in predicting the characteristics of far more complicated processes. We suggest that within the dynamical region where the Glauber model has been shown to predict accurately reaction cross sections it should in the future be used as a benchmark against which to test other models of nuclear dynamics, and it should also be used as a constraint on optical potentials used in nuclear reaction studies.

Another aspect of the elastic scattering data from these measurements is that they show evidence of the failure of the M3Y double–folding model which has been quite successful in generating the real part of the nuclear potential for heavy ion scattering at lower energies. The new data at higher energies and larger angles will provide new information for investigating possible improvements to the folding model in this region.

4. FUNDAMENTAL SYMMETRIES

4.1 0^+-0^- Isoscalar Parity Mixing in ^{14}N

E.G. Adelberger, C.A. Gossett, W. Haeberli,* P.A. Quin,* J. Sromicki,*+ H.E. Swanson, and V.J. Zeps

We are studying the isoscalar parity mixing of the 0^+-0^-;T=1 doublet in ^{14}N ($E_x \approx 8.6$ MeV) by measuring the longitudinal analyzing power (A_L) over the narrow $^{13}C+\vec{p}$ $J^\pi=0^+$ resonance (E_p=1.16 MeV) using the polarized proton beam at the University of Wisconsin EN tandem facility. The motivation, apparatus and data collection system have been describe previously.[1,2] With the DDH "best value" parity non-conserving (PNC) NN interaction and Wick Haxton's nuclear matrix element, we expect[1] a maximum PNC signal $A_L(\theta_2)-A_L(\theta_1) = -28 \times 10^{-6}$, where $\theta_1=35^\circ$ and $\theta_2=155^\circ$ are the mean angles of our detector.

The symmetry of our apparatus and the effectiveness of our beam position, angle and spin stabilization systems reduce the false asymmetries from many sources to a level of $\lesssim 1 \times 10^{-6}$. We remain sensitive to residual transverse polarization distributions in position ($\langle \epsilon \times \vec{P} \rangle_z$) and angle ($\langle \vec{\alpha} \cdot \vec{P} \rangle$) of the beam on target and a possible energy difference (ΔE) of the beam for the two spin states. The measured detector sensitivity to these quantities agrees well with our expectation (Fig. 4.1-1). We have also measured "worst case" moments of $\langle \epsilon \times \vec{P} \rangle_z \leq 4\mu$m and $\langle \vec{\alpha} \cdot \vec{P} \rangle \leq 15\mu$rad, and have improved the energy modulation limit set in Ref. 2 to $\Delta E < 0.7$ eV, using the narrow ^{27}Al(p,p) resonances at E_p=1.38 MeV. At the energy of the maximum PNC signal, our sensitivity to these beam attributes yields a false asymmetry of $\approx 15 \times 10^{-6}$, which is >50% of the expected PNC effect! Fortunately, a "magic" energy exists, where our sensitivity to these effects nearly vanishes, while the PNC signal is reduced by only 15%. We have taken two 1-week data runs at E(magic). We stabilize the beam energy to ±150 eV over the course of a 1-week run, by periodically precessing the spin 30° away from longitudinal and using the measured transverse analyzing power, $A_t(\theta_2)$ to correct the energy. After accounting for the 0.86 beam polarization and ~5.5% ^{12}C contaminant in the target, we obtain $A_L(\theta_2)-A_L(\theta_1)$ = $8.5 \pm 7.6(2.8) \times 10^{-6}$ (Fig. 4.1-2). The instrumental uncertainty is derived from the "worst case" measured beam attributes and known detector sensitivities at E(magic) ±150 eV. This PNC asymmetry corresponds to $\langle H_{weak} \rangle$ = +0.36±0.35 eV (see Sec. 4.2 for definition), inconsistent with Haxton's prediction[1] of -1.04 eV.

We plan to take one more data run at the University of Wisconsin, after which reduction of the statistical error, still the dominant uncertainty, would be difficult. The experiment will then be brought back to the University of Washington, where, with a higher expected polarized beam intensity, we should reach the systematic uncertainty limit.

References:

* University of Wisconsin, Madison, WI 53706.

\+ Present address: Jagiellonian Univ., Krakow, Poland.

1. E.G. Adelberger, et al., Phys. Rev. C 20, 2 (1984); E.G. Adelberger, et al., Phys. Rev. C 33, 5 (1986).
2. Nuclear Physics Laboratory Annual Report, University of Washington (1986) p. 29; ibid. (1985) p. 36; ibid. (1984) p. 36; ibid. (1983) p. 32.
3. J. Sromicki, et al., Nucl. Instrum. Meth. in Phys. Res. A255, 3 (1987) p. 611.

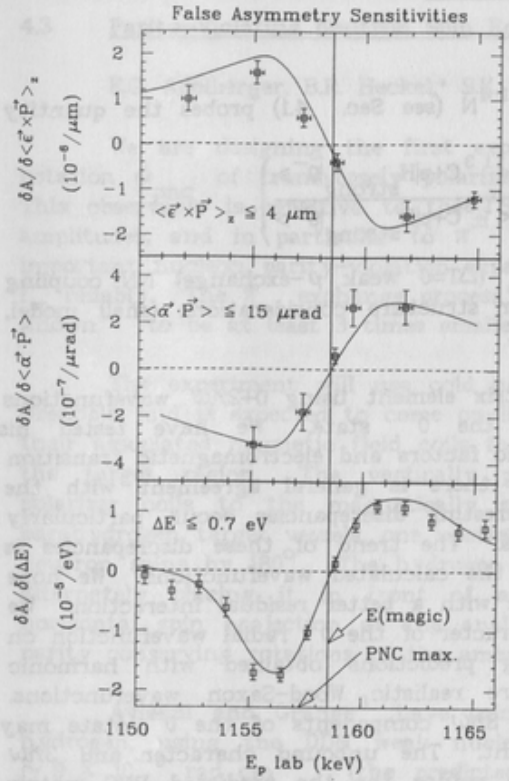

Fig. 4.1–1 The sensitivities to the three dominant sources of systematic error are plotted vs. energy, where $A=A_L(\theta_2)-A_L(\theta_1)$. "Worst case" limits for these beam attributes are also shown.

Panels 1 & 2–$\langle\vec{\epsilon}\times\vec{P}\rangle_z$ and $\langle\vec{\alpha}\cdot\vec{P}\rangle$ sensitivities. The finite beam size (angle spread) coupled with a position (angle) dependent residual transverse polarization and a non–zero transverse analyzing power (A_T) in the reaction produces a false asymmetry. We determined the detector response by measuring the position (angle) dependence of the countrates with a transversely polarized beam. The sensitivities roughly track $A_T(\theta_2)$, as expected. The solid lines are predicted sensitivities obtained by numerically integrating the cross–section over beam emittance, detector solid angle and target thickness.

Panel 3–Energy modulation sensitivity (ΔE). This arises from a difference in the energy dependence of the cross–sections for the two angles. The ΔE sensitivity was measured by modulating the target bias by ±100V. The solid line is simply $\delta\ln(\theta_2/\theta_1)/\delta E$, where θ_2/θ_1 is the countrate ratio for the two detector angles.

The good agreement between the calculations and measured values demonstrates our understanding of the detector response.

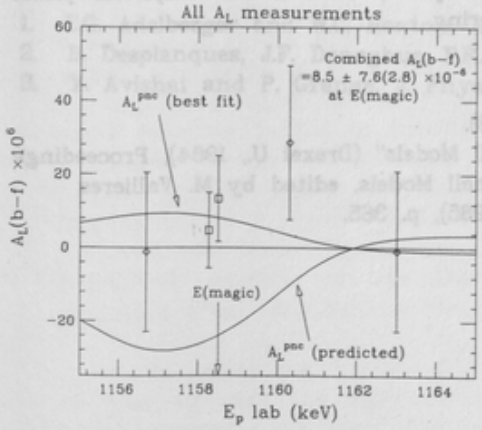

Fig. 4.1–2 All A_L measurements (with 1σ statistical error bars) are plotted vs. energy, along with the predicted and "best fit" A_L curves. We expect systematic effects as large as $\sim15\times10^{-6}$ for the three data points (diamond) not at E(magic). A_L^{pnc} (best fit) was determined from the two points at E(magic). Inclusion of the other data in the analysis, however, does not significantly alter our result.

******

4.2 Interpretation of the Parity Violating Effect in ^{14}N

E.G. Adelberger, W.C. Haxton, and V.J. Zeps

The experimental parity violating effect in ^{14}N (see Sec. 4.1) probes the quantity $\langle H_{weak} \rangle$, where

$$\langle H_{weak} \rangle \equiv \langle 0^- | H_{pnc} | 0^+ \rangle \times \text{sign} \left(\frac{\langle ^{13}C+p | H_{strong} | 0^- \rangle}{\langle ^{13}C+p | H_{strong} | 0^+ \rangle} \right).$$

Before we can extract a reliable value for the f°_{ρ} ($\Delta T=0$ weak ρ-exchange) NN coupling constant we must have confidence in the nuclear structure considerations (shell model, scattering theory) used to predict the PNC effect.

Haxton has computed the weak nuclear matrix element using $0+2\hbar\omega$ wavefunctions for the 0^+ state and $1\hbar\omega$ wavefunctions for the 0^- state. We have tested his wavefunctions by using them to predict spectroscopic factors and electromagnetic transition rates for all states with $E_x < 10.5$ MeV. While there is general agreement with the experimental values for these quantities, some interesting discrepancies occur, particularly for transitions from the predominantly $2\hbar\omega$ states. The trend of these discrepancies is symptomatic of too much configuration mixing in the calculated wavefunctions. We hope to remedy this by doing the shell model calculation with a better residual interaction. We are also investigating the effect of the unbound character of the 0^- radial wavefunction on the predicted PNC matrix element by comparing predictions obtained with harmonic oscillator wavefunctions to those made with more realistic Wood-Saxon wavefunctions. Because the 0^+ level is mostly $2\hbar\omega$, the neglected $3\hbar\omega$ components of the 0^- state may play an important role in the PNC matrix element. The unbound character and $3\hbar\omega$ components of the 0^- state are both expected to reduce the the predicted PNC matrix element. Such effects are well known[1,2], e.g.- in the calculation of the weak matrix element in ^{18}F, inclusion of the $2\hbar\omega$ components of the predominantly $0\hbar\omega$ $0^+;1$ state reduces the predicted weak matrix element by a factor of three.

While we have found that the Breit-Wigner scattering formalism describes most of the $^{13}C(\vec{p},p)$ and $^{13}C(p,\gamma)$ cross-sections very well, it slightly overpredicts the back angle elastic scattering cross-section from the broad 0^- level, consequently we are investigating accuracy of the scattering theory applied to this broad resonance. If treating the resonances as poles in the S-matrix proves to be inadequate, we will use empirical phase shifts to determine the PNC effect in the elastic scattering.

References:

1. E.G. Adelberger, et al., Phys. Rev. C 27, 2833 (1983).
2. D.J. Millener and E.K. Warburton, in "Nuclear Shell Models" (Drexel U., 1984), Proceedings from the International Symposium on Nuclear Shell Models, edited by M. Vallieres and B.H. Wildenthal (World Scientific, Singapore, 1985), p. 365.

******

4.3 Parity-Violating Neutron Spin Rotation in Parahydrogen

E.G. Adelberger, B.R. Heckel,* S.K. Lamoreaux, W.F. Rogers, and H.E. Swanson

We are designing the first experiment to measure the parity non-conserving spin rotation ϕ_{pnc} of transversely polarized neutrons propagating through liquid parahydrogen. This observable is sensitive to the $^3S_1 - {}^1P_1$, $^3S_1 - {}^3P_1$, and $^1S_0 - {}^3P_0$ transition amplitudes, and in particular to $\pi^\pm$ exchange contribution. We believe this is the most important nucleon parity-violation experiment, because it provides the best way to measure f_π reliably. The $\pi^\pm$ exchange process is quite sensitive to the neutral weak current. It is known[1] to be at least 3 times smaller than the DDH predictions.[2]

The experiment will use cold neutrons (energies < 2 meV) from the ILL reactor in Grenoble, and is expected to come on-line in early to mid 1988. Two neutron polarizers and their associated magnetic field coils form a crossed polarizer-analyzer pair which surrounds the target region. The vertically polarized neutrons pass non-adiabatically from the polarizer coils to the magnetically shielded low-field region which contains two liquid parahydrogen target vessels, one upstream and one downstream from a π-coil which rotates neutron spins by 180°. The hydrogen is periodically pumped from one vessel to the other, alternately placing it in front of and behind the π-coil. This changes the neutron horizontal spin projection at the analyzer, which helps to distinguish pnc rotations from parity conserving rotations in the ambient B field.

Avishai and Grange[3] have calculated ϕ_{pnc} for neutron-proton scattering in liquid hydrogen, using the DDH weak nucleon-nucleon interaction[2] and have found it to be $\sim 9 \times 10^{-9}$ rad cm^{-1} (the predicted transmission asymmetry of longitudinally polarized neutrons is so tiny that A_L experiments are impractical). Given the polarized neutron flux available at ILL ($\sim 5 \times 10^8$/cm^{2}sec) and our expected target size ($\sim 3 \times 3$ cm^2 area, ~ 25 cm long, 1 absorption length) we expect to achieve 4σ results in less than 30 days. Efforts are presently devoted to identifying probable systematic effects, designing and constructing the cryogenic liquid hydrogen target, and developing neutron detectors and a data aquisition system. The neutron polarimeters are already available at ILL.

References:

1. E.G. Adelberger and W.C. Haxton, Ann. Rev. Nucl. Part. Sci. 35, 501 (1985).
2. B. Desplanques, J.F. Donoghue, B.R. Holstein, Ann. of Phys. 124, 449 (1980).
3. Y. Avishai and P. Grange, J. Phys. G: Nucl. Phys. 10, 449 (1984).

******

4.4 Experimental Constraints on Intermediate-Range Composition-Dependent Interactions, Weaker than Gravity

E.G. Adelberger, J.H. Gundlach, B.R. Heckel,* K.D. McMurry, F.J. Raab,* W.F. Rogers, C.W. Stubbs,* H.E. Swanson, and R. Watanabe

Are there forces, weaker than gravity, which involve exchanged quanta with so little mass that they produce effects with macroscopic ranges? A number of speculations along this line have recently appeared. Last year Fishbach and collaborators claimed[1] that experimental evidence for such a "fifth force" was already at hand. They discovered a correlation between nuclear binding energy and differential acceleration between the various test masses reported in the original Eötvös experiment. Fishbach et.al. explained this correlation and the claimed observation by Stacey et. al. of a departure from Newtonian gravity in terms of a finite-ranged interaction 10 m $< \lambda <$ 10 km which couples to baryon number. We have tested this "fifth force" hypothesis by constructing a sensitive torsion balance. The balance is placed on a hillside at the NPL to give an enhanced sensitivity for composition-dependent forces with 1 m$<< \lambda << 10^4$ m. The balance is rotated continuously at constant ω and we search for a torque on the pendulum proportional to sinωt. We saw no evidence for "fifth force" torques on the pendulum and approximately eleven months after beginning work on this project we sent a manuscript to PRL reporting results which rule out the original "fifth force" hypothesis. The reader is referred to this publication[2] for details about our method and results. In the same issue of PRL that contained our paper Thieberger[3] reported a positive result for a Cu-H_2O accelerometer in agreement with the "fifth force" hypothesis. We have tested a scenario which could reconcile these discrepant results. In doing so we have set stringent constraints on the properties of any composition-dependent interaction which might couple to a generalized charge of the form

$$q_5 = B \cos(\theta_5) + L \sin(\theta_5),$$

where B and L refer to baryon and lepton number respectively and θ_5 is a mixing angle. If such an interaction existed with $\theta_5 = -11.1^\circ$ it would have not produced any effect in our Cu-Be detector, and given a large effect in Thieberger's Cu-H_2O accelerometer. We have tested this possibility by repeating our experiment using Aluminium and Beryllium test bodies, and find no evidence for a "new" force at essentially any value of θ_5. A paper on these results is being prepared.

References:

* Physics Department, University of Washington.

1. E. Fishbach et al., Phys. Rev. Lett., 56, 3 (1986).
2. C.W. Stubbs et al., Phys. Rev. Lett., 58, 1070 (1987).
3. P. Thieberger, Phys. Rev. Lett., 58, 1066 (1987).

******

4.5 Torsion Balance Position Readout Systems and Data Aquisition Improvements

E.G. Adelberger, R. Burton, K.D. McMurry, F.J. Raab, C.W. Stubbs, H.E. Swanson, and R. Watanabe

Independent readout systems allow us to measure the angular position of the balance in the preceding experiment, and the location of the fiber relative to the nominal center of the apparatus. From the fiber's position we obtain the instantaneous tilt of the balance. The angle readout consists of an optical lever where light from a modulated LED is reflected from a mirror on the rotating balance to a lateral effect photodiode. The asymmetry in the photocurrents from the outputs of this detector gives the centroid of the incident light spot. To minimize the effects of temperature on the measured centroid position, transconductance preamps were built using a dual FET op-amp (OPA-2111) and the photodiode detector and amplifiers were enclosed in a thick walled aluminum can with a large thermal mass. The fiber's position is also determined optically. Light from a modulated LED is incident on a slit collimator mounted at a slant in front of a dual spot photodiode. The fiber hangs between the source and the detector and casts a shadow on the slit. The relative amount of light seen by each of the two photodiodes varies as the fiber moves from side to side and the difference in the corresponding photocurrents gives a signal proportional to its displacement. Two independent assemblies are mounted orthogonally in the horizontal plane and from these we obtain the x and y components of tilt. We have recently completed a second generation of this monitor and its DC stability is excellent. With a 0.8 mil fiber, it has a sensitivity of 30 millivolts per mil and a linear range of 50 mils. We are presently working to extend this range.

Signals from the photodetectors are detected synchronously using lock-in amplifiers. For the angle readout difference signal, we have a borrowed Parc 5204 and have ordered a Parc 5208 of our own. We have also built a four channel lock-in amp around Analog Devices AD630 phase sensitive detectors. Each channel has a gain of 1000 and a two pole filter with switch selectable time constants of one and ten seconds. These are mounted in a temperature controlled box along with constant current drivers for the pulsed LED light sources. One of these channels looks at the sum of the outputs of the angle photodetector and when fed back to the corresponding LED driver holds the total light signal constant. Two additional channels are used for the x and y fiber position monitors.

An interface card was built which plugs into our IBM PC data aquisition computer. It includes a 14 bit A/D converter with a multiplexer to select 1 of 16 inputs, some digital control and sense lines, a counter/register driven by an optical shaft encoder to indicate the current position of the turntable, and a variable speed stepping motor controller. We use a stepping motor to rotate the turntable and with this interface the computer can determine the angular velocity of the table. The analog signals sampled include the outputs of the lock-in amplifiers and temperature sensors placed on the apparatus. The data aquisition program has been modified to use this interface and its reliability has been improved. We have also written a program which functions as a storage scope and gives us interactive control of the turntable's velocity. This greatly facilitates damping the pendulum after rotating the hanger to a new mirror position.

Currently our various fit and data analysis programs run on the lab's VAX780. As we plan to take the experiment to a number of remote sites, we have acquired an IBM PC/AT computer to run these programs. Most are now running and we have obtained hardcopies of the data and fits using an IBM Proprinter.

5. OTHER FUNDAMENTAL SYMMETRIES

5.1 Reconstruction of the H-atom Experiment

T.A. Trainor and P. Wong

In a previous report,[1] we described the testing and final trimming of the solenoid used to provide the 570 gauss field for the Hydrogen parity experiment. This report summarizes the testing and integration of the various systems which comprise the H-atom experiment.

The solenoid was installed in the freon container and placed on its positioning carriage. The magnetic field scans were repeated after the final installation. No significant deviation in the B-field profile was noted. A set of 3 pairs of stationary Helmholtz coils were installed to null out the earth's field. They performed acceptably by reducing the earth's field to < 1 part in 30,000 of B_z over the cavity region.

The endplate containing all of the feedthroughs was replaced by a non-magnetic stainless-steel plate. The beta-state detector assembly and feedthroughs were transferred without change, the beam dump cryopump was removed (ineffective pumping) and the beam dump mounted directly to the endplate. The NMR feedthrough was redesigned to permit non-destructive disassembly and reassembly. The rf cavities were connected to the feedthroughs and the cavity-endplate assembly installed within the solenoid. The ion pump has been restarted and provides a vacuum of 2×10^{-7} torr in the UVH chamber.

The cryopump system is being reinstalled after being contaminated by a compressor failure. The compressor has been moved into remote area $\sim$ 30 meters from the experiment because of its adverse effect on the solenoid's magnetic field.

In the NMR control system, a "parasitic resonance" due to noise injected by a switching power supply has been eliminated, and previous problems due to ground loops have not been seen. The NMR can now control the magnetic field over a wide range without going out of lock and can do it more reliably.

A simple monitor is being made to allow centering and tuning of the neutral beam using the 4-quadrant beam dump. Simple programs which will allow computer controlled DAC scans of the B-field are being developed for the initial runs which do not use the configuration expected by the Standard data acquisition programs. A new slow but reliable B-field flipping bridge will soon be built to handle the new solenoid. If the circumstances dictate, the old high performance flipping bridge will be rebuilt.

When the experiment resumes operation, the solenoid will be aligned and trimmed using scans of the resonances, and the attempt to characterize and understand stray fields will resume with a final goal of significantly reducing the upper limit on parity non-conservation in hydrogen.

Reference:

1. Nuclear Physics Laboratory Annual Report, University of Washington (1986) p. 39.

******

5.2 Trapped Antiprotons

X. Fei,* G. Gabrielse,* H. Kalinowsky,† W. Kells,+ J. Haas,† K. Helmerson,* S. Rolston,* R. Tjoelker,* and T.A. Trainor

In July, 1986 we successfully captured antiprotons in a Penning trap.[1] A cooled beam of 21 MeV antiprotons from the LEAR facility at CERN was slowed by about 3 mm of material, mostly beryllium, to maximize the yield of particles below 3 keV, as determined by an earlier run in May. Three colinear cylinders in a 6T magnetic field formed the Penning trap, with the center cylinder grounded and the ends at 3 kV. At least several hundred particles were trapped for times of order milliseconds and a significant number (5) were trapped for 10 minutes. Prospects for trapping times of hours or much longer are excellent with realizable vacuum improvements.

The immediate motivation for antiproton trapping is an improved determination of CPT invariance for hadrons by precision comparison of proton and antiproton inertial masses. In addition we can look forward to interesting atomic physics experiments with protonium and antihydrogen, especially a precision measurement of the antihydrogen gravitational mass.

We had determined in May that we could produce from a typical 200 ns LEAR pulse of 10^8 antiprotons about 10^4 antiprotons with energies below 3 keV. For the July run we replaced the time-of-flight apparatus with a Penning trap cooled to about 10 K. Particles entered the trap with the first two electrodes at ground and the last at -3 kV. About 300 ns after the pulse arrived (and the slow particles had entered the trap and turned around) the first electrode was brought down to -3 kV in about 15 ns by a specially developed krytron circuit, trapping particles less than 3 keV in energy. At some later time (the trapping time-up to 10 minutes) the last electrode was brought rapidly to ground, releasing the trapped particles to drift axially to a surface (a channel plate) where they annihilated. The annihilation pions were detected, signalling release of trapped antiprotons.

Because of a concern that the trapping efficiency might be very poor the trapped particles were released very rapidly, and the pion detectors were made very efficient to enhance signal-to-noise. In light of the observed particle numbers it is clear that the pion detectors were saturated by release of particles at short trapping times, and that the number of particles initially trapped was probably much greater than the several hundred events typically observed after milliseconds.

Having achieved trapping of antiprotons we now move on to construction of a precision trap system. The new superconducting solenoid will have a vertical bore requiring a new beam line at LEAR with a vertical 90° bend transport system. Operation will be at 5 MeV rather than 21 MeV requiring extensive redesign of the slowing foils and thin timing detector upstream of the solenoids. The lower initial energy however may permit an increase of up to 100 times in capture efficiency. The trap system will include both capture trap and precision trap in a sequence of colinear cylinders. We expect to continue operation at LEAR in early 1988.

References:

* Department of Physics, University of Washington.
† University of Mainz, Federal Republic of Germany.
+ Fermi National Accelerator Laboratory, Batavia, IL 60510.

1. "First Capture of Antiprotons in a Penning Trap: A Kiloelectronvolt Source," G. Gabrielse, X. Fei, K. Helmerson, S.L. Rolston, R. Tjoelker, T.A. Trainor, H. Kalinowsky, J. Haas, and W. Kells, Phys. Rev. Lett. 57, 2504 (1986).

6. MEDIUM ENERGY

6.1 A Feasibility Study of the ^{3}He(e,e'pp)n Reaction

P. Dreux,* B. Frois,* A. Gerard,* D. Goutte,* C.E. Hyde-Wright, J. Martino,* and S. Platchkov*

The (e,e'pp) reaction is a promising tool for the study of nucleon-nucleon correlations and the virtual photon absorption process. Such experiments are expected to be a major part of the program at future 100% duty-factor electron accelerators in the U.S. and in Europe.

In spite of the experimental difficulties in such a triple coincidence experiment at the presently available duty factor of 1.0%, this collaboration was inspired to study ^{3}He(e,e'pp), the most favorable case. The overdetermined kinematics of this reaction are expected to assist in the suppression of accidental triple coincidences relative to the true events.

In a brief (two day) run in October 1986 at Saclay a beam of 640 MeV electrons was incident on a cooled gas target. Scattered electrons were detected in the "900" spectrometer at an angle of 60 degrees and momentum 545 MeV, with an acceptance of 10% in momentum. The two protons were detected in coincidence in the "600" spectrometer at 52 degrees, each with momentum of approximately 300 MeV, within a 40% momentum acceptance. This kinematics corresponds to zero recoil momentum of the neutron. A two proton event in the "600" is identified by a coincidence between two different scintillator segments in the focal plane array.

In 16 hours of beam, approximately 1000 triple coincidence events were collected for which two distinct proton trajectories could be traced through the wire chambers of the "600". These events are mostly accidental coincidences of the type (e,p)(e,p)(e,e') uniformly distributed within the 100 ns e-p coincidence timing window and the 20 ns p-p coincidence timing window. A peak is observed in the e-p time-of-flight spectrum, indicating the presence of events of the type (e,e'p)(e,p). However, no peak is observed in either the p-p time-of-flight or (neutron) missing mass spectra.

Although we were able to verify the functioning of the acquisition hardware and software in the double proton mode, we have not been able to identify (e,e'pp) true coincidences yet. A Monte Carlo integral over the spectrometer acceptances indicates we should have a ^{3}He(e,e'pp)n counting rate of 4 counts/hr, based on the calculation of J.M. Laget.[1]

References:

* Centre d'Etudes Nucleaire, Saclay, Service de Physique Nucleaire a Haute Energie Gif-sur-Yvette, France.

1. J.M. Laget, Phys. Rev. C 35, 832 (1987).

******

6.2 Quasi-Elastic Scattering of Pions from ^{2}H, ^{3}He, and ^{4}He

I. Halpern, M. Khandaker, and D.W. Storm

Our earlier measurements of the inclusive inelastic scattering cross-sections of 100 MeV pions on ^{2}H, ^{3}He, and ^{4}He were motivated by a wish to study the interplay between quasi-elastic scattering and absorption in pion reactions with nuclei. Such studies are best done in small nuclei where the wave functions are known and final state interactions of escaping particles are minimal. This year, we have made a considerable effort to understand the accumulation of measured pion cross-sections for these three nuclei in a consistent way. Although the inelastic scattering cross-section is basically the sum of quasi-elastic scatterings from all of the individual nucleons in each nucleus, there are a number of many-body effects which differ from nucleus to nucleus and which must be taken into account in any serious interpretation of the data. These include effects of i) the momentum distribution of the target nucleons, ii) the level structure and binding energies of the nuclei, and iii) the refraction and absorption of both pions and nucleons as they travel through the nuclei.

To study these effects, a number of impulse approximation calculations and exercises were carried out. We started with fairly simple, i.e., few parameter, descriptions of the problem and introduced one major effect at a time. Our most complete calculations were DWIA calculations in which both the pion and struck nucleon waves were distorted. The assumptions and results of the various calculations are given in detail in Ref. 2. The figure below shows the general level of agreement between data and calculations in which the scattering is attributed to a single interaction with an individual target nucleon and both pion and nucleon waves are distorted. The fits are seen to be quite good both in magnitude and spectral shape. They were found to depend only weakly on the choices of pion optical-model parameters where these parameters are required to match elastic scattering data. The fact that even the low energy tails in the spectra are reasonably accounted for confirms our assumption that there is very little contribution to the observed spectra from multiple scattering. Although the absolute cross-sections at angles back of 60° are well reproduced, we found that none of our calculations was able to account for the sharp drop off in yield which we observed forward of 60°.

References:

1. Nuclear Physics Laboratory Annual Report, University of Washington (1986) p. 42.
2. M.A. Khandaker, "A Study of the Inclusive Inelastic Scattering of 100 MeV Pions from ^{2}H, ^{3}He, and ^{4}He," Ph.D. Thesis, University of Washington, 1987.

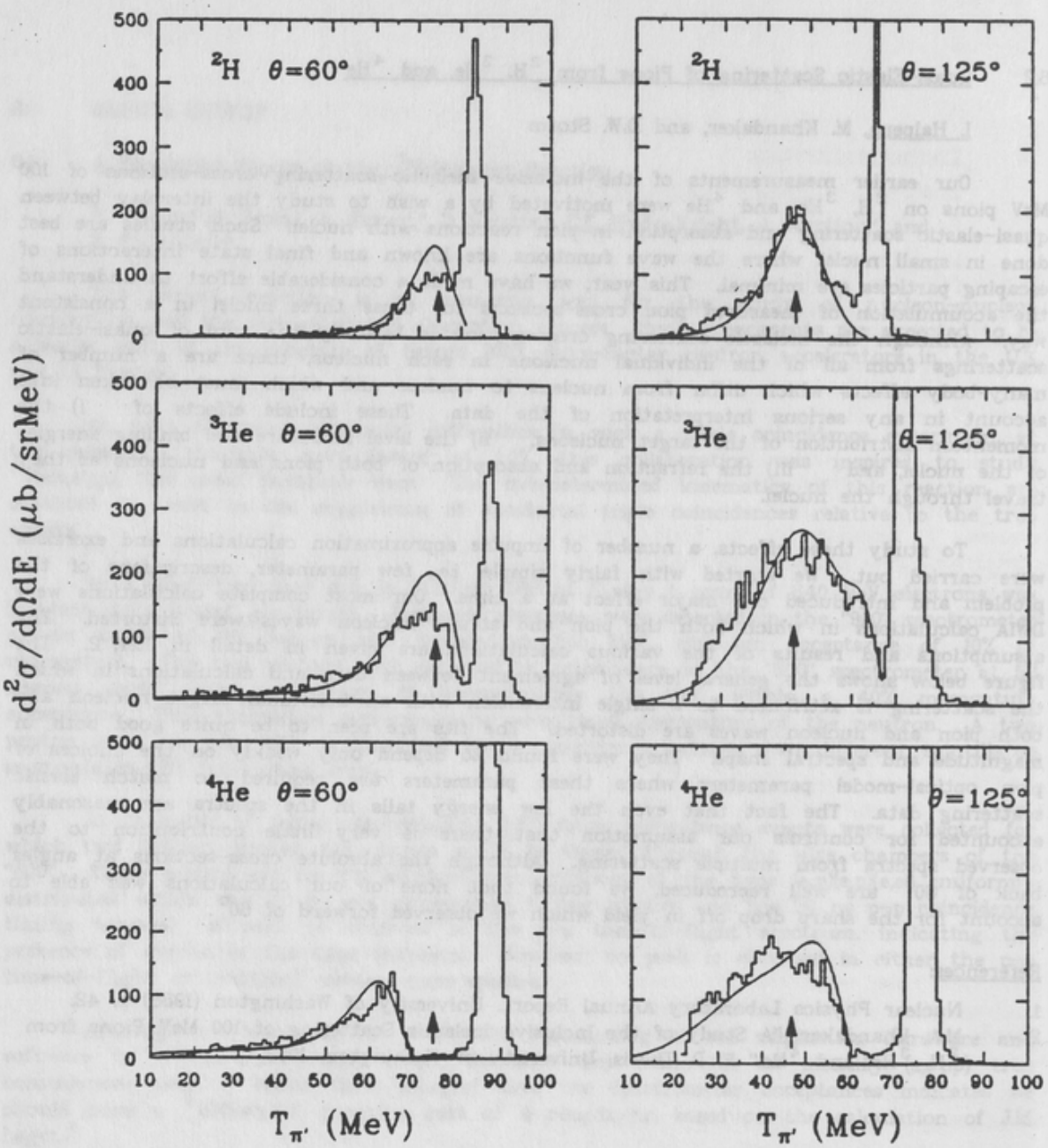

Fig. 6.2–1 Examples of measured spectra (histograms) and calculated spectra (solid curves) for the inclusive inelastic scattering of positive pions form ^{2}H, ^{3}He, and ^{4}He at 100 MeV. The calculations assumed that the scattering was due to a single interaction with one nucleon in the nucleus. The wave functions for the pions and struck nucleons were both distorted in these calculations. It is seen that the shapes of the inelastic spectra are reasonably well reproduced but that the ratios of relative cross-sections 60° /125° are slightly overpredicted by the calculations.

******

6.3 π^+/π^- Inelastic Scattering Cross-section Ratios at 100 MeV

J.F. Amann,* K.G.R. Doss,† D. Drake,* I. Halpern, M. Khandaker,+ J. Nelson,x D.P. Rosenzweig, D.W. Storm, D.R. Tieger,x and S.A. Woodx

The simple model which we have developed to describe inelastic pion scattering in the (3,3) resonance reproduces the observed magnitudes of the differential π^+ cross-sections at angles in the back hemisphere quite well, including their dependence on incident energy and on target mass.[1] It also accounts for the observed ratios of charge exchange to normal scattering cross-sections for both π^+ and π^-. The model fails, however, to predict correctly the ratios in the literature between π^- and π^+ inelastic cross-sections. Because of the simplicity of the model and its successes and because it is now possible to make significantly better measurements than in the older experiments, it seemed appropriate to repeat the measurement of the π^- and π^+ inelastic cross-sections in several nuclei.

Measurements were made using the Clamshell pion spectrometer at the Low Energy Pion channel at LAMPF. Both π^- and π^+ scattering spectra were obtained for C, Ca, and Pb at 100 MeV and five angles between 50° and 140°. At each angle essentially complete inelastic continuum spectra were observed using three overlapping spectrometer bites. A hydrocarbon target was used to calibrate the spectrometer and to determine the necessary efficiencies.

The data were recorded using the Los Alamos Q system, and replay analysis is underway on our Vax using this system. This experiment is the first to use the Clamshell to measure such a broad continuum spectrum, and we are working on some of the problems which arise in such a situation. In the high momentum bite, some of the pions are energetic enough to range through the stopping scintillator of the spectrometer, while in the lowest momentum bite some of the pions do not even reach it. The problem of setting up consistent criteria for positive and negative pions is complicated by the contributions of stars to the pulse height for negative pions. Still another problem is that of determining the backgrounds which are characteristic of the different momentum bites. We are working on solving these problems. When we have done so we expect that the measured spectra will be found to match in their overlap regions, and that we will have determined the π^+/π^- ratios for quasi-elastic scattering cross-sections on the level of 5 to 10%.

References:

* Los Alamos National Laboratory (LAMPF), Los Alamos, NM 87545.
† University of Saskatchewan, Saskatoon, Canada.
+ Now at the University of Maryland, College Park, MD 20742.
x Massachusetts Institute of Technology, Cambridge, MA 02139.

1. K. Aniol et al., Phys. Rev. C 33, 208 (1986).

******

6.4 Properties of the E2 Isovector Giant Resonance seen in (γ,n) Studies

P.T. Debevec,* A. Freytag,* C.A. Gossett, I. Halpern, T. Murakami,† D.P. Rosenzweig, and D.W. Storm

Because of the repairs and modifications which were being carried out this past year on the University of Illinois microtron, it was not possible to schedule an experimental run in our survey of the E2 isovector resonance using the (γ,n) reaction. We have been analyzing the data of our most recent run on Ca (near the resonance) and on Pb (well past the resonance).

Among the more interesting features of these data are the following: 1) The shapes of the forward-to-back asymmetry curves are very similar for the three targets (Pb, Cd and Ca) which we have studied so far.[1,2] These curves all rise smoothly to maximum values of 0.7±0.1. The photon energies at which the rises occur decrease with increasing target mass number at a rate consistent with the presence of an E2 isovector giant resonance. In Pb, the only target for which we have substantial data beyond the resonance, the asymmetry is found to remain high at the higher energies. 2) The photoneutron cross-sections fall off rapidly with increasing energy, and finally 3) There is a dramatic drop at photon energies beyond the resonance of the 90° yield compared to the average yield at 55° and 125°.

The displacements to higher energies of the asymmetry curves as the target mass number is reduced and the rapid fall-off of the cross-sections with increasing energy are consistent with interpretation of the data in terms of an E2 isovector giant resonance. The persistence of the large asymmetries at high energy, despite the contrary implications of calculations using the direct/semi-direct model, suggest however that these higher energy asymmetries may not be entirely due to giant resonances but to some other process, perhaps photoabsorption on quasi-deuterons.[3] If, however, the absorptions are still mainly single particle absorptions, the small 90° yields at the higher energies imply an increase of the ratio of quadrupole to dipole absorption.

References:

* University of Illinois, Urbana, IL 61801.
† Michigan State University, East Lansing, MI 48824.

1. T. Murakami, I. Halpern, D.W. Storm, P.T. Debevec, L.J. Morford, S.A. Wender, and D.H. Dowell, Phys. Rev. C 35, 479 (1987).
2. D.W. Storm, I. Halpern, C.A. Gossett, T. Murakami, D.P. Rosenzweig, D.R. Tieger, P.T. Debevec, A. Freytag, L.J. Morford, S.A. Wender, and D.H. Dowell, Workshop on Isovector Excitations in Nuclei, Vancouver, Canada, Oct. 1986, to be published in Canadian J. of Phys.
3. H. Schier and B. Schoch, Nucl. Phys. A 229, 93 (1974).

******

6.5 Photoabsorption Mechanisms at Energies Above the Giant Resonances

C.A. Gossett, I. Halpern, D.D. Leach, and D.P. Rosenzweig

As we were preparing for the completion of our survey of the E2 isovector resonance using the γ,n reaction, it occurred to us that by substituting a plastic scintillator for the carbon target which we had been planning to use, it becomes possible to study the so-called quasi-deuteron photoabsorption mechanism with only a slight modification of the apparatus already in place for the resonance studies. There is roughly one classical sum-rule worth of total photoabsorption cross-section between the giant resonance region (where single nucleon excitation dominates) and the meson threshold.[1] Yet good data[2] in this energy region are scarce and the mechanisms responsible for this large cross-section remain poorly understood.

Any charged-particle detection system to be used in conjunction with the monochromator at the University of Illinois would have to include an active target since the fluxes are necessarily limited and the required target thicknesses are of the order of the typical ranges of the emitted charged particles. In order to design a system to detect the charged particles from medium energy photoreactions, we have constructed a prototype plastic scintillation counter and have been studying its properties using proton and alpha particle beams of appropriate energies from our tandem Van de Graaff. The scintillator in this detector is a 3" × 4" slab of BC-400, 1 cm thick, and will be viewed by two RCA 8575 phototubes through lightguides placed at opposite ends of the scintillator. A preliminary run with 16 MeV protons and 24 MeV α particles shows that within the region on the scintillator illuminated by the bremsstrahlung beam, the variation in pulse height for either of these test beams is less than 10%. The width of a line for a narrow monochromatic beam of over 20 MeV which hits any one spot of the scintillator is also no larger than 10%. Monte Carlo simulations using Stanford's EGS4 electron-gamma shower code predict that the electromagnetic background streaming through the active target will not significantly reduce the pulse height resolution for the charged particles produced in the photoreactions.

During our next run at Illinois on the E2 isovector survey, we expect to include a feasibility run with a counter system for coincident charged particles. On the basis of what we learn we will design a final arrangement for a study of photoreaction mechanisms above 30 MeV.

References:

1. A. LePretre et al., Nucl. Phys. A 367, 237 (1981).
2. I.V. Dogyust et al., Yad. Fiz. 35, 810 (1982); Yad. Fiz. 40, 1382 (1984).

7. ACCELERATOR MASS SPECTROMETRY (AMS)

7.1 Accelerator Mass Spectrometry (AMS)*

D.R. Balsley, G.W. Farwell, P.M. Grootes,+ D.D. Leach, and F.H. Schmidt

In our experiments to date we have measured $^{14}C/^{12,13}C$ and $^{10}Be/^{9}Be$ ratios in the range of 10^{-11} to 10^{-15}, with applications in several fields of the geochemical, oceanographic, and atmospheric sciences. The work has received partial support from sources available to our collaborators in the Quaternary Isotope Laboratory and the School of Oceanography. Radiocarbon studies under way or completed during the past year include the following:

A. Measurements of organic ^{14}C concentrations in deep-sea surface sediments from locations in the equatorial Pacific, the south Pacific, and the northwest Atlantic were completed. Surprisingly, variations are seen within the bioturbated layer (the top few cm) of the sediments. The results of modeling studies of the data now suggest that up to 50% of the total organic carbon in the sedimentary mixed layer is degradable on a time scale of a thousand years or less.[1]

B. In another joint effort with University of Washington oceanographers, supported in part by a NASA grant, we are engaged in an integrated isotopic biogeochemical study of Alaskan tundra methane. Methane is the most important of the non-CO_2 gases that contribute to the atmospheric greenhouse effect and that could, in the aggregate, contribute as much to atmospheric warming as CO_2. (This study will continue for at least two more years.)

C. AMS measurements for study of the contamination of very old sea shells through carbon exchange are partially completed, and analysis is under way.

D. The technology of preparation of very small graphitized carbon sputter ion source samples for use in AMS has been advanced and we now have the capability to work with samples of 1 mg or less.[2] (See also Sec. 7.2 of this report.)

E. It now appears that 60,000 years is a conservative rather than an optimistic assessment of the effective ^{14}C background of the ion source-accelerator elements of our AMS system and procedures; contamination introduced during sample preparation is the limiting factor in attempts to measure carbon samples older than about 50,000 years.[3] Some recent results are summarized below in Table 7.1-1. Our very low ^{14}C background for AMS will be exploited as appropriate scientific opportunities arise.

F. A paper summarizing the work first presented at the 12th International Radiocarbon Conference (Trondheim, Norway, June, 1985) has been published.[4]

References:

* Our work was supported in part by the National Science Foundation (Grant EAR-8115994, Environmental Geosciences Program).

+ Quaternary Isotope Laboratory and Departments of Geological Sciences and Physics.

1. "Organic Carbon in Deep-Sea Sediments: C-14 Concentrations," S. Emerson, C. Stump, P.M. Grootes, M. Stuiver, G.W. Farwell, and F.H. Schmidt, (to be published in Nature).

2. "Ion Source Sample Preparation Techniques for Carbon-14 AMS Measurements," D.R. Balsley, G.W. Farwell, P.M. Grootes, and F.H. Schmidt, presented at Fourth International Symposium on Accelerator Mass Spectrometry, Ontario, Canada, April, 1987 (to be published in Nucl. Instr. Methods).

3. "Early Expectations of AMS: Greater Ages and Tiny Fractions. One Failure? – One Success," F.H. Schmidt, D.R. Balsley, and D.D. Leach, presented at Fourth International Symposium on Accelerator Mass Spectrometry, 1987 (to be published in Nucl. Instr. Methods).

4. "Radiocarbon Dating with the University of Washington Accelerator Mass Spectrometry System," Pieter M. Grootes, Minze Stuiver, George W. Farwell, Donald D. Leach, and Fred H. Schmidt, Radiocarbon 28, 237 (1986).

Table 7.1-1

^{14}C Background Measurements

Source	Sample	Equivalent Radiocarbon Age (years)[a) b)]
I.	"Machine" only: no ions injected[c)]	≥90,000[d)]
II.	Aluminum blank	≥90,000[d)]
III.	Geological graphite	
	A. Powdered and encapsulated under argon, sintered, decapsulated in argon, installed under argon	69,000±1700
	B. Same as A, except prepared in air	63,800±1100
	C. Same as A, except used in source, removed, and reused two weeks later	65,650±1970
	D. Same as B, except used in source, removed, and reused two weeks later	65,470±1710
	E. Prepared from solid material, with fresh surface	
	1st sample	65,800±2800
	2nd sample	58,590±1050
IV.	Commercial graphite rod	41,160± 510
V.	Marble to CO_2 to graphite	
	A. Marble powdered and dissolved	47,960± 670
	B. Solid marble dissolved	49,690± 700
VI.	Anthracite to CO_2 to graphite	up to 52,000
VII.	^{12}C ion implant in Al	~61,000

a) Half-life = 5568 years
b) Midpoint of upper and lower ages
c) $^{14}N \sim 0.75$ c/sec; total ~ 4 c/sec
d) No counts observed (as compared to standard sucrose at 50 c/sec)

******

7.2 Ion Source Sample Preparation Techniques for ^{14}C AMS Measurements

D.R. Balsley, G.W. Farwell, P.M. Grootes, and F.H. Schmidt

The ability to produce consistent, high-output ion source samples from small amounts of material is a key factor in AMS research. Our group has invested considerable time in developing graphite samples for ^{14}C measurements. The best material for producing C beams with a Cs sputter ion source is solid graphite. It produces high intensity beams with high efficiency, and lends itself to production of samples with good geometrical characteristics. By this we mean samples which are initially identical and geometrically symmetric, and which show consistent, axially symmetric cratering.

In an earlier report[1] we described our method for making graphite pellets using a pitch binder and high temperature heating. Controlling the fraction of binder in small samples proved to be infeasible and in 1983 a system was developed that produces excellent graphite samples without the use of a binder.

For most sample material, we start with CO_2 produced by combustion of pretreated carbonaceous material. This is converted to graphite powder by hydrogen reduction with an iron catalyst.[2] 95% to 100% reduction is achieved; the iron is 5% or less (by atom) of the carbon (i.e., typical Fe:C mass ratios are between 1:4 and 1:5). Carbonate samples are converted to CO_2 by acid hydrolysis.

To make a sample suitable for use in a sputter ion source, 1 to 5 mg graphite powder (or, in some cases, amorphous carbon powder) is encapsulated in tantalum, compressed to $\sim$ 14 kbars and heated in vacuum to $\sim 2500^{\circ}$ C. In this process the filamentous graphite produced by the catalytic reduction process is re-graphitized into a solid mass (if the initial material was amorphous carbon, it is converted to graphite in this step). The capsule (a can, 3.18 mm O.D. $\times$ 2.38 mm long) is then pressed into an Al sample holder disk and the end is cut off in a lathe, exposing a smooth, flat graphite surface 2.38 mm in diameter. We have recently modified the encapsulation process to reduce the size of the exposed surface to 1.59 mm dia., requiring a factor of two less material for a successful sample.

Since 1984 we have made over 500 encapsulated samples. The samples produce up to 65 μA $^{12}C^-$ ions in our sputter source. The average output of our 44 most recently run samples, all of which were made from catalytically reduced graphite powder, was 89% of that of commercial graphite run under similar ion source conditions. Common ^{12}C outputs during data runs range from 20 to 40 μA. Only 5 samples had outputs less than 75% of that of commercial graphite. Our failure rate is now essentially zero for the catalytically reduced graphite and less than one in ten for amorphous carbon. For a more detailed description of these techniques, see ref. 3.

References:

1. Nuclear Physics Laboratory Annual Report, University of Washington (1982) p. 116.
2. J.S. Vogel, J.R. Southon, D.E. Nelson, and T.A. Brown, Nucl. Instrum. Methods 233 [B5], 289 (1984).
3. D.R. Balsley, G.W. Farwell, P.M. Grootes and F.H. Schmidt, Proc. of 4th Int. Symp. on AMS, Nucl. Instrum. Methods, to be published in 1987.

8. NUCLEAR REACTIONS – POLARIZATION

8.1 Polarization of Protons from the $(^3\vec{He}, \vec{p})$

J.L. Allen,* A.R. Crews,* D. Jordan,† S.L. Rosell,+ W.G. Weitkamp, and H. Willmes#

As a continuation of earlier work exploring spin dependent effects in nuclear reactions to the continuum[1] we have been preparing to measure the polarization of protons from the $(^3He, \vec{p})$ reaction leaving the residual nucleus in an excited state. Our activities have been divided into two parts, preparation of the momentum filter and polarimeter and measurement of cross sections for the $(^3He, p)$ reaction on a variety of possible target nuclei.

A number of problems have been overcome to prepare the magnetic momentum filter/spectrograph for use in this measurement. Previous measurements suggested that the image spot at the exit of the momentum filter is not constant in either shape or position. We investigated this and found that, after improvements in the magnet control system electronics, the spot shape is stable and is slightly smaller than previously measured. We have devised a detector system to monitor the position of the spot in the polarimeter entrance slits and learned how to correct the magnetic field to properly center the spot.

The polarimeter,[2] which employs scattering from ^4He, can be calibrated either by allowing protons of known polarization to enter it so that the effective analyzing power can be determined directly, or by a calculation in which the well-known cross section and analyzing power for the scattering of protons from ^4He are integrated over the finite solid angle and target thickness of the polarimeter. We have made preliminary measurements of the analyzing power using polarized protons from elastic scattering of protons on ^{12}C. A computer code to calculate the expected analyzing power is nearing completion.

In a double scattering experiment of this type, a major problem is to achieve a high counting rate to minimize statistical uncertainties. In the absence of any other overriding criterion, we will use the target with the largest inelastic cross section for these measurements. We have found only one set of $(^3He, p)$ cross-section measurements in the literature[3] at energies larger than a few MeV. Since these measurements covered only a limited range of target mass, we measured the $(^3He, p)$ cross section for the targets listed in Table 8.1–1 below. The entire proton spectrum was measured, but the cross sections at only two representative proton energies are given. Uncertainties are about 20%. Clearly ^{47}Sc and ^{59}Co are the best choices for this measurement.

References:

* The Boeing Company, Seattle, WA 98124.
† Present address: Massachusetts Institute of Technology, Cambridge, MA 02134.
\+ Tacoma Community College, Tacoma, WA 98465.
\# The University of Idaho, Moscow, ID 83843.
1. W.G. Weitkamp, I. Halpern, T.A. Trainor, S.K. Lamoreaux, and Z.Y. Liu, Nucl. Phys. A 417, 405 (1984).
2. Nuclear Physics Laboratory Annual Report, University of Washington (1984) p. 81.
3. A. Chevarier et al. Nucl. Phys. A 231, 64 (1974).

Table 8.1-1

Measured cross sections (mb/sr-MeV) for the (^{3}He, p) reaction at two outgoing energies, T_p. 30° proton angle, 27 MeV incident energy.

Target	T_p = 14 MeV	T_p = 24 MeV
^{27}Al	7.0	2.4
^{47}Sc	36	6
^{58}Ni	22	4
^{59}Co	44	8
^{120}Sn	2.4	0.4

9. RESEARCH BY OUTSIDE USERS

9.1 Total Body Calcium by Neutron Activation

C.H. Chesnut,* B.L. Lewellen,* R. Murano,* and S.M. Ott*

Since 1969, the cyclotron has been used to produce neutrons to measure in vivo total body calcium by neutron activation analysis in humans. Starting in 1982, we began studying an alternate method of studying bone mass in human patients, using the differential absorption of two gamma rays of different low energies. With this method, it is possible to make quantitative measurements with good spatial resolution of bones which are particularly vulnerable to bone-wasting disease, for instance, the neck of the femur and the vertebrae, with very low radiation doses. Although this method shows low bone mass in osteoporotics as does the measurement of total body calcium by neutron activation, the correlation is not very close.[1] The relatively low cost and simplicity of the procedure, in addition to the advantages noted above, have led us to prefer this new method to neutron activation. Thus in December of 1986 we measured our last patient by neutron activation, concluding 17 years of using this method.[2]

References:

* Department of Radiology, University of Washington.

1. "Ability of Four Different Techniques of Measuring Bone Mass to Diagnose Vertebral Fractures in Post-Menopausal Women," S.M. Ott, R.F. Kilcoyne, C.H. Chesnut, Journal of Bone Mineral Research (in press).
2. Nuclear Physics Laboratory Annual Reports, University of Washington (1969-1986).

******

9.2 Irradiation of Optical Materials

T.L. Criswell,* K.L. Ballou,* G. Bohnhoff-Hlavacek,* and V.S. Starkovich*

Reflection of light from transparencies (e.g., the inside of windshields, CRT screens, or instrument covers) is a chronic problem. Existing antireflective coatings, while reducing reflection, often work in too narrow a band of frequencies, are absorptive, or produce excessive diffuse scattering. The fundamental cause of reflection is the abrupt change in the index of refraction at the interface between the two media, air and the transparency. If the change in the index can be smoothed over distances of the order of the wavelength of light, the reflectivity will be reduced. Such smoothing can be achieved by producing a dendritic surface with an areal-average index. A method of producing such surfaces has been developed by adapting techniques used in nuclear track-etch detectors. Dielectric materials are irradiated with high fluences of heavy ions and the resulting damage tracks are chemically etched away. The remaining walls of the etch pits approximate the desired shape. The exact shape of the pit wall depends on the damage threshold of the material, the stopping power of the ion, and the etch process. The present study covers a wide selection of plastics and glasses, finding optimum ion-etch combinations to produce the desired antireflective surface for each material. Over 400 samples were irradiated this year, concentrating on optical plastics. A large-sample irradiation facility was designed in anticipation of future work on components.

Reference:

* Boeing Aerospace Company, Seattle, WA 98124-2499.

9.3 Non-Destructive Measurements of Power FET Single Event Burnout Cross Sections

D.L. Oberg* and J.L. Wert*

Power FETs have been increasingly utilized in many space craft systems. It has recently been observed that destructive burnout of N-channel power Mos-FET devices can be caused by single heavy ions, such as are found in cosmic rays. Previous measurements of HEXFET burnout susceptibility have been destructive. Devices were irradiated while the device voltage was increased until the device burned out. Such a technique is not conducive to providing a statistically meaningful burnout probability for various values of Linear Energy Transfer (LET) and drain to source voltage (V_{ds}). A new technique to measure burnout cross sections by observing "potentially destructive" current pulses is presented here. This, in turn, will improve calculations for the probability of failure during a mission.

The circuit used employs a 1 kΩ load resistor connected between the high voltage supply and drain lead of the device. Current limiting is provided by this resistor. The drain current pulses are sensed by a Tektronics CT-2 current transducer attached to the source lead, which is grounded. These pulses are counted with a NIM fast counting system and appear to be caused by the discharge of the HEXFET gate-drain capacitor.

Most of the testing has been done using the University of Washington Nuclear Physics Laboratory tandem Van de Graaff accelerator. Ions are accelerated up to approximately 120 MeV (depending on ion) and are scattered by a foil at the center of scattering chamber. Fig. 9.3-1 shows the test setup. The ion fluence is determined by

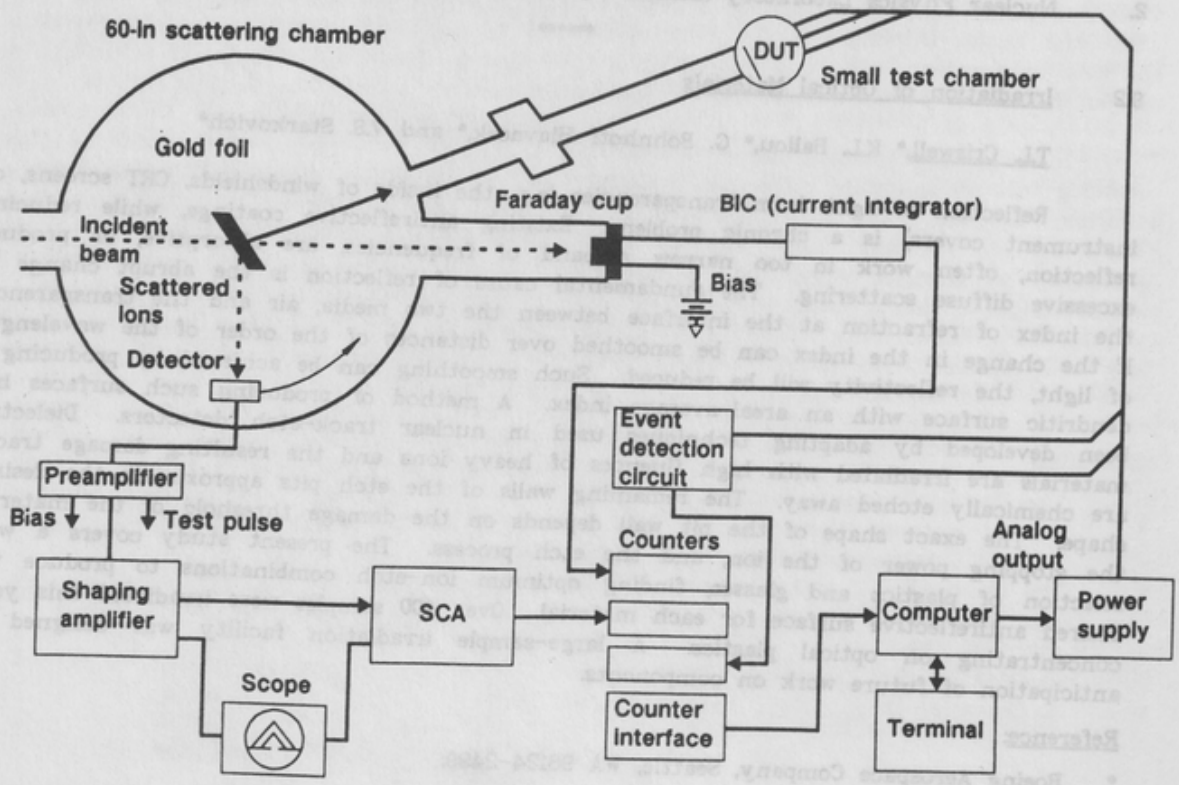

Fig. 9.3-1 Van de Graaff test setup for studies of burnout cross-sections of power FETs.

monitoring the beam current and converting to ion flux by monitoring the Rutherford scattering peak with a surface barrier detector. Our portable test system (also in Fig. 9.3-1) is used to control and monitor the beam as well as adjust V_{ds} and calculate cross sections.

Burnout cross section is defined as the number of potentially destructive current pulses divided by the fluence. The probability of destructive burnout in an actual circuit depends on the cross section, heavy ion spectrum, and actual circuit parameters, such as duty cycle, load resistance, and inductance. Burnout cross section data are shown in Figs. 9.3-2 for an IRF 350 HEXFET. Data are shown for 87 MeV iodine ions as well as 85 MeV chlorine ions.

Reference:

* Boeing Aerospace Company, Seattle, WA 98124-2499.

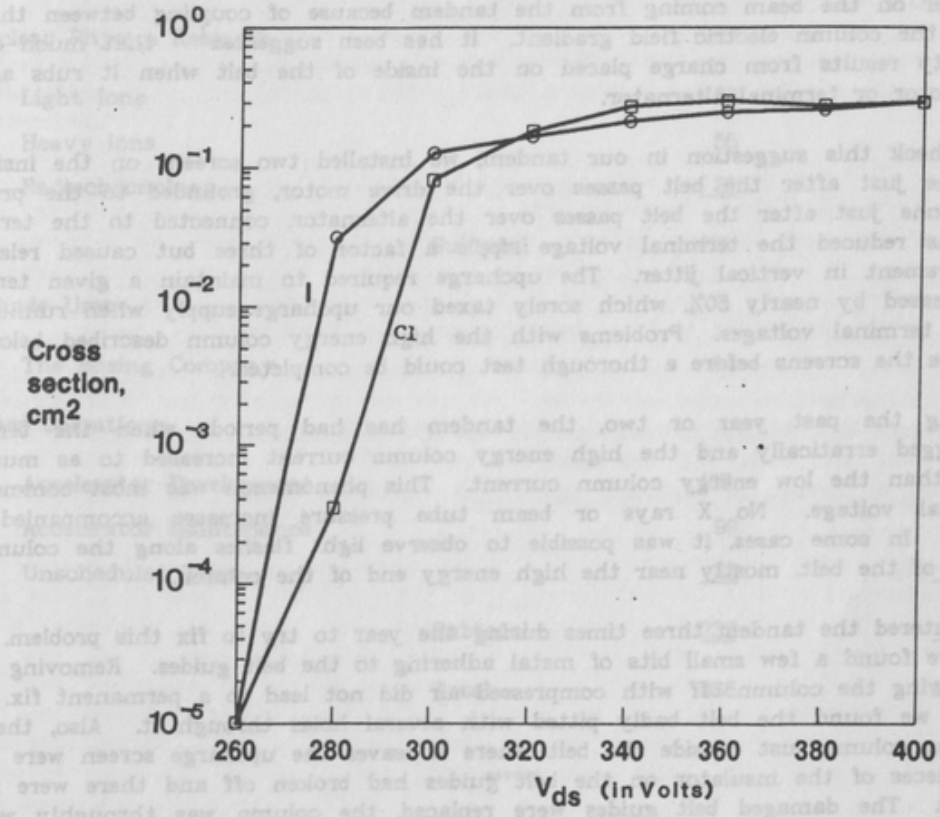

Fig. 9.3-2 Burnout cross sections for the IRF 350 power FET with 87-MeV iodine ions and 85 MeV cholorine ions as a function of V_{ds}.

10. ACCELERATORS AND ION SOURCES

10.1 Van de Graaff Accelerator Operations and Development

D.R. Balsley, J.R. Cromie, D.J. Hodgkins, C.E. Linder, F.H. Schmidt, R.E. Stowell, J.J. Tomasko, T.D. Van Wechel, and W.G. Weitkamp

Major emphasis by the accelerator staff has again been placed on completing the superconducting booster described in Sec. 13. However, we did spend time investigating a possible solution to an old Van de Graaff problem, belt charge ripple, and have apparently fixed another aggravating problem with the high energy column.

The charge carried by a tandem belt is not uniformly distributed on the belt. This causes terminal voltage ripple and, when inclined-field beam tubes are installed, causes vertical jitter on the beam coming from the tandem because of coupling between the belt charge and the column electric field gradient. It has been suggested[1] that much of the nonuniformity results from charge placed on the inside of the belt when it rubs against the drive motor or terminal alternator.

To check this suggestion in our tandem, we installed two screens on the inside of the belt, one just after the belt passes over the drive motor, grounded to the pressure vessel, and one just after the belt passes over the alternator, connected to the terminal. These screens reduced the terminal voltage ripple a factor of three but caused relatively little improvement in vertical jitter. The upcharge required to maintain a given terminal voltage increased by nearly 50%, which sorely taxed our upcharge supply when running at the highest terminal voltages. Problems with the high energy column described below led us to remove the screens before a thorough test could be completed.

During the past year or two, the tandem has had periods when the terminal potential sagged erratically and the high energy column current increased to as much as 30% higher than the low energy column current. This phenomenon was most common at high terminal voltage. No X rays or beam tube pressure increases accompanied this phenomenon. In some cases, it was possible to observe light flashes along the column in the vicinity of the belt, mostly near the high energy end of the column.

We entered the tandem three times during the year to try to fix this problem. The first time, we found a few small bits of metal adhering to the belt guides. Removing these bits and blowing the column off with compressed air did not lead to a permanent fix. The second time we found the belt badly pitted with several holes through it. Also, the belt guides on the column just outside the belt where it leaves the upcharge screen were badly damaged. Pieces of the insulator on the belt guides had broken off and there were many spark tracks. The damaged belt guides were replaced, the column was throughly washed and inspected, and the belt replaced.

Within a few weeks, the phenomenon was again noted. We again found the belt guides damaged. However, the new belt showed only minor signs of damage, just a few discolored spots. We replaced all suspect belt guides and carefully inspected the column again. We also replaced the tank gas and encouraged the operators to be follow more conservative procedures in raising the terminal voltage. The machine appears to be fixed, since it has since run several weeks at terminal voltages in the vicinity of 9.5 MV without problems.

During the year from April 16, 1986 to April 15, 1987 the tandem operated 2937 hours. Additional statistics of accelerator operations are given in Table 10.1-1.

References:

1. M. Letournel and J.-C. Oberlin, Rev. Phys. App. 12, 1383 (1977).

Table 10.1-1
Tandem Accelerator Operations
April 16, 1986 to April 15, 1987

Activity	Days Scheduled	Percent
A. Nuclear Physics Research		
Light Ions	36	10
Heavy Ions	55	15
Radiochronology	27	7
Subtotal	118	32
B. Outside Users		
The Boeing Company	14	4
C. Other Operations		
Accelerator Development	102	28
Accelerator Maintenance	99	27
Unscheduled Time	32	9
Subtotal	233	64
Total	365	100

******

10.2 Measurement of the Flux of the Polarized Atomic Beam Source

C.A. Gossett and T. Nirider

We have measured the flux of the atomic hydrogen beam from the polarized atomic beam source using a compression tube technique. The flux is collected at the exit of the fourth sextupole magnet of the source in an upright cylindrical can of approximately one liter volume fitted with an ionization gauge. The response of the device is calibrated for hydrogen by leaking hydrogen gas into the cylinder at a known rate and noting the corresponding pressure rise. The atomic beam flux measurement technique thus relies on the recombination of the atomic beam on the walls of the cylinder before detection in the ionization gauge.

The atomic hydrogen beam is polarized in electron spin by magnetic separation. Atoms with one electron spin state are focussed by the sextupole magnets of the source and the acceptance solid angle for this beam is much larger than the geometric solid angle. Hence by switching the sextupole magnets off and on and noting the pressure rise in the cylindrical can, one may measure directly the flux of the beam component of interest.

The atomic beam flux has been measured as a function of the operation parameters of the source; sextupole field, dissociator gas pressure, rf power level and coupling, atomic beam skimmer size and distance between the dissociator nozzle and the skimmer. The observed intensity of $4\text{–}6 \times 10^{15}$ atoms/sec is unexpectedly insensitive to the variation of the source parameters and is approximately 5 times lower than is measured for similar sources[1,2]. We are continuing to investigate the origin of these puzzling results.

References:

1. W. Haeberli, M.D. Barker, C.A. Gossett, D.G. Mavis, P.A. Quin, J. Sowinski, and T. Wise, Nucl. Instr. and Meth. 196, 319 (1982).
2. J. Alessi, A. Kponou, R. Raymond, and Th. Sluyters, IEEE Trans. Nucl. Sci. NS–30, 2708, (1983).

******

10.3 Polarized Ion Source

R. Hobbs, J.R. Olson, T.A. Trainor, and V.J. Zeps

In March–May, 1986 the polarized source was moved from its off–line development site to a permanent location in the tandem tunnel. Installation of the 90°–90° beam transport system from spin precessor output to tandem beam line was completed in September. The AB source output was tripled in this interval, so that by mid November the source output at the 90°–90° system input was 1 μA H^- at 40keV with about 7 mA Cs° through the ionizer. A peak beam of 2 μA H^- at 15 mA Cs° was observed, but this cesium intensity is too great at present for stable long–term operation. The first polarized beam through the tandem was observed in December. Transmission from spin precessor to tandem entrance was about 75% and transmission through the accelerator was 50% at 12 MeV to produce an accelerated beam of 300–350 nA.

In March, 1987 the rf transition units, rf generators and a temporary TTL spin reversal system were installed. In April ^4He (p,p) ^4He elastic scattering was used to optimize the rf transitions. Both weak and strong field transitions were tuned to ~100% efficiency resulting in a beam polarization of 0.86 for both spin states within 1%. The spin precessor was also calibrated.

The 90°–90° beam transport system uses two 90°, 20 cm radius electrostatic inflectors to bring the beam from the spin precessor axis 90 cm across to the parallel tandem beam line. These inflectors are cylindrical, so each inflector has attached entrance and exit quadrupole singlets to compensate for the inflector astigmatism. All four singlets focus in the vertical plane. A waist formed by the spin precessor quadrupoles just before the first singlet is propagated to a second waist at the system symmetry point between the inflectors and then to a third waist at the output. A 10 cm diam. einzel lens with adjustable axial position is used immediately after this waist to reduce the divergence angle and match the beam into optics downstream. All of the beam arriving at the entrance to the 90°–90° system is transmitted through 1 cm diameter apertures at the entrance and midpoint. Three quarters of this beam are transported to the entrance of the accelerator.

The rf units for hydrogen have been optimized. The weak field unit is a series–resonant circuit with a nine–turn 2 cm diameter coil coaxial with the atomic beam and a small tapered dipole magnet producing about 7 gauss at optimum. The resonant circuit is driven with a 14 MHz, 75 watt amateur radio transmitter. The 10 m transmission line (RG–58U) is terminated at the rf unit with a quarter–wave open–end stub to locate a voltage node near the rf unit. Full polarization is achieved with 10–20% of the available power. Some care was taken to provide magnetic shielding from the ionizer 2 kG field on the one hand and the strong–field unit ~~140 G field on the other. Nevertheless, the B–field distribution in the region of the weak–field rf unit depends nonlinearly on the ionizer field because of saturation in the ionizer field termination plate. This does not seem to affect performance for hydrogen.

The strong–field rf unit is a series–resonant structure produced by ANAC, Inc. It is driven by a 60 watt MCL rf generator at about 1450 MHz. Proper tuning of this unit is very critical to assure sufficient field amplitude. It was found that even at full output the generator must be located as close to the transition unit as possible (less than 3 m cable, RG–8U). At the required power level the resonant structure temperature was observed to rise 30–50° C corresponding to a shift in resonant frequency of 10–20 MHz. This leads to considerable instability until thermal equilibrium is achieved on resonance. About 1/4 of the rf power (based on observed temperature rise) is absorbed by the quartz tube through

which the atomic beam passes.

Polarization in the two spin states (plus and minus) was measured as a function of reversal rate. Most of the variation up to 2–3 kHz was accounted for by flight time of the atomic beam between the two rf units and the ionizer. Results indicated that introduction of appropriate time delays between the spin controller and data acquisition system would permit reversed rates up to 1 kHz with full polarization and dead time near 10%.

While the present routine output of the polarized source is about 1μA the expectation based on scaling from experience at Wisconsin is an output of 5–10 μA. The output of the AB source at the last six-pole has been measured by comparison to a calibrated hydrogen leak to be about 4×10^{15}/sec. The intensity entering the ionizer has been measured by reference to calculated pumping speeds to be 2×10^{15}/sec. These numbers are indeed 5–10 times smaller than expected for this AB source. Two other AB sources of this particular design are in operation. One, at the Brookhaven AGS, operates in pulsed mode at very low duty cycle with a cryogenic dissociator nozzle, tapered first six-pole, and extra pumping in the rf transition region. The output is $5\text{–}10 \times 10^{16}$/sec (the instantaneous H^- output in the pulse is about 20 μA). The other, at the Karlsruhe cyclotron, operates continuously with a cryogenic nozzle. The output of polarized beam has been several times less than expected. Although these three sources are identical in general structure the nozzle differences make comparison difficult. It is unlikely that the UW AB source would run effectively with a cryogenic nozzle in crossed-beams mode because of the large power deposited by the cesium beam (10's of watts).

The lifetime of the source operating at 1 μA output in April was about 36 hours. The failure mode was breakdown of insulators in the neutralizer region, specifically breakdown across the main ionizer insulators due to buildup of sputtered metal, and breakdown of an einzel lens presumably due to cesium buildup. It is probable that both of these problems can be eliminated.

Aside from these problems the output of the source is very stable. The cesium reservoir temperatures for the neutralizer and cesium gun are well regulated and the AB source is an inherently stable device. Short-term (5–10 min.) variation in intensity is less than 1%.

Ultimate limitation of source lifetime will be sputtering of neutral cesium defining apertures in the rf and six-pole regions and the skimmer and nozzle. Sapphire apertures are presently used in the rf region with good result. The skimmer has recently been replaced with an aluminum unit. It is important that ferrous material (even stainless steel) not be sputtered in the region of the six-poles to avoid building up shorting bridges between poles. The six-poles should also be shielded with sapphire or aluminum. This required strategy argues against the use of a tapered first six-pole because such a unit would present a large unshieldable ferrous surface to the cesium beam for sputtering.

The dissociator nozzle was observed to be sputtered about 1/2 mm deep during the April run. This result and the relative expense and inconvenience of dissociator replacement suggests that the nozzle should be a separate item with independent water cooling and a gasket seal to the dissociator bottle proper. The bottle should have a substantial glass plug at the closed end to serve as a target for the cesium beam passing through the nozzle aperture. This arrangement would provide for easy nozzle replacement and an opportunity to experiment with nozzle design and materials.

******

10.4 Direct Extraction Source Operations

J.G. Douglas, G.C. Harper, D.J. Hodgkins, and T.A. Trainor

As part of the injector platform installation the direct extraction ion source (DEIS), which has been in operation in this laboratory for almost 20 years, was moved on to the zero-degree port of the platform switching magnet where it has been in operation since January. As part of the move we upgraded the ion source power supplies (Glassman and Sorenson), changed from a pyrex and copper rod filament holder to all stainless steel and ceramic, and added an anticorona ring on the back end of the ion source.

Running on pure oxygen we have produced up to 70 μA of $^{16}O^-$. Running a mixture of H_2 and CCl_4 we have produced over 25 μA of $^{35}Cl^-$. Running on pure H_2O one can produce over 20 μA of OH^-, and with enriched ^{18}O water one can produce 10-20 μA of $^{18}O^-$.

Since the DEIS move we have observed significantly shorter filament lifetimes. We have not yet established whether this is due to running on pure oxygen for example rather than a more conventional H_2-O_2(1.5%) mixture as in the past, or to the change from copper to stainless steel filament posts, or to some unknown change in the ion source operation. Our goal is to provide the experimenters with a reproducible and reasonable range of choices between filament lifetime and beam intensity.

Throughout the history of this ion source the quality of the bunched beam has been quite variable. To ensure optimum operation of the booster linac we have developed the injector platform mass analysis system for use as an energy analyzer with resolution of $E/\Delta E \sim 5000$. This system shows that the DEIS can easily be adjusted to yield energy spreads from less than 10 eV to more than 50 eV where a 20 eV spread would correspond to a bunch width minimum of about 1 ns at 50 keV. Presumably the large energy spreads are produced by plasma oscillations in the kHz to Mhz range. In fact, the energy distribution can be made to be double peaked at times, characteristic of a simple sinusoidal energy variation.

By looking at the arc light intensity fluctuations in the source with a fiber optic and correlating this signal with the variations in energy spread we hope to develop a simple diagnostic for tuning the ion source to ensure optimum bunching performance.

******

10.5 Model 860 Sputter Source Installation

J.G. Cramer, J.G. Douglas, G. Harper, D.J. Hodgkins, and T.A. Trainor

A model 860 sputter ion source has been purchased from General Ionex Corp. to serve as a very intense source of heavy ions for the injector platform. In conjunction with the very good mass analysis system on the platform this should enable production of usable beams of rare isotopes from natural targets while avoiding excessive loading of the injector high voltage or tandem charging systems. The model 860 typically produces beams of 100–300 μA from targets like carbon or copper.

In the model 860 design, the negative ion beam energy is determined by the sum of two voltages, one of which primarily determines the focussing of the positive cesium sputtering beam and the other which determines focussing of the negative ion beam. This system has two drawbacks. 1) The beam energy will change if either focus supply is adjusted. With a high resolution analysis system this would make beam tuning intolerable. 2) Two power supplies, at least one of which (cesium focus) will be loaded nearly to maximum output, contribute to beam energy fluctuations.

We have modified the model 860 to overcome these difficulties. We have added a third high voltage supply which directly determines the sputter target bias voltage with respect to platform ground, and hence the beam energy, independent of the focussing voltages. This supply provides only the negative beam output current and so minimizes beam energy fluctuations. In order to decouple this beam energy supply from the focussing supplies we have added an additional acceleration gap which has a non–zero voltage gradient to the extent that the focus voltages do not add up to the beam energy.

The source was modified shortly after receipt from General Ionex. It has been operated briefly after installation on the injector platform. A 40 μA beam of ^{12}C was extracted at 25 keV, and operation of the new biasing system was as expected. Some difficulty has been encountered in introducing a controlled amount of cesium into the ionized region through the long thin tube provided. However, our experience is too little at present to conclude that this is a major operational difficulty.

******

11. NUCLEAR INSTRUMENTATION

11.1 Electrostatic Deflector for Studying Spin Distributions at Near-Barrier Energies

S. Gil, D.D. Leach, S.J. Luke, L.T. Nirider, and R. Vandenbosch

This year we have begun a new effort to improve the technique for obtaining the spin distribution of the compound nucleus produced in fusion reactions at near barrier-energies.[1] One of the techniques that has been used during the last few years in our laboratory[1] for determining gamma multiplicities, M_γ, is based on using a high resolution GeLi detector in coincidence with several NaI detectors. The GeLi detector was used for tagging the different evaporation residues produced in the reaction. From the ratio of coincidence to singles spectra we obtained the M_γ for the dominant even-even evaporation products. This method has at least two important shortcomings: a) low efficiency due to the combination of the low cross sections in the region of interest (σ < 50 mb) and the low efficiency of the GeLi detector, b) possible bias due to the greater sensitivity of this technique in tagging even-even residual nuclei. This last limitation is expected to be more important in the cases of more symmetric projectile-target combinations, where there is larger fractionation of the yield.

An alternative approach would consist in using the evaporation residues as a tag of the fusion events directly. Since fusion products are strongly peaked at 0^0 degree, a large detection efficiency can be achieved if it is possible to separate and suppress the beam particles from the residues. The ratio of these residues in coincidence with the NaI detectors to the residues singles would yield a M_γ value that will be insensitive to any bias due to channel fractionation.

We are particularly interested in combinations of projectile-target systems that lead to compound nuclei in the mass region of 150 to 180 amu. At near-barrier energies the fusion products have relatively small energy per nucleon (0.15 to 0.7 MeV/A) as compared to that of the beam (3.7 to 5. MeV/A). Therefore an electrostatic deflector can be effectively used for separating the residues from the beam.

Our design consists of three parts: an electrostatic deflector box, a detector chamber and a new scattering chamber. The deflector box can be isolated from the rest of the system enabling us to change targets and manipulate the particle detectors without compromising the conditioning of the deflector itself. The deflector plates are located at 18 cm from the target and are made of (polished) stainless steel with dimensions of 5 cm high, 25 cm long and 1.25 cm thick. The separation and orientation of the plates can be easily changed. The plates are located in a stainless steel box designed to hold up to ±70 KV. A turbo-molecular pump provides the vacuum to this module. The detector chamber contains a beam stop and a large area particle detector, both of which can be moved without breaking the vacuum. The particle detector system consists of a position-sensitive Breskin counter[2] followed by a large-area solid state detector. The Breskin counter provides a position and a timing signal and the solid state detector gives the energy of the particles. This system, when operated with a pulsed beam, would provide us with the energy and time of flight of the particles, which will enable us to separate the fusion products from the elastic and other direct products.

The scattering chamber is a cylindrical aluminum box 25 cm in diameter and 25 cm height and can accommodate several NaI detectors around it. The major components of

our deflector system have already been purchased and the different parts are currently being built in our local shop.

References:

1. Nuclear Physics Laboratory Annual Report, University of Washington (1986) p. 21.
2. A. Breskin et al., Nucl. Instrum. Methods 221, 363 (1984).

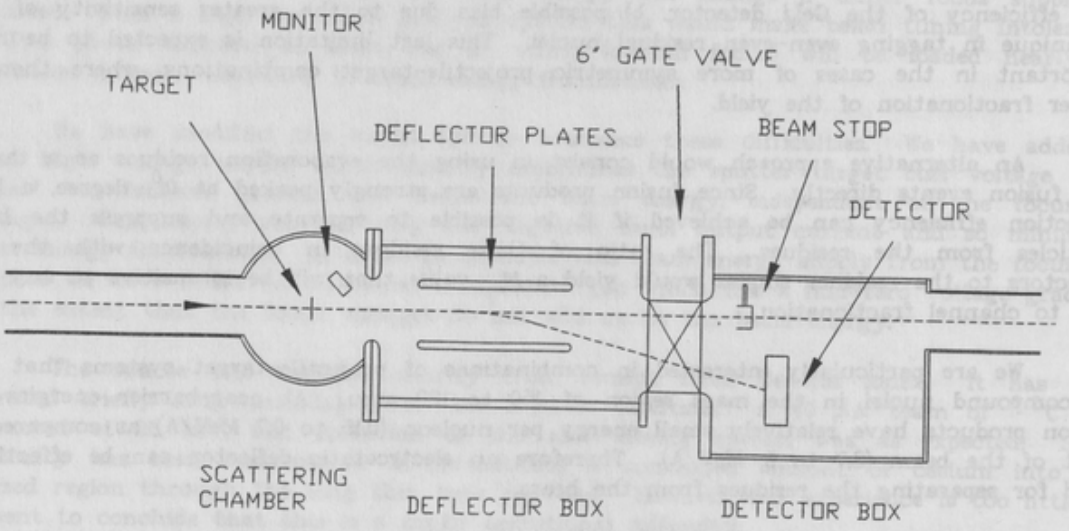

Fig. 11.1-1 Schematic view of the electrostatic deflector.

******

11.2 Design and Construction of Electronic Equipment

T. Earle, H. Fauska, J.M. Lacroix, D.K. Morris, D.B. Newell, L. Prewitt, J.M. Stehfest, R.E. Stowell, and T.D. Van Wechel

Again this year, a majority of the electronics shop time was devoted to projects on the booster linac, described in Sec. 13 of this Annual Report. A list of the major projects follows:

a. A magnet control chassis was designed and constructed to allow computer control of the H.P. power supplies for the inter-cryostat quadrupole magnets.

b. The forty rf control modules constructed last year[1] were further modified to make the conditioning input independent of amplifier error loop gain and quiescent power setting.

c. A second auxiliary electronics chassis was designed to allow computer control of the following: cryostat heaters, power on/off for the rf amplifiers and intercryostat magnet power supplies, remote reset of rf amplifiers tripped off due to excessive vswr, and remote measurement of rf amplifier forward and reflective power levels. Seven of these chassis were built for the linac's six satellite control stations and for the buncher station.

d. Additional modifications to the seven auxiliary electronics I chassis constructed last year[1] were made as a result of further testing. This was primarily in the circuitry for the fiber optic data link from the linac stations to the control room.

e. Several additional electronic control chassis for the cryogenics system were designed and constructed (see Sec. 13.4).

f. The magnet controller chassis described last year[1] was tested extensively after installation of the three 90 degree bending magnets. Some minor modifications were made.

g. A remote control scheme to allow control room operation of the pretandem beam buncher built last year[1] was designed.

h. The vacuum controller chassis built last year[1] was expanded to include a second card cage for additional output units.

i. Extensive testing, debugging and some minor modifications were made to the seven linac resonator controller chassis described last year.[1]

j. The forty commercial rf amplifiers that drive the linac resonators were modified and adjusted, including rewiring for 208 VAC power inputs, uniform trip points for excessive vswr and addition of remote reset capabilities for tripped amplifiers.

k. Several printed circuit cards for 120 VAC power control and reed relay signal switching were designed and constructed for the diagnostics group (see Sec. 13.7).

Reference:

1. Nuclear Physics Laboratory Annual Report, University of Washington (1986) pp. 57, 70, 73, 75.

11.3 Target Preparation

G.M. Hinn

In the table below are listed a few of the more interesting targets prepared in the target laboratory during the past year.

Target	Starting Form	Final Form	Method of Preparation	Backing	Thickness in mg/cm^2
$^{6}Li_2O$	metal	oxide	evaporation oxidation	self supporting	2–4
$^{nat}C, ^{12}C, ^{13}C$	C	C strip	E-Gun	2 μgC 10 mil Ta	.01
^{11}B	metal	metal	E-Gun	self supporting	>1
^{71}Ga	oxide	oxide	evaporation	10 mil Ta	0.1–0.2
^{166}Er	oxide	metal	reduction evaporation	self supporting	0.3
$^{nat,180}Hf$	oxide	metal	E-Gun	self supporting	.5
^{208}Pb	oxide	metal	H_2 reduction	self supporting	1
^{nat}Se	metal	metal	evaporation	10 mil Pt	1
$^{152,154}Sm$	oxide	metal	reduction evaporation	C	0.1–0.2
$YBa_2Cu_3O_{6.5}$ super-conductor high T_c	powder	sintered pellet	sintering	none	100

a. Stripper Foils. We have changed from slackening the foils by reducing the size of the foil ring support by compression to applying a slight suction to one side of the foil in order to slacken the foil while it dries. This is in preparation for a 200 position stripper foil wheel to be built and installed in the Tandem in the near future.

b. $^{6}Li_2O$. 2–4 mg/cm^2 $^{6}Li_2O$ foils have been made for the University of New Hampshire which is conducting an experiment at the University of Mainz, Germany. These foils have served quite well as oxygen targets and continue to be in demand.

c. $YBa_2Cu_3O_{6.5}$ High T_c Superconductor. Some initial experiments to produce LN_2 cooled high T_c superconductors have proven successful.

******

11.4 Investigations of "Warm" Superconductors

J.G. Cramer, G.M. Hinn, and M.B. Kurup

We have been pursuing some investigations of the new "warm" superconductors for possible use in acceleration cavity or nuclear instrumentation applications at our laboratory. Our first step in this work was to produce a pellet of $YBa_2Cu_3O_x$ that when cooled in liquid nitrogen exhibited the magnet repulsion characteristic of superconductors. This was accomplished by firing a stoichiometric mixture of Y_2O_3, $BaCO_3$, and CuO at 1000° C for 10 hours. We fired this material as a loose powder, then reground it to powder form, compressed it to a pellet, and fired it again. The material from this pellet was then reground to a fine powder. We have been seeking a substrate material which will support a thin surface layer of the superconducting material and preserve the superconductivity of the surface layer. We have tried substrates of copper, gold-plated copper, copper oxide, single-crystal silicon, and brass. Of these, only brass has shown some promise, but the resulting coatings have so far not been superconducting.

Another investigation has involved the addition of fluorine to the $YBa_2Cu_3O_x$ material. It has been observed that incomplete oxidation of the basic material is associated with optimum superconductivity. We speculated that fluorine in replacing oxygen sites in the crystal might function as an electron donor, thereby promoting superconductivity. We produced $YBa_2Cu_3F_4O_x$ but were unable to observe superconductivity in this material. Our speculation is apparently valid, however. Six weeks after our work was initiated, a publication[1] appeared which reports the observation that $YBa_2Cu_3F_2O_x$ fired in air is superconducting at 155° K. We are continuing these investigations.

Reference:

1. S.R. Ovshinsky, R.T. Young, D.D. Allred, G. DeMaggio, and G.A. Van der Leeden, Phys. Rev. Lett. 58, 2579 (1987).

12. COMPUTER SYSTEMS

12.1 Data Acquisition System Enhancements

C.A. Gossett, H.P. Readdy, R.J. Seymour, and D.P. Rosenzweig

The principal data acquisition system is a DEC PDP 11/60 with a CAMAC-based experiment interface controlled by a BiRa MBD-11 microcomputer. The 11/60 uses the RSX-11M operating system, an RL-01 and RL-02 disk drive, a 1600 bpi 75ips tape drive, a Printronix P-300 printer/plotter with a Trilog Tektronix hardcopy board, a DEC VT-11 graphics display and a Tektronix or NDS terminal. The CAMAC crate connects to twelve Tracor Northern TN-1213 ADCs, plus occasional LeCroy 2249As, 2251s and 2256As. We have 15 NPL-built 10 digit scalers connected to an IEEE-488 bus. The IEEE bus also connects to target arm angle readouts and beamline magnet controllers.

Minor software enhancements have been made, including one to MULTI to allow replacement of the obsolete Tektronix terminal by an NDS terminal. This allows the use of a raster terminal but still provides intensification of new scatterplot points.

******

12.2 Data Analysis System Enhancements

C.A. Gossett, H.P. Readdy, R.J. Seymour, and D.P. Rosenzweig

Our data analysis system consists of an 8 megabyte VAX 11/780 with 1 gigabyte of System Industries disks, two 75ips 1600 bpi tape drives and one 50 ips Telex 6250 bpi drive, a Printronix P-300 printer/plotter, an HP 7475a pen plotter, an AED-512 color graphics display, two modems and thirty local terminals. It is connected via DECnet/Ethernet to the Booster console MicroVAX II.

The 780's memory was doubled to 8.0Mb with a memory bank purchased from the Physics Department. This overfilled the VAX system cabinet, and an alternative was developed to avoid purchasing a $5000 expansion cabinet from DEC, a solution which received a "VAX wizard" award at the fall 1986 Decus symposium. A sidecar was built providing sufficient air flow, mounting rigidity, and power and signal wiring for the Systems Industries SBI adaptor.

A Lasermaster printer was added to the system for printing letter quality and Autocad drafting documents. Additional fonts and characters were defined. An IBM PC-AT clone was programmed to handle file transfers from the VAX and output to the printer. PCTEX was installed on the IBM PC-AT as an alternative to Superscript in formatting documents.

There were the usual updates to the lab-standard analysis programs HP and MUSORT to correct errors, enhance performance and add minor features.

We now run the Q suite of programs for Doug Rosenzweig's analysis (see Sec. 6.3).

******

12.3 Microcomputer Installations

C.A. Gossett, H.P. Readdy, D.P. Rosenzweig, K. Schuh, and R.J. Seymour

We added a second PC-AT clone for use in mechanical drafting with Autocad. Autocad version 2.18 was updated to version 2.52, and a menu program, Allegro, was installed as a user interface to Autocad.

Two IBM PC-ATs and an IBM PC serve as data acquisition systems for dedicated experiments (see Adelberger's group's reports).

As mentioned above, another PC-AT clone drives the Laser printer.

******

12.4 Network Installations

C.A. Gossett, W. Haxton, H.P. Readdy, R.J. Seymour, and D.P. Rosenzweig

In conjunction with Nuclear Theory, we are currently upgrading our installed VAX system by adding MicroVAX 2's in the form of VAXstation GPX's. At this time we have installed three, have one trying to come up and one more expected soon. The full details will be covered in next year's annual report.

******

12.5 Modifications of the Statistical Model Code CASCADE

C.A. Gossett and M. Kicinska-Habior

The code CASCADE[1] calculates evaporation spectra based on the statistical model for compound-nucleus reactions (Hauser-Feshbach theory). The code came to our laboratory[2] via Oxford and KVI where the original version based on Ref. 1 was modified to include the decay of the giant dipole and giant quadrupole resonances built on excited nuclear states and was modified for use on VAX 11/780 systems.

In 1984 we wrote a code CASFIT which is used quite extensively in the laboratory in the analysis of high energy gamma decay following heavy ion collisions (see Sec. 2). The code incorporates the CASCADE program into a least squares fitting routine in which the variable parameters are an overall normalization (which in practise is fixed at 1.0) and six parameters describing the energy locations, widths and fraction of sum rule strengths for, in general, a two-component Lorentzian form for the giant dipole resonance (GDR) strength function. The energy dependent line shape and efficiency of the 10"x10" NaI detector is folded with the statistical model calculation, and the GDR parameters varied in order to fit the high energy portion of the measured γ-decay spectra. The parameter uncertainties are extracted in the fitting procedure from the curvature matrix. The uncertainties in several quantities of interest which combine the fitted parameters, such as the total strength, ratio of strengths, ratio of energies, and mean resonance energy for a two-component GDR shape, are determined after accounting for the cross correlations of the parameters.

In the past year the CASCADE and CASFIT codes have received major modification. The CASCADE program was changed to allow for variable dimensioning of the spin and energy arrays to accommodate calculations at high energies and spins and for calculation and fitting with variable length energy bins for the particle evaporation and gamma decay spectra. Several errors in the code used for folding the measured NaI line shape with the statistical model calculation were corrected and the code modified to adapt to the variable length energy bins from CASCADE. We have also added an option to CASCADE which allows the level density used to be calculated according to the Reisdorf approach.[3] We have modified a version of the CASCADE code which accounts for the effect of isospin and parity, to be used in the fitting routines. In order to reduce the computation time required in fitting spectra, particularly at high excitation for which the decay cascades are quite long, we have added options to the CASFIT code which allow preliminary fits to be performed in a quick yet approximate manner. Rather than reevaluate the entire decay cascade at each step in the derivative and γ-decay spectrum shape calculation, the full cascade is calculated once and further steps involve reevaluation of the γ-decay spectrum only. This method is particularly useful for fits in which the initial parameter values are best estimates only and may differ significantly from the final fit values, and in cases in which one wishes to test, in a timely manner, the sensitivity of the fitted GDR parameters to the parameters of the statistical model calculation.

References:

1. F. Pühlhofer, Nucl. Phys. A 280, 267 (1977).
2. Nuclear Physics Laboratory Annual Report, University of Washington (1984) p. 85.
3. W. Reisdorf, Z. Phys. A 300, 465 (1981).

13. BOOSTER LINAC PROJECT

13.1 Construction of the Superconducting Booster Accelerator

R. Abel, J.F. Amsbaugh, J. Annis, J. Barei, M.K.M. Brown, M. Bryce, R.S. Burton, R.C. Connolly, R.L. Cooper, D.T. Corcoran, J.G. Cramer, J.R. Cromie, J. Davis, S. Doub, J.G. Douglas, T. Earle, M. Farley, H. Fauska, A.M. Flanagan, R.W. Floyd, B.J. Fulton, M. Gabre, L.L. Geissel, G.C. Harper, D.J. Hodgkins, B.P. Holm, M.A. Howe, T.J. Irwin, J.A. Katterman, J.M. LaCroix, T.H. Lau, D.D. Leach, Q.-X. Lin, C.E. Linder, J.R. Longwill, J.-Q. Lu, T.A. Meadows, D. Morris, D.B. Newell, R.A. Nielsen, D. Paschke, D. Pengra, L. Prewitt, M.G. Ramirez, H.P. Readdy, R. Rose, S. Rosell, D. Rosenzweig, B. Sanborn, D. Schaafsma, K. Schuh, A. Schroeder, K. Seymour, R.J. Seymour, L. Sima, H. Simons, D. Sours, J.M. Stehfest, D.W. Storm, R.E. Stowell, H.E. Swanson, J.J. Tomasko, T.A. Trainor, R. Vandenbosch, T.D. Van Wechel, W.G. Weitkamp, D.I. Will, A. Willman, and J. Wootress

As has been discussed previously, the superconducting booster accelerator is expected to produce proton energies of 36 MeV and energies of up to 20 MeV/A for the lighter heavy ions dropping to 10 MeV/A around mass 40. Quarter wave resonators were chosen to optimize the range of masses that could be effectively accelerated. The linac consists of 36 superconducting resonators in 12 large cryostats plus two resonators operating as bunchers in two smaller cryostats.

During the past year we have been involved in an intense period of construction, installation, and assembly. As subsystems were completed they were tested. In addition, tests on the entire accelerator were performed with particle beams. By the time this report is being prepared (June, 1987) we have installed all components of the accelerator except the last piece of beam line. All of these components have been operated, and in nearly all cases the systems or subsystems perform as expected.

The eight major tasks and some sub-tasks of the booster project are described in the following sections in more detail. The sections are referenced in parentheses. Our accomplishments for this year can be summarized as follows: 1) Most of the work for the injector deck (13.2) was done this year. The deck construction is complete, although more work remains on the controls. The isolation transformer failed and is being rebuilt by the supplier. 2) The cryogenic system (13.3) has been in regular operation this year. The automatic control (13.4) of the distribution system was completed and has been working reliably. 3) The high beta resonator construction was completed and all the resonators required for the booster have been plated and installed (13.5). 4) The vacuum systems (13.6) have been installed and are remotely controlled, monitored, and protected by the satellite computer. 5) The beam diagnostics (13.7) and the controls for the diagnostics have been installed and are used regularly. 6) The control system (13.8) is nearly completed, and the remote readouts of all the parameters have been installed at the main control console. 7) The main control program (13.9) is completely operational and permits operation of all the systems of the linac from the main control console. 8) All the beam transport elements have been installed (13.10), and some effort has gone into additional studies of the beam dynamics, although substantial additional work will be needed in this area. 9) The radiation monitoring systems (13.11) have been installed and are being connected into an interlocked safety system. And, finally 10) a foil stripper for the Tandem (13.12), which will increase the capacity from 50 to 200 foils, is being prepared. This stripper is based on an NEC system.

We have performed several beam tests with sections of the accelerator and finally with the entire accelerator. In this final test we accelerated an ^{16}O beam to 170 MeV. During this test we used 19 of the 24 low beta accelerating resonators and 10 of the 12 high beta ones. The high energy buncher (low beta resonator) was used as well. (The seven resonators not used were suffering from mechanical problems with either the tuners or the couplers that prevented us from moving them to the appropriate operating point.) The average accelerating field obtained with the low beta resonators was 2.76 MV/m while that with the high beta resonators was 2.23 MV/m. The average power consumed by liquid helium was 6 W for each low-beta and 11 W for each high-beta resonator. These tests are presented in more detail in the section 13.13.

In general, we are pleased with the results with the Booster so far. Our original construction milestone "All systems tested and accepted" by July 1987 still appears to be realistic, as it is essentially achieved already. Our diagnostic systems enable us to tune the booster effectively and to learn what qualities of the beam need improvement. The control system enables us to monitor and adjust all systems of the machine conveniently and reproducibly. We have had no unpleasant surprises with our original design, and we feel that an appropriate effort in tuning and improving various components or systems will give us the beam quality that we expected at the initiation of the project.

We are now looking forward to the commissioning phase of the project in which our efforts will no longer be focused on construction of a number of separate systems but will be concentrated on getting all those systems to operate together to produce high quality beams. In spite of the fact that the accelerator looks finished, there remains a lot of work associated with tuning and beam development. For the long term, it is expected that there will still be substantial manpower requirements for maintaining the large cryogenic system and the 14 cryostats with 38 independently controlled resonators and rf systems. There will be additional efforts required for developing and tuning different beams if we are to achieve the full capability of the accelerator. Thus the staff required will be substantially smaller than that involved in the construction of the machine, but will be substantially larger than that that has previously been involved with the laboratory accelerator.

******

13.2 Injector Platform

J. Barei, J. Davis, J.G. Douglas, M. Gabre, G.C. Harper, D. Hodgkins, T. Lau, D.B. Newell, A. Schroeder, J. Tomasko, T.A. Trainor, and L.B. Van Houten

Platform assembly has been completed, with two ion sources installed and one of them in regular service. The direct extraction ion source (DEIS) was moved from its former site in December and put into service in January. A General Ionex Model 860 sputter source has been installed and is still in development.

Operation of the platform at high voltage has been limited due to repeated failures of the 10 kVA, 300 kV isolation transformers supplied by Hipotronics. This situation is still unresolved after two separate units of different design were supplied and suffered breakdowns.

Despite the transformer problems the platform has been tested at 300 kV and has delivered ion beams up to 250 keV. Except for the transformer problem the high voltage performance is excellent. Total power supply current at 300 kV is about 220 μA of which 20–40 μA is corona discharge. Voltage noise on the platform, as monitored with a capacitor plate, is, except for the power supply noise, due to AC capacitively coupled through the isolation transformer ($\sim$ 1/2 V_{pp}) and to random fluctuations from the corona discharge. These latter have a skewed distribution, with most of the variation within 5 V, about 20% of the variation within 5–10 V, and a few percent within 10–20 V of the maximum value. The power supply has achieved a 6 V_{pp} noise performance when attached to the platform.

The mass analysis system of object and image slits and a precision double-focusing 90° magnet has provided resolution $m/\Delta m$ from 200 at full transmission for various heavy ion beams up to about 5,000 for analysis of ion source noise. This makes possible measurement of time-averaged ion source noise spectra with a resolution of about 10 eV in order to improved bunching performance. This resolution is especially important for the DEIS which can be operated inadvertently in a noisy regime with an energy spread as large as 40–50 eV.

Both ion sources, the DEIS and the Model 860, require isolated power supplies operating at high voltage with respect to the platform. A separate isolated rack and isolation transformer are provided on the platform for this purpose. Because two ion sources share this rack a high voltage switch isolated to 50 kV has been developed which disconnects the unused ion source from the rack so that maintenance can be performed.

Beam line optics from the injector platform to the FN tandem have also been installed, consisting of two 15 kV electrostatic quadrupole triplets, a 10 cm einzel lens and electrostatic (2) and magnetic (2) steerers. This system provides for operating the platform at ground potential (for light ions), as well as at potentials up to 300 kV.

The platform control system provides for completely manual operation or for alternative control of some parameters by computer. The computer control is based on a DEC Falcon microprocessor communicating with a set of three multiplexing analog and two-state I/O units on the platform via fiber optics. Each unit has eight ports of each type (these are ANAC 736 units purchased some years ago). The Falcon also controls beam line components at ground potential via conventional DEC I/O ports.

1987AR

13.3 Booster Cryogenic System Performance

D.T. Schaafsma, D.I. Will, and J.A. Wootress

This article summarizes operating experience since helium refrigerator startup in August of 1985. Our cryogenic system consists of a Koch Process Systems 2830 S Helium Refrigerator (comprised of three RS screw compressors and one cold box with three double piston expansion engines), a Beechcraft Cryogenic Distribution System, and fourteen Janis Research cryostats.

For ease of communication we call the refrigerator expanders the top, middle and wet engines. The top engine has operated 15,000 hours at ≈ 150 rpm. It has required six sets of o-rings with grease felts, two sets of piston pins with bearings, one rebuild of its valves, and one replacement of cam follower arm bushings. One of the replacements of piston pin with bearings occurred because of defective pin bearing caps, one of which broke away from its cup and severely scored the aluminum piston crosshead and its steel guide. After replacing the crosshead and guide so we could continue operating, we sleeved the guide. The scoring of the crosshead itself appears to be confined to nonessential surfaces only. We believe both are usable spares. Our middle engine has operated 8000 hours at ≈ 150 rpm. It has required three sets of o-rings with grease felts. Our wet engine has operated 2000 hours at 50 to 100 rpm. Only minimal o-ring wear was observed at the two prophylactic replacements. Finally, we have pressed bronze piston pin bushings into four of our six aluminum crossheads to eliminate the scoring which occurred with pin bearing replacement.

As of July, 1987, each compressor has run 11,000 hours. Each came equipped with an oil removal system consisting of four Balston mist filters in series followed by a one meter long warm charcoal bed. When we changed the charcoal in compressor number one at 5000 hours, we found less than one inch of the bed contaminated. On that basis we plan to change charcoal in a second compressor between 10,000 and 12,000 hours.

Our cryogenic distribution system delivers liquid helium and liquid nitrogen to our cryostats and returns cold helium vapor to the refrigerator within one vacuum jacket. Icing and blockage of fluid lines have occurred every few months during start-up. Deriming is done by cycling the vacuum with helium gas while purging the blocked line(s).

The twelve large accelerator cryostats and two buncher cryostats built by Janis Research have performed well. Loaded heat leak is three watts to helium per large cryostat. We have had two liquid nitrogen tank ruptures in the large cryostats. These failures occurred because we were unaware of these tanks' low working pressure rating, 5 psig. Failures occurred during initial cooldown from bakeout temperatures of 350 K. To prevent further failures we limit liquid delivery rate during cooldown with a 1/8 " orifice. Double pressure relief valving has been installed on each cryostat liquid nitrogen tank with cracking pressures of 2.5 and 5.0 psig. In addition, Janis changed the liquid nitrogen tank design for our last four cryostats plus the two replacement tanks to provide higher working pressure. We have repaired the two ruptured units for spares.

Liquid nitrogen consumption varies from 300 to 400 gallons per day. Combined static and operating liquid helium heat load is somewhat over 300 watts during maximum power input achieved thus far. It was easily handled by the refrigerator.

13.4 Cryogenics Control System

M.A. Howe, H.P. Readdy, D.T. Schaafsma, and D.I. Will

The original goals for control of the cryogenic system have largely been achieved; later additions are close to implementation. The eventual objective is to create a cryogenic system that is largely self-monitoring and self-regulating.

The PDP 11/23+ microcomputer currently regulates liquid cryogen levels in 14 cryostats by changing the settings of 28 valves (one LHe and one LN_2 per cryostat) to maintain constant level sensor readings. The control loop has variable setpoint and proportional closure range (proportional integrating differential loop). The valves can be run in manual mode as well as in the automatic loop.

The remaining two original goals, the pressure building loop and the dewar heater loop, are close to completion. The stepping motor used to operate the (gross) pressure building valve can be run from the computer, but as yet it is not installed and there is no automatic control loop to facilitate computer regulation of the dewar pressure. The dewar heater loop consists of a control circuit driven by a DAC voltage from the computer, a true RMS power meter, and the heater itself. This hardware has been installed and is ready to be tested.

The PDP 11/23+ will also be able to start and stop the three Koch compressors on operator command from the linac control console. It will also receive binary status reports indicating whether the compressors are on or off, loaded or unloaded. The compressors themselves will have automatic load time delay relays installed to ensure that they run at optimum efficiency with a minimum of operator involvement.

The Koch refrigerator will also be controlled from the computer link, as well as manually. Users will be able to start, stop and control the speed of the three expansion engines and open or close five valves including the pressure building valve, the Joule-Thompson valve, and three heat exchanger bypass valves. The hardware for this system is installed and waiting to be wired and tested. Status reports on engine speeds, seven temperatures and three pressures throughout the refrigerator are read by the computer.

Computer control will also be available for the distribution system vacuum, including starting and stopping the forepump and turbomolecular pump and opening and closing the gate valve to the vacuum space. This hardware is at the same level of development as the refrigerator control system. Indications of five ion gauge pressures at the distal arms of the system and sixteen Pirani gauge pressures at the field joints to all the cryostats and on the system foreline are currently sent to the PDP 11/23+.

A recurrent problem with the linac computers has been loss of power, momentary or prolonged, due to an external problem in the power lines. To circumvent this, we have purchased an uninterruptable power supply which will give us eight minutes of backup power in which to set the various system components described above in fail safe mode. Measures are also being taken to automate the restart procedure to prevent the loss of helium gas when the liquid evaporates and triggers overpressure reliefs.

The system hardware consists of the two microcomputer card cages, the Aydin/Carroll Touch color touch screen, four interface card cages (manufactured in house),

the EPD uninterruptable power supply, five ion gauges and controllers, sixteen Pirani gauges and controllers, 29 level sensors, six gauge pressure transducers, two differential pressure transducers, turbomolecular pump and controller, and various control relays. All devices external to the microcomputer rack (and thus at a different ground potential), are optically isolated at the computer.

Local control is done by an 11/23+ computer programmed in Micropower Pascal. The clock regularly signals a device I/O process and a process which scans user input via the touchscreen and calls procedures and/or other processes to change control values and perhaps monitor input on a different schedule. The control loop is directed to run on a varying schedule, as are a stepmotor process and an engine/pump/compressor control process. A process which handles input from the MicroVAX runs whenever there is input from the serial line.

The remaining hardware has been installed and now needs to be wired and tested; documentation exists for the entire system. Changes in software will be implemented at such time as operator familiarity with the system is suitable to provide a reliable control algorithm.

******

13.5 Resonator Production and Plating Status

D.T. Corcoran, M.A. Howe, and T.A. Meadows

The booster production run of resonators came to an end early this year with completion of high beta resonator #13. This gives the booster its total complement of 28 low beta resonators (three are spares) and 15 high beta resonators (two are spares).

Various difficulties were noted during the production of the high beta resonators. The problems were of the same type that were seen in the low beta resonators.[1] The majority of the problems were failed braze joints. In the low beta resonators we removed the drift tubes and brazed new ones in place which proved to be expensive and time consuming. It was found that the bad spots on the braze joints could be fixed with low temperature solder (60/40 tin-lead). Early test results show no problems with a patch of this kind.

All of the resonators needed for the linac were lead plated and installed in cryostats. The success rate for getting a high quality surface was about 75% for both low and high beta resonators. There was no one persistent problem that accounted for the unsuccessful platings. The most dramatic development was that of periodic reverse pulse plating which consists of our normal pulse plating[2] with brief polarity reversals. This greatly reduces the growth of "fuzz" and "trees" giving a very shiny, high quality surface.

References:

1. Nuclear Physics Laboratory Annual Report, University of Washington (1986) p. 68
2. Nuclear Physics Laboratory Annual Report, University of Washington (1984) p. 93.

******

13.6 Vacuum Systems and Beam Line Installation

J.F. Amsbaugh, J. Davis, and A.M. Flanagan

During the last year installation of the booster linac vacuum system has progressed. This system has been described in previous reports.[1,2,3] To date, all 14 cryostats have been installed along with their associated pumping systems. The beamlines needed to transport beam from the tandem to linac, between the two halves of the linac and finally to the experimental areas have been installed. Typical pressures are 1–5 $\times$ 10^{-7} torr in beamlines and around 5 $\times$ 10^{-6} torr in the cryostats before cooling, but 3 $\times$ 10^{-8} torr after the liquid nitrogen heat shield is filled. Operating pressures with liquid helium in the cryostat providing cryopumping and the turbomolecular pump system valved off is 1–6 $\times$ 10^{-9} torr, although one cryostat has developed a small helium leak that requires constant pumping to maintain good vacuum. In the next few weeks, the remaining vacuum system installations will be finished. Included are a vacuum upgrade of the tandem object beamline and analyzing magnet to prevent contaminating the vacua in the rebuncher/debuncher and buncher cryostats.

The vacuum control computer is a LSI 11/23+ in a Q–bus crate. The current configuration has 256 status inputs, 160 control outputs, and 96 ADCs. This information is displayed on a 19" color monitor equipped with a touch screen for operator input. A list processor control program has been developed so that changes in the system, interlock overrides, and installation do not require rebooting a new control program and no need to shut the entire vacuum system down. A hard disk and controller are being added to speed loading the program and associated constraint files and to provide reboot after power failures. This also will speed up future software development. A procedure for an automatic restart of the vacuum system after a power failure has been installed and tested.

The interface between the I/O boards and the various devices must present an orderly relation between computer address and the terminal strips connected to the device. The interface must also be isolated electrically to avoid ground loops. The output interface consists of an array of solid state relays and monitors the data valid line from the computer. If the data valid is missing for longer than 16 msec then the output are all latched off. The devices controlled are 'safe' in the off mode. The input interface senses device status via relays and/or switches in the device. The ADC interface has an array of unity gain instrumentation amplifiers to isolate the local ion gauge controller ground from the computer ground. This interface hardware has been completed and tested.

References:

1. Nuclear Physics Laboratory Annual Report, University of Washington (1985) p. 86.
2. Nuclear Physics Laboratory Annual Report, University of Washington (1986) p. 70.
3. J.F. Amsbaugh et al., "The Vacuum System of the University of Washington Booster–Linac," Twentieth Symposium of Northeastern Accelerator Personnel, Nov. 1986, Notre Dame, IN, to be published.

******

13.7 Beam Diagnostics

R.C. Connolly, H. Fauska, M.A. Howe, T.J. Irwin, D.D. Leach, H.P. Readdy, and W.G. Weitkamp

A system of diagnostic instruments is used to measure the profile, location, energy, current and time structure of the beam at various places along the beamline. The instruments are operated from the control console via four touch-screen pages. Each page shows a section of the beamline with the diagnostic instruments in their actual location. The touch-screen pages show which instruments are activated and the operating parameters of each one. The instrument signals are read on logarithmic current meters, oscilloscopes and an electrometer in the control console. When a diagnostic instrument is turned on, the signal is automatically switched to the appropriate read-out device. An alphanumeric display is associated with each read-out device to show which instrument is connected to it. The system is about 90% complete.

Beam profiles are measured with ten beam profile monitors (BPM's) purchased from National Electrostatics Corporation (NEC). The control console has two oscilloscopes so two BPM's can be observed simultaneously. Each of the two BPM channels has a touch-screen controlled amplifier so gains can be remotely adjusted to be appropriate for the beam. The BPM displays show the vertical and horizontal beam profiles with vertical and horizontal oscilloscope traces.

Beam apertures are located at the entrances of the cryostats and of the 90° bending magnets. These protect the resonators and restrict the beam to the center of the beamline. Each aperture has four 90° pie-slice shaped jaws to provide steering information.

Adjustable slits are located at the five locations where it is necessary to have horizontal waists. Four of these locations have a single horizontal slit and one location has both a vertical and a horizontal slit. Three of the horizontal slits are homemade. One of the homemade slits is still being tested prior to installation. The slit currents and the aperture currents are read on the logarithmic current meters.

Six Faraday cups (FC's) are available for measuring beam currents. Five are from NEC and one is a beam stop on the through port of the 90° magnet at the end of the south row. The FC currents are read on the electrometer.

An energy monitor is located at the linac entrance, at the end of the south row and at the linac exit. Each consists of a solid state detector and gold scattering foil. The signals are remotely switched into the control room.

The time widths of the beam pulses are measured with time structure monitors located at the entrances to the south and north rows. A tungsten wire is inserted into the beam and a beam-induced signal is detected with a microchannel plate detector. The signal is from X-rays with proton beams and from secondary electrons with heavier ion beams. The detectors are sensitive to both. It has proven necessary to shield the detectors with 1/8" of tantalum from X-ray sources other than the wire. A stand-alone pulse height analyser in the control room is used for the time structure monitors and the energy monitors.

A detector to measure transverse beam emittances has been purchased from Danphysik. It is in house and control software has been written. Testing of the emittance system is now in progress.

13.8 The Linac Control System

R. Burton, M.A. Howe, J.M. LaCroix, D.B. Newell, H.P. Readdy, J.M. Stehfest, and H.E. Swanson

The linac control system consists of an operator's console built around a MicroVAX II computer, 10 satellite PDP 11 processors stationed along the linac itself, and the analog input and output and bitwise parallel interfaces between these satellites and the linac components themselves. A star communications network connects the console to each of the satellites. An operator monitors and controls most of the linac using color graphics displays, touch screens, electroluminescent text displays, and assignable knobs and trackballs. While this system comprises all aspects of linac operation, the vacuum, cryogenic distribution, beam diagnostics, and injector parts are described in detail elsewhere in this report. A progress report on the control console software is also found in a separate section. In overview, we can control the basic linac from the console. Any linac parameter can be set to a previously logged value and tuned with a knob. All dipole magnets can be NMR stabilized to the desired field. Beam transport magnets and resonator phases can be adjusted interactively while observing beam diagnostic devices such as slit and cup currents and scanners. The vacuum and cryogen levels can be monitored and required actions taken remotely. Some aspects of the control system completed this past year are discussed in the following paragraphs.

The fiber optic analog bus link between each satellite and the operator's console can now be used for monitoring the phase and amplitude error signals of all resonator controllers. Analog signals are converted to a frequency of LED pulses on the satellite side of the link and are converted back to voltage signals at the console where they are displayed on a dual trace oscilloscope. A small text display below the scope informs the operator which resonator is being displayed. Resonators may now be brought on-line and tuned from the operators console.

We have completed the interface for the knobs, trackballs, and local displays to the console microVAX. This uses a single board version of an IBM PC. Each operator station has two knobs and two track balls. The PC displays the parameter's name and value on small electroluminescent display panels adjacent to the knobs. It also drives similiar displays identifying the beam diagnostic devices being shown on the oscilloscopes and meters, and as mentioned above, shows what is on the analog bus. A status panel using two color LED's tells which resonators are on and whether they are phase and amplitude locked. This augments the "fast out of lock" system which can act as inhibit should any resonator go out of lock. The maximum message rate to the microVAX is set and moving the knobs faster just increases the value of the increment or decrement.

Each rf amplifier has a four port directional coupler for measuring the forward and reflected power of the resonator. We have installed Schottky diode detectors to allow the computer to read these quantities and display them on the resonator pages. We can also remotely control the AC power to the rf amps, intercryostat quad supplies and cryostat heaters. This completes the control functions planned for the resonator satellites.

******

13.9 Master Control Program Status

R.S. Burton, M.A. Howe, H.P. Readdy, R.J. Seymour, and H.E. Swanson

The booster master control program (CSX) is now being used for all system tests of the NPL linac hardware. The version of CSX that is running currently supports control of all resonators, dipoles, quadrupoles, cryogenic systems, vacuum systems, diagnostics, knobs, console status lights, and console meter and scope labels. In addition, there are provisions for downloading satellites, logging and restoring system parameters, charting system parameters verses time, running user written programs and command files, and monitoring system communication.

There is some additional code which needs to be written to enable remote control of the injector deck, some refrigerator and LHe dewar parameters. The remaining work probably represents about 5% of the total program. The programming for the injector deck will comprise the majority of the remaining code and can not be completed until the injector deck satellite programing is completed.

This year the MicroVAX II host computer was upgraded. A 70 megabyte hard disk was added bringing the total amount of disk storage space to 100 megabytes. In addition, the system random access memory was increased to six megabytes.

The knob satellite subsystem was also completed. It consists of an Ampro Little Board/186 (an IBM PC clone) which controls four knobs and four track balls on the booster console. Under control of CSX, a knob or track ball can be connected to any booster parameter.

Work is also starting on a subset of CSX which will constantly monitor all vital booster parameters and warn the operator if they are outside their normal ranges. Also some work is being done in the areas of automating some of the booster setup and operation activities.

******

13.10 Beam Dynamics

I. Ben Zvi, J.G. Cramer, J.-Q. Lu, and D.W. Storm

(a) Beam Transport Magnets. The beam transport magnets for the "180°" and "90°" systems of the linac were received from Brucker and have been installed. Both the 180° system and the 90° system have now been successfully tested with beam. These are the last two new magnetic transport systems of the linac, and this phase of the project is considered complete.

(b) Beam Dynamics Calculations. We have continued development of beam dynamics software for the booster. In particular, a new beam dynamics program LYRAN has been written by Ben Zvi and Lu. It is based on the program LYRA written by A.H. Scholldorf for the Stony Brook linac, but in LYRAN the calculational strategy of the program has been completely restructured so that all rays in the beam bundle are transported through the accelerating structures together, element by element. This new structure greatly improves the running speed on the VAX by eliminating the extensive page faulting that the was a serious problem for LYRA calculations. It also has made possible the addition of a search mode which permits searching of selected machine conditions to produce certain desired beam characteristics.

13.11 Radiation Safety System

H. Fauska, C.E. Linder, and W.G. Weitkamp

We are enlarging the radiation safety system[1] at the accelerator to accommodate booster operations. The sensors for this system consist of Bonner spheres for neutrons and proportional counters for gamma rays. The sensors produce audible clicks at the rate of 1 click/sec = 1 mrem/hr to provide first level warning of radiation danger. The sensors also have relay contacts which close when the dose equivalent exceeds 100 mrem/hr, the "high radiation" level.

The accelerator area is divided into eight zones, each of which can be isolated from the rest of the laboratory by shielding doors or personnel barriers. A programmable controller will monitor the "high radiation" contacts on all the sensors and the status of all the shielding doors and barriers. When a sensor in one of the zones shows high radiation, the programmable controller will shut off the beam entering the zone unless all doors and barriers allowing entry into the zone are closed.

The gamma monitors detect X radiation resulting from conditioning resonators as well as gamma radiation from the beam. The resonators are sometimes conditioned by an auxiliary amplifier which is not hard wired in place and is therefore difficult to interlock. Consequently, when a gamma monitor senses high radiation in the vicinity of the resonators and a barrier allowing personnel access to the resonator area is open, a loud whistle will alert the operator to the potential hazard.

We have also installed a Bonner sphere outside the building at the point where we expect the highest neutron field to be produced. In the unlikely event that the dose equivalent exceeds 0.2 mrem/hr at this point (which is about 100 m from the nearest normally inhabited building), the beam will be turned off.

The status of all radiation sensors, shielding doors and barrier are displayed on a board in the control room. Radiation levels are displayed by LED bar indicators which turn red when a high radiation level is present. This board is operated directly by the programmable controller so that the radiation safety system is completely independent of the VAX computer which controls the operation of the booster.

Several problems had been overcome in setting up this system. The purchased sensors did not entirely satisfy our needs. Neither the gamma monitors nor the Bonner spheres produce the clicking sound required, so the necessary circuitry had to be added. The Bonner spheres did not operate with the sensors located as far from the electronics as specified by the manufacturer. Also these spheres were quite susceptible to electrical noise. Rebuilding the sphere preamps so they could be moved to the immediate vicinity of the spheres corrected this problem.

All the hardware for this system has been purchased and most is installed. The system is operational; it lacks only a small amount of wiring, programming and final checkout to be completed.

References:

1. Nuclear Physics laboratory Annual Report, University of Washington (1968) p. 68.

13.12 Tandem Foil Stripper

J.J. Davis and W.G. Weitkamp

The existing foil stripper in the tandem terminal holds 38 foils on a spiral disk.[1] This capacity has proven to be inadequate for heavy ion operations. Since we expect operation of the booster to increase demand for heavy ions, the booster project includes installation of a larger capacity foil stripper.

The design criteria for this installation are as follows:

1. It must be possible to insert either a foil or the gas stripper tube into the beam.
2. It must be possible to bias foils to up to 10 kV for the "terminal ripple remover."[2]
3. Transverse electric fields must be minimized so that the beam isn't steered sideways.

After surveying the various types of available mechanisms, we have chosen to install an NEC Model FS-6 foil changer. This device holds 200 foils on inserts which are attached to a metal band by spring clips. The mechanism is mounted on an insulating bushing so the foils can be biased.

In order to fit the foil changer into the terminal with the foils downstream of the gas stripper tube, it is necessary to mount it in the horizontal plane with the axis of the mechanism 60° to the axis of the beam. A system of shields will insure that the beam doesn't encounter transverse electric fields.

An electrostatic vertical steerer in the terminal of the tandem has proven invaluable because it enables the operator to vertically center the beam as it leaves the tandem. As part of this project we will add a horizontal steerer to the terminal as well so that we can correct for horizontal as well as vertical misalignment of the beam.

The foil stripper mechanism has been delivered, the detail drawings are nearly complete and the installation will be completed this fall.

References:

1. W.G. Weitkamp and F.H. Schmidt, Nucl. Instrum. Meth. 122, 65 (1974).
2. G.W. Roth and W.G. Weitkamp, Nucl. Instrum. Meth. 115, 501 (1974).

******

13.13 Tests of the Superconducting Booster Accelerator and Operation Experience

J.F. Amsbaugh, R.C. Connolly, G.C. Harper, M.A. Howe, D.D. Leach, D.P. Rosenzweig, D.W. Storm, and T.D. Van Wechel

During the past year we have carried out several tests with beams through the booster. The first tests involved only the buncher. Then we had three accelerating cryostats, then six, and finally all twelve. The names listed above represent only those individuals who actively participated in operating the tests; however it should be emphasized that most of the staff was involved in preparing and trouble-shooting equipment for the tests.

The object of the tests has been two-fold; first they permit a realistic study of the simultaneous long term operating status of all the equipment. Second, the tests provide an opportunity to begin to learn how to tune the booster and to study the quality of its operation with particle beams.

The final test, using all 12 accelerating cryostats, involved all systems of the booster and all components except for the rebuncher and the final quadrupole doublet. During this test all the systems except the injector deck operated for several days under remote control from the main control computer. (The deck remote controls are not complete.) With the exceptions that will be mentioned below, all these systems operated satisfactorily. The earlier tests involved fewer cryostats and can be viewed as preliminary to the final one.

Using magnetic analysis, we are able to measure the beam energy change produced by each resonator and thereby determine the average accelerating field $\langle E_a \rangle$ in that resonator. These values were generally within 10 to 15% of the values obtained from the rf calibrations, but on average were a little lower. The beam determined values of $\langle E_a \rangle$ will be quoted from here on.

Of the 24 low beta resonators, five were not operable because of failure of the mechanical linkage of the coupler or tuner. Of the remaining 19, the average value of $\langle E_a \rangle$ was maintained at 2.8 MV/m for the several days duration of the tests. The design goal for $\langle E_a \rangle$ is 3.0 MV/m. These resonators stayed phase and field locked and could be turned on and off and locked at will. The average power consumed, as determined by helium boil off, was consistent with that expected from the rf measurements, and was 6 W per resonator. The low beta half of the accelerator produced an ^{16}O beam of 107 MeV using the 6+ charge state from the tandem. Using the 8+ charge state from the second stripper before the linac, the energy was 123 MeV. The energy of the beam at the linac entrance was 56 MeV.

Of the 12 high beta resonators, 2 were not operable because of failure of the tuner drive linkage. The remaining 10 were used in the final test, which was also the first time they were operated with a beam. Their average $\langle E_a \rangle$ was 2.2 MV/m. This average was depressed by one particularly poor resonator operating at 0.9 MV/m. The median $\langle E_a \rangle$ was 2.4 MV/m. The power, as determined by boil off, was 11 W per resonator. We expect that by operating appropriate resonators at higher power, as well as by replating or replacing the several worst ones, we will be able to increase the average $\langle E_a \rangle$ to the design value of 3.0 MV/m for both high and low beta. The 8+ ^{16}O beam emerged from the high beta half of the accelerator with 170 MeV. All but two of the high beta resonators exhibited no

problems with phase or field lock. Those two require some adjustments in their electronics.

For the future, it is clear that we will have to improve the width of the bunches from the tandem as well as eliminate a drift in the low energy buncher phase lock system. At present the low energy buncher is phase locked to a resonant detector that is located just upstream of the high energy buncher. The locking system removes time variations in the bunch arrival due to 60 Hz ripple on the ion energy, due to belt ripple on the tandem, and so on. Observation of the phase locking error signal indicates that this lock performs very well with residual drifts of a few picoseconds. However, either due to drifts in the resonant frequency of the detector or due to other long term drifts in the electronics, we see shifts of several hundred picoseconds in the phasing between the beam and the high energy buncher. We are presently studying this phenomenon and expect to resolve it during the next month or two. The bunch widths (entering the high energy buncher) are substantially in excess of one nanosecond, while bunches of one nanosecond or less are expected. Part of this width should be reduced by the use of the elevated injector deck.

We plan to open and repair the four cryostats which contain the resonators whose couplers or tuners are inoperable. This work should be done by the end of June. Installation of the final piece of beamline and the final quadrupole doublet is scheduled for the first half of July. The isolation transformer for the injector deck is also expected to be installed during July. Further tests with beam will be carried out near the end of July.

14. APPENDIX

14.1 Nuclear Physics Laboratory Personnel

Faculty

Eric G. Adelberger, Professor
David Bodansky, Professor
John G. Cramer, Professor; Director, Nuclear Physics Laboratory
George W. Farwell, Professor Emeritus
Cynthia A. Gossett, Research Assistant Professor
Pieter M. Grootes, Joint Senior Research Associate, Geological Sciences
Isaac Halpern, Professor
Charles E. Hyde-Wright, Assistant Professor
Eric B. Norman, Affiliate Assistant Professor[1]
Fred H. Schmidt, Professor Emeritus
Kurt A. Snover, Research Professor
Derek W. Storm, Senior Research Scientist; Director, Superconducting Booster Project
Thomas A. Trainor, Research Associate Professor
Robert Vandenbosch, Professor
William G. Weitkamp, Research Professor; Technical Director, Nuclear Physics Laboratory

Research Staff

Ilan Ben-Zvi, Visiting Scientist[2]
Salvador Gil, Research Associate
Marta Kicinska-Habior, Research Associate
Munther Hindi, Visiting Scientist[3]
Steven K. Lamoreaux, Research Associate
Qui-Xun Lin, Visiting Scientist[4]
Jian-Qin Lu, Visiting Scientist[5]
Warren F. Rogers, Research Associate

Predoctoral Research Associates

John A. Behr
Keith J. Davis[6]
Gerald Feldman[7]
Patricia B. Fernandez
Alejandro Garcia
Holger K. Glatzel[8]
Jens H. Gundlach
Stephen E. Kellogg[9]
Mahbubul A. Khandaker[10]
S. John Luke
Brian McLain
Douglas P. Rosenzweig
Christopher W. Stubbs[11]
Ryoji Watanabe
Peter Wong
Valdis J. Zeps

Professional Staff

John F. Amsbaugh, Research Engineer
David Balsley, Research Engineer
Roger C. Connolly, Reseach Engineer
Jim Davis, Research Engineer
J. Greg Douglas, Visiting Controls Engineer[1 2]
Harold Fauska, Senior Research Scientist[1 3]
Gregory C. Harper, Research Engineer
Gervas M. Hinn, Research Scientist/Target Maker
Robert D. Hobbs, Research Engineer
David J. Hodgkins, Research Engineer
Mark A. Howe, Research Engineer
Donald D. Leach, Research Scientist
Thomas A. Meadows, Research Scientist
David B. Newell, Research Engineer
L. Thomas Nirider, Research Engineer[1 4]
H. Pamela Readdy, Computer System Engineer
David Schaafsma, Research Engineer
Richard J. Seymour, Computer System Manager
Rod E. Stowell, Electronics Engineer/Electronic Shop Supervisor
H. Erik Swanson, Research Physicist
Louis P. Van Houten, Research Engineer[1 4]
Timothy D. Van Wechel, Electronics Engineer
Douglas I. Will, Research Engineer

Technical Staff

Robert L. Cooper, Instrument Maker
Dean T. Corcoran, Engineering Technician
James R. Cromie, Accelerator Technician
Louis L. Geissel, Instrument Maker, Student Shop Leadman
Brian P. Holm, Instrument Maker
John M. LaCroix, Electronics Technician
Carl E. Linder, Engineering Technician
George E. Saling, Accelerator Technician[1 3]
Kenneth Schuh, Drafting Technician
Byron A. Scott, Instrument Maker[1 3]
Hendrik Simons, Instrument Maker, Shop Supervisor
John M. Stehfest, Electronics Technician
Jay J. Tomasko, Accelerator Technician
John A. Wootress, Accelerator Technician
Allen L. Willman, Instrument Maker[1 3]

Administrative Staff

Ronald Floyd, Buyer[1 4]
Barbara J. Fulton, Administrative Secretary
Holly L. Johnson, Office Assistant[1 4]
Rebecca Nielsen, Office Assistant
Maria G. Ramirez, Budget Coordinator

1. Permanent Address: Lawrence Berkeley Laboratory, University of California, Berkeley, CA 94720.
2. Permanent Address: Department of Nuclear Physics, Weizmann Institute of Science Rehovot, Israel.
3. Now at: Tennessee Technological University, Cookeville, TN 38505.
4. Permanent Address: Peking University, Beijing, People's Republic of China.
5. Permanent Address: Peking University, Beijing, People's Republic of China.
6. Now at: Boeing Aerospace, Seattle, WA 98124.
7. Now at: Duke University, Durham, NC 27706.
8. On leave: D-792 Heidenheim, Federal Republic of West Germany.
9. Now at: California Institute of Technology, Pasadena, CA 91125.
10. Now at: University of Maryland, College Park, MD 20742.
11. Department of Physics, University of Washington, Seattle, WA 98195.
12. Permanent Address: Group 3 Technology Ltd., Auckland, New Zealand.
13. Retired - part time employee.
14. No longer associated with the Nuclear Physics Laboratory.

Part Time Staff

Robert Abel*
James Annis*
Darrell Armstrong
James Barei
David Badt*
Melanie Bryce
Frederick L. Bahr*
Donald W. Black*
Margaret K.M. Brown*
Richard Burton
Steven P. Doub
Tony Earle*
Marc Farley*
Ann Flanagan
Mulugetta Gabre*
Tefera Gulelat*
David Hamann
Timothy J. Irwin
Lee W. Jackson*
James Katterman*
Peter Kaloupis*
John Kevcheval
Te Lau
Mark Lemmon
Wei Liu*
James R. Longwill
Gary S. Malkasian
Henry McDonald*
Margaret McEwen*
Kevin McMurry
Denton K. Morris
Joseph R. Olson
Darren Paschke
David Pengra*
Harold Poskanzer*
Lee Prewitt
Robert Rose*
Sharon Rosell
Barbara Sanborn*
Alan Schroeder
Kristen Seymour*
David Sours*
Jeff Sowers
Jeff Stodola*
Rob Vander Stoep*
Sun Yao Wong*
Blair Zajec*

* No longer associated with the Nuclear Physics Laboratory.

******

FRONT ROW: CORNWALL, PASCHKE, BAREI, DAVIS, GIL, HOBBS, HYDE-WRIGHT, CRAMER, STEHFEST, TRAINOR, SCHMIDT, FULTON, WEITKAMP, NAKAMOTO, PREWITT, DOUGLAS, ROGERS

MIDDLE ROW: WOOTRESS, CONNOLLY COOPER, GEISSEL, SIMONS, SWANSON, FARWELL, WONG, VAN WECHEL, RAMIREZ, SWARTZ, ROSENZWEIG, ROSELL, WILL, BALSLEY

BACK ROW: HALPERN, STORM, LEACH, HODGKINS, GROOTES, LACROIX, AMSBAUGH, FERNANDEZ, HARPER, MCLAIN, MCMURRY, BURTON, SEYMOUR, IRWIN, CORCORAN, STUBBS, WATANABE, ADELBERGER

14.2 Degrees Granted, Academic Year 1986–1987

Ph.D. Degrees:

"The Calibration of Sub-Coulomb Heavy Ion Proton Transfer Reactions," Keith J. Davis, Ph.D. Thesis, University of Washington (1987).

"A Study of the Inclusive Inelastic Scattering of 100 MeV Pions from ^{2}H, ^{3}He and ^{4}He," Mahbubul Khandaker, Ph.D. Thesis, University of Washington (1987).

"The Nucleosynthesis of $^{180}Ta^{m}$," Stephen E. Kellogg, Ph.D. Thesis, University of Washington (1987).

"Giant Dipole Resonances Built on Excited Nuclear States Observed in Proton Capture and Heavy-Ion Fusion," Gerald Feldman, Ph.D. Thesis, University of Washington (1987).

Master's Degrees:

"Cryogenic System Design for a Superconducting Booster," Douglas I. Will, Master's Thesis, University of Washington (1987).

"Proton Emission from ^{3}He Induced Reactions," Alan R. Crews, Master's Thesis, University of Washington (1987).

"Measurement of the Neutral Hydrogen Beam Flux in the University of Washington Colliding Beams Polarized Ion Source," L. Thomas Nirider, Master's Thesis, University of Washington (1987).

14.3 List of Publications

Published Papers:

"Giant Resonances in Excited Nuclei," K.A. Snover, Ann. Rev. Nucl. Part. Sci. 36, 545 (1986).

"Energy Modulations of a Polarized Proton Beam Associated with Polarization Reversal," J. Sromicki, P.A. Quin, W. Haeberli, E.G. Adelberger, C.A. Gossett, H.E. Swanson, and V.J. Zeps, Nucl. Instrum. Methods, A255, 611 (1987).

"Reply to 'Parity Violating Asymmetries in the Scattering of Transversely Polarized Protons'," E.G. Adelberger, P. Hoodbhoy, and B.A. Brown, Phys. Rev. C 33, 1840 (1986).

"Fission Probes of Sub-Barrier Fusion Cross Section Enhancements and Spin Distribution Broadening," T. Murakami, C.-C. Sahm, R. Vandenbosch, D.D. Leach, A. Ray, and M.J. Murphy, Phys. Rev. C, 34, 1353 (1986).

"Total Reaction Cross Section for ^{12}C on ^{12}C, ^{40}Ca, ^{90}Zr and ^{208}Pb between 10 and 35 MeV/Nucleon," C.-C. Sahm, T. Murakami, J.G. Cramer, A.J. Lazzarini, D.D. Leach, D.R. Tieger, R.A. Loveman, W.G. Lynch, M.B. Tsang, and J. Van der Plicht, Phys. Rev. C 34, 2165 (1986).

"Search for the Beta-Decay of ^{180}Lu to $^{180}Hf^{m}$," S. Kellogg and E.B. Norman, Phys. Rev. C 34, 2248 (1986).

"Linear Momentum and Angular Momentum Transfer in the Reactions of ^{16}O with ^{154}Sm," M.N. Namboodiri, R.K. Choudhury, L. Adler, J.D. Bronson, D. Fabris, U. Garg, P.L. Gonthier, K. Hagel, D.R. Haenni, Y.W. Lui, Z. Majika, G. Mouchaty, T. Murakami, J.B. Natowitz, G. Nebbia, R.P. Schmitt, S. Simon, J.P. Sullivan, and D.H. Youngblood, Phys. Rev. C 35, 149 (1987).

"Forward-to-Backward Asymmetry of the (γ,n) Reaction in the Energy Range 20-30 MeV," T. Murakami, I. Halpern, D.W. Storm, P.T. Debevec, L.J. Morford, S.A. Wender, and D.H. Dowell, Phys. Rev. C 35, 479 (1987).

"Isomeric Levels in ^{180}Lu and the Nucleosynthesis of $^{180}Ta^{m}$," K.T. Lesko, E.B. Norman, D.M. Moltz, R.M. Larimer, S.G. Crane, and S. Kellogg, Phys. Rev. C 34, 2256 (1986).

"Nonequilibrium Population of Magnetic Substates and Excitation-Energy Division in the Decay of an Orbiting Complex," A. Ray, D.D. Leach, R. Vandenbosch, K.T. Lesko, and D. Shapira, Phys. Rev. Lett. 57, 815 (1986).

"First Capture of Antiprotons in a Penning Trap: A Kiloelectronvolt Source," G. Gabrielse, X. Fei, K. Helmerson, S.L. Rolston, R. Tjoelker, T.A. Trainor, H. Kalinowsky, J. Haas, and W. Kells, Phys. Rev. Lett. 57, 2504 (1986).

"Search for an Intermediate Range Interaction," C.W. Stubbs, E.G. Adelberger, F.J. Raab, J.H. Gundlach, B.R. Heckel, K.D. McMurry, H.E. Swanson, and R. Watanabe, Phys. Rev. Lett. 58, 1070 (1987).

"Gamma Ray Production Cross Sections for Alpha-Particle Induced Reactions on ^{19}F and ^{23}Na," E.B. Norman, K.T. Lesko, T.E. Chupp, P. Schwalbach, M.A Faccio, Radiation Effects 94, 307 (1986).

"Radiocarbon Dating with the University of Washington Accelerator Mass Spectrometry System," P.M. Grootes, M. Stuiver, G.W. Farwell, D.D. Leach, and F.H. Schmidt, Radiocarbon 28, 237 (1986).

Papers to be Published or Submitted:

"Organic Carbon in Deep-Sea Sediments: C-14 Concentrations," S. Emerson, C. Stump, P.M. Grootes, M. Stuiver, G.W. Farwell, and F.H. Schmidt, Nature, to be published.

"LYRAN: A Program for the Analysis of Linac Beam Dynamics," J.-Q. Lu, I. Ben-Zvi, and J.G. Cramer, submitted to to Nucl. Instrum. Methods.

"A Pretandem Harmonic Buncher," Q.-X. Lin and T.D. Van Wechel, submitted to Nucl. Instrum. Methods.

"The ^{37}Cl Solar Neutrino Capture Cross Section," E.G. Adelberger and W.C. Haxton, submitted to Phys. Rev. C.

"Statistical GDR Decay of Highly Excited States of ^{63}Cu," M. Kicinska-Habior, K.A. Snover, C.A. Gossett, J.A. Behr, G. Feldman, H.K. Glatzel, J.H. Gundlach, and E.F. Garman, submitted to Phys. Rev. C.

"Rapid Response of Tree Cellulose Radiocarbon Content to Changes in Atmospheric $^{14}CO_2$ Concentration," G.W. Farwell, P.M. Grootes, D.D. Leach, F.H. Schmidt, and M. Stuiver, submitted to Tellus.

Conference Presentations, Proceedings, and Invited Talks:

"The Vacuum System of the University of Washington Booster-Linac," J.F. Amsbaugh, Twentieth Symposium of North Eastern Accelerator Personnel, Nov. 1986, Notre Dame, IN, to be published.

"A 300 KV Isolation Platform at the University of Washington," G. Harper, Twentieth Symposium of North Eastern Accelerator Personnel, Nov. 1986, Notre Dame, IN, to be published.

"University of Washington Nuclear Physics Laboratory--Report to SNEAP," W.G. Weitkamp, Twentieth Symposium of North Eastern Accelerator Personnel, Nov. 1986, Notre Dame, IN, to be published.

"A Computer Program for Predicting Tandem Parameters," Report to SNEAP 1985, W.G. Weitkamp, in Proc. of the Symposium of Northeastern Accelerators Personnel, 1985, Rev. Sci. Instrum. 57, 740 (1986).

"Status of the University of Washington Supeconducting Booster," Report to SNEAP 1985, J.F. Amsbaugh, R.C. Connolly, D.T. Corcoran, J.G. Cramer, M.A. Howe, D.W. Storm, H.E. Swanson, T.A. Trainor, R. Vandenbosch, L.P. Van Houten, W.G. Weitkamp, and D.I. Will, in Proc. of the Symposium of Northeastern Accelerators Personnel, Rev. Sci. Instrum. 57, 761 (1986).

"Superconducting Tests of Beta=0.1 and Beta=0 Resonators, Report to SNEAP 1985, D.W. Storm, J.F. Amsbaugh, D.T. Corcoran, and M.A. Howe, in Proc. of the Symposium of Northeastern

Accelerators Personnel, Rev. Sci. Instrum. 57, 773 (1986).

"The NPL Superconducting Linac Control System," Report to SNEAP 1985, H.E. Swanson, M.A. Howe, L.W. Jackson, J.M. LaCroix, H.P. Readdy, D.W. Storm, and L.P. Van Houten, in Proc. of the Symposium of Northeastern Accelerators Personnel, Rev. Sci. Instrum. 57, 784 (1986).

"Heavy Ion Fusion and Fission Reactions," R. Vandenbosch, Beijing International Symposium on Physics at Tandem, May, 1986, Peking, China.

"Giant Resonances in Hot Nuclei," K.A. Snover, Invited talk presented at the Nuclear Structure Workshop, Niels Bohr Institute, Copenhagen, May 1986.

"Heavy Ion Fusion Reactions," (4 lectures) R. Vandenbosch IX Workshop on Nuclear Physics, July, 1986, Tandar Laboratory, Buenos Aires, Argentina.

"Giant Resonances in Excited Nuclei," K.A. Snover, invited lectures presented at the International School of Heavy Ion Physics - The Response of Nuclei Under Extreme Conditions, Erice, Italy, Oct. 1986; Plenum Press, to be published.

"Giant Dipole Resonances in Excited Nuclei," K.A. Snover, in International Symposium on Weak and Electromagnetic Interactions in Nuclei, ed. H.V. Klapdor, Springer-Verlag, Heidelberg, p. 148, 1986.

"Nuclear Structure of Heated Nuclei from the Statistical Decay of the Giant Dipole Resonance," C.A. Gossett, Workshop on Nuclear Structure at Moderate and High Spin, Berkeley, October, 1986 (invited talk).

"Ion Source Sample Preparation Techniques for Carbon-14 AMS Measurements," D.R. Balsley, G.W. Farwell, P.M. Grootes, and F.H. Schmidt, presented at Fourth International Symposium on Accelerator Mass Spectrometry, Niagara-on-the-Lake, Canada, April, 1987, (to be published in Nucl. Instrum. Methods).

"Early Expectations of AMS: Greater Ages and Tiny Fractions. One Failure? - One Success," F.H. Schmidt, D.R. Balsley, and D.D. Leach, presented at Fourth International Symposium on Accelerator Mass Spectrometry, Niagara-on-the-Lake, Canada, April, 1987, (to be published in Nucl. Instrum. Methods).

"Parity and Time-Reversal Violation in Nuclei and Atoms," E.G. Adelberger, in Intersections between Particle and Nuclear Physics, ed. D.F. Geesaman, AIP Conf. Proc. No. 150, p. 1117, 1986.

"(γ,n) Studies of the Giant Isovector E2 Resonance in Lead, Cadmium, and Calcium," D.W. Storm, I. Halpern, C.A. Gossett, T. Murakami, D.P. Rosenzweig, D.R. Tieger, P.T. Debevec, A. Freytag, L.J. Morford, S.A. Wender, and D.H. Dowell, Workshop on Isovector Excitations in Nuclei, Vancouver, Canada, Oct. 1986, to be published in Canadian J. of Phys.

"Electroproduction de Kaons sur les Noyaux," C.E. Hyde-Wright, presented at the Conference Photoproduction et Electroproduction de Mesons sur le Nucleon et sur les Noyaux, Clermont-Ferrand, Nov. 1986, to be published by Laboratoire de Physique Corpusculaire, Universite de Clermont-Ferrand II Aubiere 63170 France, P. Bertin, ed.

"The Nucleon–Nucleon Weak Interaction," E.G. Adelberger, in the Investigation of Fundamental Interactions with Cold Neutrons, ed. G.L. Greene, NPS Special Publication 711, U.S. Department of Commerce, Feb. 1986.

"Symmetries in Nuclei," E.G. Adelberger, in Current Problems in Nuclear Physics, eds. T. Paradellis and S. Kossionides, Hellenic Physical Society Conf. Series 1, 177 (1986).

"Nuclear Probes of Fundamental Symmetries," E.G. Adelberger, in International Symposium on Weak and Electromagnetic Interactions in Nuclei, ed. H.V. Klapdor, Springer–Verlag, Heidelberg, p. 592, 1986.

"Progress Report on an Experiment to Measure $\Delta I = 0$ Parity Mixing in ^{14}N," H.E. Swanson, V.J. Zeps, E.G. Adelberger, C.A. Gossett, J. Sromicki, W. Haeberli, and P. Quin, in International Symposium on Weak and Electromagnetic Interactions in Nuclei, ed. H.V. Klapdor, Springer–Verlag, Heidelberg, p. 648, 1986.

"Symmetry Violation in Nuclear Reactions," E.G. Adelberger, in New Scope of Heavy Ion Science, Part I, eds. A Arima, H. Kamitsubo, S. Kubono, and S. Nagamiya, Supp. Jour. Phys. Soc. Japan 54, 501 (1985).

"Parity and Time Reversal Violation in Nuclei," E.G. Adelberger, to be published in Proc. of V Int. School in Neutron Physics, Oct. 1986, Alushta, USSR.

"High Energy Gamma Emission Following Heavy Ion Collisions," C.A. Gossett, [Energetic Products of Heavy Ion Collisions], Fourth Gull Lake Nuclear Physics Conference, Gull Lake, Michigan, May 17–20, 1987.

Abstracts:

"The Calibration of Sub–Coulomb Heavy Ion Proton Transfer Reactions," K.J. Davis, T. Murakami, S. Gil, M. Khandaker, A. G. Lazzarini, D.D. Leach, R. A. Loveman, and J.L. Osborne Bull. Am. Phys. Soc. 31, 785 (1986).

"ℓ–Forbidden Beta Decay of ^{207}Tl," M.M. Hindi, E.G. Adelberger, S.E. Kellogg, and T. Murakami, Bull. Am. Phys. Soc. 31, 874 (1986).

"Temperature and Spin Dependence of the GDR Strength Function of ^{63}Cu," M. Kicinska–Habior, J.A. Behr, G. Feldman, H. Glatzel, C.A. Gossett, J.H. Gundlach, and K.A. Snover, Bull. Am. Phys. Soc. 31, 1205 (1986).

"High Energy Gamma Emission Following Heavy Ion Collisions," C.A. Gossett, J.A. Behr, J.H. Gundlach, K.A. Snover, K.T. Lesko, and E.B. Norman, Bull. Am. Phys. Soc. 31, 1205 (1986).

"Low Energy Resonances in ^{13}N Studied via $^{12}C(\vec{p},p)$," E.G. Adelberger, C.A. Gossett, V.J. Zeps, and J. Sromicki, Bull. Am. Phys. Soc. 31, 1209 (1986).

"An Attempt to Measure the γ–branch of the Unbound 5.17 MeV Level of ^{14}O," P.B. Fernandez, E.G. Adelberger, M. Khandaker, and M.M. Hindi, Bull. Am. Phys. Soc. 31, 1209 (1986).

"Forward–to–Backward Asymmetries in the (γ,n) Reaction Around the E2 Isovector Giant

Resonance," A. Freytag, D. Dale, P.T. Debevec, C.A. Gossett, I. Halpern, T. Murakami, D. Rosenzweig, D.W. Storm, and D.R. Tieger, Bull. Am. Phys. Soc. 31, 1215 (1986).

"A Scanner for Low-Energy Polarized Proton Beams," V.J. Zeps, E.G. Adelberger, C.A. Gossett, H.E. Swanson, P.A. Quin, and J. Sromicki, Bull. Am. Phys. Soc. 31, 1226 (1986).

"A System for Controlling the Position, Angle, and Spin Direction of a Polarized Proton Beam," H.E. Swanson, E.G. Adelberger, C.A. Gossett, and V.J. Zeps, Bull. Am. Phys. Soc. 31, 1226 (1986).

"Neutron Spin Rotation and Study of P&T Violation Effects in Nuclei," S. Saha, E.G. Adelberger, and B. Heckel, Bull. Am. Phys. Soc. 31, 1230 (1986).

"Experimental Constraints on Intermediate Range Interaction Between Baryons," C.W. Stubbs, E.G. Adelberger, F.J. Raab, J.H. Gundlach, B.R. Heckel, K.D. McMurry, H.E. Swanson, and R. Watanabe, Bull. Am Phys. Soc. 32, 1049 (1987).

"Parity Mixing of the Ex $\approx$ 8.6 MeV $0^+,0^-$; T=1 Doublet in $^{14}N^*$," V.J. Zeps, E.G. Adelberger, A. Garcia, C.A. Gossett, H.E. Swanson, W. Haeberli, P.A. Quin, and J. Sromicki, Bull. Am. Phys. Soc., 32, 1061 (1987).

"GDR Decays and the Shape of $^{90}Zr^*$ at Moderate Temperature and Spin," J.H. Gundlach, J.A. Behr, G. Feldman, C.A. Gossett, M. Kicinska-Habior, and K.A. Snover, submitted to First Topical Meeting on Giant Resonance Excitation in Heavy Ion Reactions, Padova, Italy, Sept. 1987

"Spin Dependence of the Giant Dipole Resonance Strength Function in Highly Excited Nuclei in the Mass Region A=39-45," M. Kicinska-Habior, J.A. Behr, C.A. Gossett, J.H. Gundlach, G. Feldman, and K.A. Snover, submitted to First Topical Meeting on Giant Resonance Excitation in Heavy Ion Reactions, Padova, Italy, Sept. 1987

"The Giant Dipole Resonance in Highly Excited ^{92}Mo and ^{100}Mo," M. Kicinska-Habior, J.A. Behr, C.A. Gossett, J.H. Gundlach, G. Feldman, and K.A. Snover, submitted to First Topical Meeting on Giant Resonance Excitation in Heavy Ion Reactions, Padova, Italy, Sept. 1987

"Excited-State Giant Dipole Resonances in Proton Capture," G. Feldman, J.A. Behr, D.H. Dowell, C.A. Gossett, J.H. Gundlach, M. Kicinska-Habior, and K.A. Snover, submitted to Sixth International Symposium on Capture Gamma-Ray Spectroscopy, Belgium, Sept. 1987.

Other Publications by Members of the Laboratory and Other Laboratory Research:

"Electroexcitation of M4 Transitions in ^{17}O and ^{18}O," D.M. Manley, B.L. Berman, W. Bertozzi, J.M. Finn, F.W. Hersman, C.E. Hyde-Wright, M.V. Hynes, J.J. Kelly, M.A. Kovash, S. Kowalski, R.W. Lourie, B. Murdock, B.E. Norum, B. Pugh, and C.P. Sargent, Phys. Rev. C 34, 1214 (1986).

"Electroexcitation of 4^- States in ^{16}O," C.E. Hyde-Wright, W. Bertozzi, T.N. Buti, J.M. Finn, F.W. Hersman, M.V. Hynes, M.A. Kovash, J.J. Kelly, S. Kowalski, J. Lichtenstadt, R.W. Lourie, B.E. Norum, B. Pugh, C.P. Sargent, B.L. Berman, F. Petrovich, and J.A. Carr, Phys. Rev. C 35, 880 (1987).